Time-Stepping Schemes for Nonlinear Hamiltonian Systems Based on the Discontinuous Galerkin Method

Chair for Applied Mechanics

Department of Mechanical Engineering

University of Kaiserslautern

Germany

LTM

Master's Thesis

(submitted for a diploma in mechanical engineering)

written by

cand. ing. Michael Gross

supervised by

Dr.-Ing. Peter Betsch

finished on

March 16, 2000

recorded as

D02/00

Abstract

A family of implicit multi-level one-step time-stepping schemes for Hamiltonian systems is developed. The implicit multi-level one-step schemes are based upon the discontinuous Galerkin finite element approximation of Hamilton's canonical equations and possess numerical dissipation. For comparison, energy conserving time-stepping schemes which rely on the continuous Galerkin finite element method are also dealt with. The following two natural systems are considered: the planar circular pendulum and the two-body central force problem. In particular, constant and linear time finite elements are investigated. The influence of exact and numerical quadrature in time on the algorithmic total energy and angular momentum of the associated time-stepping schemes is examined in detail. In this connection the numerical dissipation properties of the time-stepping schemes under consideration are also inspected. Numerical examples for the circular pendulum deal with linear motions (harmonic oscillator) as well as nonlinear motions. For the two-body problem Hooke's central force law (isotropic harmonic oscillator) and inverse square law of force (Kepler's problem) are considered.

Contents

1 Introduction

This paper concernes the time integration of the Hamilton's canonical equations. Instead considering a finite difference method from the outset, we employ the finite element method for the temporal discretization. The Hamiltonian point of view implies an intependent approximation of the generalized coordinates and momenta. The starting point of the present time finite element method is the weighted residual statement (weak form) of Hamilton's canonical equations in symplectic notation. We solve the corresponding system of first-order ordinary differential equations by applying time-stepping schemes emanating from the so-called discontinuous Galerkin method; see Eriksson et al. [12].

This Galerkin finite element method, often accredited to Lasaint & Raviart [27], relies upon the use of discontinuous trial and test functions of the same space. In comparison, the continuous Galerkin method is based on continuous trial and test spaces with a test space dimension reduced by one compared with the trial space dimension. According to Eriksson et al. [12] the identical function spaces turns out to be an advantage in the error analysis and also gains improved stability properties for parabolic problems in comparison to the continuous Galerkin method. However, in contrast to the continuous Galerkin method, one has to give up the requirement that the initial condition is exactly satisfied.

In particular we examine in the present paper for constant and linear time finite elements the conservation properties which hold for the following two holonomic, scleronomous constrainted (natural) systems:

- the planar circular pendulum and
- the two-body central force problem.

The total energy and the total angular momentum are especially of interest because these two constants of the motion play a central role in mechanics and therefore it is also a great advantage to be able to conserve them exactly after each time step (algorithmic conservation). According to LaBudde & Greenspan [26] the application of conventional numerical methods to systems of ordinary differential equations of motion of classical mechanics leads to conservation of the total energy and angular momentum only to the order of the truncation error.
Moreover, from the numerical viewpoint the energy conservation of a time-stepping scheme is diserable for unconditional stability within the nonlinear regime; see Betsch & Steinmann [9] and Hughes [18].

Since, according to the papers of Bauchau & Joo [5], Bauchau & Theron [6], Chung & Hulbert [11], Hoff & Pahl [17], Hulbert [20], Johnson [22], Johnson et al. [23], Neumann & Schweizerhof [30] and Ruge [32], for instance, a time discontinuous Galerkin approximation leads to numerical dissipation in time and space-time finite element methods, we aim to obey the conservation laws by a suitable numerical quadrature. Note that within the scope of the continuous Galerkin finite element method P. Betsch

and P. Steinmann have achieved a conservation of algorithmic total angular momentum in their papers Betsch & Steinmann [7, 8] by specific quadrature rules. In general, we consider in the present paper so-called interpolating quadrature rules according to Isaacson & Keller [21] and in particular, we restrict ourselves to the midpoint rule, the trapezoidal rule and the Gaussian quadrature rules.

In addition, we have implemented the considered two natural systems and in the present paper we illustrate the analytical results by numerical examples. We have taken as reference for the computations the energy conserving continuous Galerkin finite element method according to Betsch & Steinmann [7, 9].

The remainder of this thesis is organized in the following manner: Part I aims at the derivation of the time-stepping schemes emanating from the discontinuous Galerkin method. First we review in Section 2 the Hamiltonian formulation of equations of motion: subsequent to an introduction of Hamilton's canonical equations, we identify the hamiltonian as the total energy of natural systems and thus as a constant of motion for natural systems. In Section 3 we derive the implicit multi-level one-step time-stepping schemes from the discontinuous Galerkin finite element method. Section 4 elaborates upon the algorithmic hamiltonian of the discontinuous Galerkin method.
Part II comprises the consideration of the circular pendulum. Section 5 starts with an introduction of the conservation of total angular momentum for only one particle which we apply as well to the circular pendulum as to the two-body problem. We determine in Section 6 a time finite element formulation for the harmonic oscillator which means the circular pendulum for small oscillations. We consider exact quadrature and the quadrature rules named above. In Section 7 we examine the algorithmic total energy of the harmonic oscillator for exact and numerical quadrature. Section 8 is devoted to an elaboration of a time finite element formulation for the circular pendulum for arbitrary motions. Owing to the nonlinear conservative force, we gain time-stepping schemes for linear time finite elements within the symplectic notation only by numerical quadrature. Note that Betsch & Steinmann [9] show a possibility applying exact quadrature outside the symplectic notation. Section 9 is dedicated to the algorithmic total angular momentum of the circular pendulum. Since we apply polar coordinates for generalized coordinates, the calculation is almost trivial. Section 10 shows how we obtain algorithmic total energy conservation by a nonstandard quadrature rule.
Part III describes the application of the time-stepping schemes to the two-body central force problem. Section 11 begins with a reduction of this problem with six degrees of freedom to an equivalent planar one-body problem with two degrees of freedom. In Section 12 we give the Hamiltonian formulation of the equivalent one-body problem. In Section 13 we create a time finite element formulation for the isotropic harmonic oscillator, ie Hooke's central force law, which is based upon the equivalent one-body problem. Section 14 concerns the algorithmic total energy of the isotropic harmonic oscillator where we take into consideration exact quadrature as well as interpolating quadrature rules. In Section 15 we investigate the algorithmic total angular momentum of the isotropic harmonic oscillator for exact and numerical quadrature. In Section 16 we

turn to a time finite element formulation for arbitrary nonlinear central force laws and consider the inverse square law of force (Kepler's problem) in detail. Section 17 examines the conservation properties of algorithmic total angular momentum of the equivalent one-body problem only for interpolating quadrature rules owing to the arbitrariness of the central force law. Section 18 shows a possibility to obtain algorithmic total energy conservation by a nonstandard quadrature rule. Section 19 concludes with a summary and impulses for further investigations into the described finite element formulation.

Part I
The Galerkin Finite Element Formulation

2 The Hamiltonian formulation of equations of motion

The starting point for the Galerkin approximation developed below is the Hamiltonian formulation of the equations of motion. In this section we give a brief account of classical mechanics which will be needed for the subsequent derivation of numerical time-stepping schemes from a finite element formulation. For more details, we refer to Arnold [3] and Goldstein [14].

2.1 The canonical equations of Hamilton

We consider mechanical systems with n_{dof} degrees of freedom and holonomic, scleronomous (natural) constraints. The state of the system is described by independent generalized coordinates q_i, $i = 1, \ldots, n_{dof}$. Let the generalized coordinate q_i be the ith component of a $n_{dof} \times 1$ column matrix $\mathbf{q}$. Furthermore, let $T(\mathbf{q}, \dot{\mathbf{q}}, t)$ be the total kinetic energy of the system, where $\dot{\mathbf{q}} = d\mathbf{q}/dt$ is the generalized velocity vector, then the motion of the system is described by the following equation:

$$\frac{d}{dt}\left(\partial_{\dot{\mathbf{q}}} T\right) - \partial_{\mathbf{q}} T = \mathbf{Q}, \tag{1}$$

where $\mathbf{Q}$ denotes the $n_{dof} \times 1$ column matrix of generalized forces Q_i, $i = 1, \ldots, n_{dof}$. We assume that the motion of the system is influenced by generalized forces Q_i which are associated with a conservative force field, ie $\mathbf{Q} = -\partial_{\mathbf{q}} V$. The potential $V(\mathbf{q}, t)$ of the field is a function only of $\mathbf{q}$ and time t. Therefore, we define a new function L as

$$L(\mathbf{q}, \dot{\mathbf{q}}, t) = T(\mathbf{q}, \dot{\mathbf{q}}, t) - V(\mathbf{q}, t). \tag{2}$$

L is called the lagrangian or Lagrange function. Now the equation (1) takes the form

$$\frac{d}{dt}\left(\partial_{\dot{\mathbf{q}}} L\right) - \partial_{\mathbf{q}} L = \mathbf{0}, \tag{3}$$

where $\mathbf{0}$ denotes a $n_{dof} \times 1$ zero matrix. We refer to equation (3) as Lagrange's equation of motion.
Lagrange's equation generally leads to n_{dof} nonlinear differential equations of second-order. In view of the finite element formulation which we develop below, we prefer the Hamiltonian formulation of the mechanical systems. Hamilton described the motion by $2n_{dof}$ independent variables. Therefore, the equations of motion are in terms of $2n_{dof}$ first-order differential equations. It is natural to choose half of the $2n_{dof}$ independent variables to be the independent generalized coordinates q_i, $i = 1, \ldots, n_{dof}$. Owing to the relation $\dot{\mathbf{q}} = d\mathbf{q}/dt$, the generalized velocity vector $\dot{\mathbf{q}}$ depends on $\mathbf{q}$. To obtain the other half of the $2n_{dof}$ independent variables, Hamilton used the Legendre transformation

$$H(\mathbf{q}, \mathbf{p}, t) = \mathbf{p} \cdot \dot{\mathbf{q}} - L(\mathbf{q}, \dot{\mathbf{q}}, t), \tag{4}$$

where Legendre defined the new vector variable $\mathbf{p}$ as

$$\mathbf{p} = \partial_{\dot{\mathbf{q}}} L. \tag{5}$$

The function $H(\mathbf{q}, \mathbf{p}, t)$ is called the Hamiltonian function or brief the hamiltonian. According to definition (5) we refer to the new vector variable $\mathbf{p}$ as the generalized momentum vector. Note that according to Arnold [3] the Legendre transformation requires a convex total kinetic energy T to be unique. This condition is generally fulfilled for scleronomous constrained (natural) systems, of which the total kinetic energy is a positive definite quadratic form in the generalized velocities. Taking into account equation (5), the total differential of the hamiltonian H leads to the canonical equations of Hamilton given by

$$\dot{\mathbf{q}} = \partial_{\mathbf{p}} H, \tag{6}$$

$$\dot{\mathbf{p}} = -\partial_{\mathbf{q}} H. \tag{7}$$

The equation (3) of Lagrange is equivalent to Hamilton's canonical equations (6) and (7) if the condition

$$\partial_t H = -\partial_t L \tag{8}$$

is fulfilled. Note that for scleronomous constrained systems condition (8) is satisfied.

2.2 The conservation of the hamiltonian of natural systems

Natural systems are described by generalized coordinates which do not depend on time explicitly. Furthermore, the generalized forces can be derived from a potential V. Hence the total kinetic energy is a quadratic form with respect to $\dot{\mathbf{q}}$. A lemma on the Legendre transformation of quadratic forms implies that the hamiltonian H of natural systems is the total energy (see Arnold [3]):

$$H = T + V. \tag{9}$$

For a system which hamiltonian does not depend explicitly on time, ie $\partial_t H = 0$, the Hamilton's canonical equations leads to

$$\dot{H} \equiv \partial_t H = 0. \tag{10}$$

Thus the hamiltonian of natural systems is a constant of the motion.

3 The discontinuous Galerkin (dG) method

We deal with the discontinuous Galerkin finite element method within the scope of the Hamiltonian formulation of the equations of motion. Galerkin finite element methods are based on piecewise polynomial approximation. The discontinuous Galerkin method is defined by using discontinuous trial and test functions of degree k; see Eriksson et al. [12]. In the following, we refer to a discontinuous Galerkin method of degree k as the dG(k) method.

We obtain a compact representation of Hamilton's canonical equations (6) and (7) if we introduce the following matrix notation:

$$\mathbf{z} = \begin{bmatrix} \mathbf{q} \\ \mathbf{p} \end{bmatrix}. \tag{11}$$

The variable $\mathbf{z}$ takes the shape of a $2n_{dof} \times 1$ column matrix. The canonical equations are now equivalent to the equation

$$\dot{\mathbf{z}} = \mathbf{J}DH(\mathbf{z}), \tag{12}$$

where $DH(\mathbf{z})$ designates the Jacobian matrix of the hamiltonian H with respect to $\mathbf{z}$ and the skew-symmetric $2n_{dof} \times 2n_{dof}$ hypermatrix $\mathbf{J}$ takes the form

$$\mathbf{J} = \begin{bmatrix} \mathbf{O} & \mathbf{I} \\ -\mathbf{I} & \mathbf{O} \end{bmatrix}. \tag{13}$$

According to Arnold [4] the hypermatrix $\mathbf{J}$ is called the symplectic unit matrix and we refer to equation (12) as Hamilton's canonical equations in symplectic notation; see Goldstein [14]. The matrices $\mathbf{O}$ and $\mathbf{I}$ are the $n_{dof} \times n_{dof}$ zero and identity matrix respectively.

With respect to the initial condition $\mathbf{z}(t_0) = \mathbf{z}_{(0)}$ the equation (12) forms the following initial value problem: find $\mathbf{z} : I_t \to \mathcal{R}^{2n_{dof}}$ such that

$$\begin{cases} \dot{\mathbf{z}}(t) = \mathbf{J}DH(\mathbf{z}(t)) \quad \text{for} \quad t_0 < t \leq T, \\ \mathbf{z}(t_0) = \mathbf{z}_{(0)}, \end{cases} \tag{14}$$

where $I_t = [t_0, t_0 + T]$ denotes the time interval of interest.

To obtain a numerical solution of this initial value problem (14) on the time interval I_t, we perform a discretization in time. For the given interval I_t, we let $t_0 < t_1 < \ldots < t_N$ be a partition of I_t into subintervals $I_n = [t_{n-1}, t_n]$ of length $h_n = t_n - t_{n-1}$, $n = 1, \ldots, N$. In view of a finite element formulation, we introduce a transformation $T_n : t \mapsto \alpha(t)$ to a master element $I_\alpha = [0, 1]$, defined by

$$T_n : \alpha(t) = \frac{t - t_{n-1}}{t_n - t_{n-1}} \equiv \frac{t - t_{n-1}}{h_n}. \tag{15}$$

In other words, we substitute the variable α and the derivative $d(\bullet)/d\alpha$ for the time t and the time derivative $d(\bullet)/dt = h_n^{-1} d(\bullet)/d\alpha$ respectively. Accordingly, the initial value

$k=0$	$M_1 = 1$
$k=1$	$M_1 = 1-\alpha$
	$M_2 = \alpha$
$k=2$	$M_1 = (2\alpha-1)(\alpha-1)$
	$M_2 = -4\alpha(\alpha-1)$
	$M_3 = \alpha(2\alpha-1)$
$k=3$	$M_1 = -\frac{9}{2}(\alpha-\frac{1}{3})(\alpha-\frac{2}{3})(\alpha-1)$
	$M_2 = \frac{27}{2}\alpha(\alpha-\frac{2}{3})(\alpha-1)$
	$M_3 = -\frac{27}{2}\alpha(\alpha-\frac{1}{3})(\alpha-1)$
	$M_4 = \frac{9}{2}\alpha(\alpha-\frac{1}{3})(\alpha-\frac{2}{3})$

Table 1: Lagrange basis functions $M_I(\alpha)$ of polynomial degree $0 \leq k \leq 3$.

problem on the master element I_α reads: find $\mathbf{z} : I_\alpha \to \mathcal{R}^{2n_{dof}}$ such that

$$\begin{cases} \mathbf{z}'(\alpha) = h_n \mathbf{J} DH(\mathbf{z}(\alpha)) \quad \text{for} \quad 0 < \alpha \leq 1, \\ \mathbf{z}(0) = \mathbf{z}_0, \end{cases} \tag{16}$$

where the prime indicates differentiation with respect to α: $(\bullet)' = d(\bullet)/d\alpha$.
With regard to the discontinuous Galerkin method, in the following we search for an approximate solution of the initial value problem (16) in the space of polynomials. Let $\mathcal{P}^k(0,1)^{2n_{dof}}$ denote the space of $2n_{dof}$-dimensional polynomials of degree k on the interval I_α which in general take the form $\mathbf{z}^h(\alpha) = \sum_{I=1}^{k+1} c_I \alpha^I$. However, as basis of $\mathcal{P}^k(0,1)^{2n_{dof}}$, we choose the Lagrange basis $\{M_I\}_{I=1}^{k+1}$ associated to the distinct $k+1$ nodes $\alpha_1 < \alpha_2 < \ldots < \alpha_{k+1}$ in I_α, determined by the requirement that $M_I(\alpha_J) = \delta_{IJ}$, the Kronecker delta. The explicit expression for the basis function M_I is

$$M_I(\alpha) \;=\; \prod_{\substack{J=1 \\ J \neq I}}^{k+1} \frac{\alpha - \alpha_J}{\alpha_I - \alpha_J}, \quad 1 \leq I \leq k+1. \tag{17}$$

We refer to Table 1 for examples involving Lagrange basis functions $M_I(\alpha)$ of polynomial degree $0 \leq k \leq 3$.

Remark 3.1 *In respect to the definition of the nodal basis, the case $k = 0$ corresponds to the case with only one node α_1. Thus in equation (17) the indices I and J are equal. Hence at the first sight the definition (17) does not hold for this case since $I \neq J$ is required. However, that equation (17) for arbitrary k holds, the sense of the restriction $I \neq J$ in equation (17) implies that $(\alpha - \alpha_J)/(\alpha_I - \alpha_J)$ is equal to one if $I = J$ for arbitrary k. Therefore, we obtain in equation (17) at the case $k = 0$ the nodal shape function $M_1 = 1$.*

Figure 1: The jump in the approximate solution on the master element I_α; eg k=1.

The polynomial $\mathbf{z}^h(\alpha) \in \mathcal{P}^k(0,1)^{2n_{dof}}$ has the value $\mathbf{z}_I = \mathbf{z}^h(\alpha_I)$ at the nodes α_I, $I = 1, \ldots, k+1$. Hence the polynomial $\mathbf{z}^h(\alpha)$ may be expressed in terms of the corresponding Lagrange basis as

$$\mathbf{z}^h(\alpha) = \sum_{I=1}^{k+1} M_I(\alpha)\, \mathbf{z}_I, \tag{18}$$

so that the values $\{\mathbf{z}^h(\alpha_I)\}_{I=1}^{k+1}$ are the coefficients of $\mathbf{z}^h(\alpha)$ with respect to the Lagrange basis. Note that we also refer to the Lagrange basis and the Lagrange basis functions as a nodal basis and the nodal shape functions respectively. Now we may formulate the dG(k) approximation for the initial value problem (16) as follows: find a trial function $\mathbf{z}^h \in \mathcal{P}^k(0,1)^{2n_{dof}}$ such that

$$\int_0^1 \mathbf{J}\delta\mathbf{z}^h \cdot \left[\left(\mathbf{z}^h\right)' - h_n \mathbf{J} DH(\mathbf{z}^h)\right] d\alpha + \mathbf{J}\delta\mathbf{z}_1 \cdot [\mathbf{z}^h]_0 = 0, \tag{19}$$

for all test functions $\delta\mathbf{z}^h \in \mathcal{P}^k(0,1)^{2n_{dof}}$, where $[\mathbf{z}^h]_0 = \mathbf{z}_1 - \mathbf{z}_0$ denotes the amount of a jump at $\alpha = 0$. Within the scope of a finite element formulation, let $\mathbf{z}^h(\alpha = 0^-) \equiv \mathbf{z}_0$ and $\mathbf{z}_1 = \mathbf{z}^h(\alpha = 0^+)$ denote the limit at $\alpha = 0$ on the left and on the right respectively; cf Figure 1. We also refer to the equation (19) as the weak form of the initial value problem (16).

In this method the trial and test spaces are the same. To prevent that the nodal values $\mathbf{z}_I$ of the trial function are over-determined, we give up the requirement that $\mathbf{z}^h$ satisfies the initial condition $\mathbf{z}_0$ exactly. Instead, the initial condition is satisfied weakly because of the presence of the term $\mathbf{J}\,\delta\mathbf{z}_1 \cdot [\mathbf{z}^h]_0$. For that reason, we get a jump $[\mathbf{z}^h]_0$ in the master element I_α.

The test function $\delta\mathbf{z}^h$ is also an element of the space $\mathcal{P}^k(0,1)^{2n_{dof}}$ such that it takes the form given in (18):

$$\delta\mathbf{z}^h(\alpha) = \sum_{I=1}^{k+1} M_I(\alpha)\, \delta\mathbf{z}_I. \tag{20}$$

Further, the nodal shape functions $M_I(\alpha)$ take the form (17). Now we obtain the derivative of the trial function (18) with respect to α as follows:

$$\left(\mathbf{z}^h\right)'(\alpha) = \sum_{I=1}^{k+1} M_I'(\alpha)\,\mathbf{z}_I. \tag{21}$$

Next we introduce the equations (20) and (21) into the weak form (19). With regard to the arbitrariness of the $\delta\mathbf{z}_I$ on each subinterval I_n, we get the following set of algebraic equations:

$$\sum_{J=1}^{k+1} \int_0^1 M_I M_J' d\alpha\,\mathbf{z}_J - h_n \int_0^1 M_I \mathbf{J} DH(\mathbf{z}^h) d\alpha + \delta_{I1}[\mathbf{z}^h]_0 = \mathbf{0}, \tag{22}$$

for $I = 1, \ldots, k+1$, where we introduced the Kronecker delta δ_{I1} owing to the identity $\delta\mathbf{z}_1 = \delta_{I1}\delta\mathbf{z}_I$. Henceforth $\mathbf{0}$ denotes a column zero matrix which has, with a few exceptions, the dimensions $2n_{dof} \times 1$.
With the $k+1$ equations in (22), we obtain a family of implicit multi-level one-step schemes of which we define a specific member by the selection of the polynomial degree k and a specific quadrature rule for evaluation of the integrals in (22).

4 The algorithmic hamiltonian of the dG method

In this section we give a proof for the decay of the hamiltonian H provided that particular conditions hold; also see Bauchau & Joo [5]. Let us consider the weak form (19):

$$\int_0^1 \mathbf{J}\delta\mathbf{z}^h \cdot \left[\left(\mathbf{z}^h\right)' - h_n \mathbf{J} DH(\mathbf{z}^h)\right] d\alpha + \mathbf{J}\delta\mathbf{z}_1 \cdot [\mathbf{z}^h]_0 = 0.$$

First we choose the test space such that the following condition holds

$$\delta\mathbf{z}^h = \mathbf{J}^{-1} DH(\mathbf{z}^h). \tag{23}$$

Taking into account equation (23) the weak form leads to

$$\int_0^1 DH(\mathbf{z}^h) \cdot \left(\mathbf{z}^h\right)' d\alpha - h_n \int_0^1 DH(\mathbf{z}^h) \cdot \mathbf{J} DH(\mathbf{z}^h) d\alpha + DH(\mathbf{z}_1) \cdot [\mathbf{z}^h]_0 = 0. \tag{24}$$

On account of the form of the symplectic matrix $\mathbf{J}$ the bilinear form $DH(\mathbf{z}^h) \cdot \mathbf{J} DH(\mathbf{z}^h)$ vanishes (cf Betsch & Steinmann [8]) and equation (24) can be written as

$$\int_0^1 DH(\mathbf{z}^h) \cdot \left(\mathbf{z}^h\right)' d\alpha + DH(\mathbf{z}_1) \cdot [\mathbf{z}^h]_0 = 0. \tag{25}$$

We now use the Fundamental Theorem of Calculus to evaluate the integral (cf Betsch & Steinmann [8]):

$$\int_0^1 DH(\mathbf{z}^h) \cdot \left(\mathbf{z}^h\right)' d\alpha = H(\mathbf{z}_{k+1}) - H(\mathbf{z}_1), \tag{26}$$

where $\mathbf{z}_{k+1}$ denotes the nodal value of H at the node $k+1$. Employing equation (26) in equation (25) leads to

$$H(\mathbf{z}_{k+1}) - H(\mathbf{z}_1) + DH(\mathbf{z}_1) \cdot [\mathbf{z}^h]_0 = 0. \tag{27}$$

Note that we refer to $H_i = H(\mathbf{z}_i)$, $i = 0, \ldots, k+1$, as the algorithmic hamiltonian at the ith node of the master element I_α. Furthermore, we may write the algorithmic hamiltonian H_0 by means of Taylor's theorem in the following form:

$$H_0 = H(\mathbf{z}_0) \equiv H(\mathbf{z}_1 - [\mathbf{z}^h]_0) = H(\mathbf{z}_1) - DH(\mathbf{z}_1) \cdot [\mathbf{z}^h]_0 + \frac{1}{2}\mathcal{H}_\xi [\mathbf{z}^h]_0 \cdot [\mathbf{z}^h]_0, \tag{28}$$

where $\mathcal{H}_\xi \equiv D^2 H(\mathbf{z}_\xi)$ denotes the Hessian matrix of the hamiltonian H at $\mathbf{z}_\xi$ with $\mathbf{z}_\xi \in [\mathbf{z}_0, \mathbf{z}_1]$; see eg Apostol [1]. We substitute equation (27) for $H(\mathbf{z}_1)$ in equation (28) and obtain

$$H_{k+1} - H_0 = -\frac{1}{2}\mathcal{H}_\xi [\mathbf{z}^h]_0 \cdot [\mathbf{z}^h]_0. \tag{29}$$

Accordingly, the behavior of the algorithmic hamiltonian H_{k+1} depends on the definiteness of the Hessian matrix $\mathcal{H}_\xi$:

$$\begin{cases} H_{k+1} - H_0 < 0, & \text{for } \mathcal{H}_\xi \text{ positive definite.} \\ H_{k+1} - H_0 = 0, & \text{for } [\mathbf{z}^h]_0 = 0 \text{ or } \mathcal{H}_\xi \text{ indefinite.} \\ H_{k+1} - H_0 > 0, & \text{for } \mathcal{H}_\xi \text{ negative definite.} \end{cases} \tag{30}$$

Therefore, a positive definite Hessian matrix $\mathcal{H}_\xi$ leads to a decay of the algorithmic hamiltonian H_{k+1}, negative definiteness implies growth of the algorithmic hamiltonian H_{k+1} and apart from vanishing of the jumps, according to Zurmühl & Falk [35] only an indefinite Hessian matrix $\mathcal{H}_\xi$ may end up in a conservation of the algorithmic hamiltonian H_{k+1}.
For this proof to hold: (i) the test space condition (23) and (ii) the Fundamental Theorem of Calculus has to be fulfilled. Note that the test space condition is generally fulfilled for the dG(0) method. Moreover, we will see in the sections below that the condition (ii) is for the dG(0) method also fulfilled if interpolating quadrature rules according to Isaacson & Keller [21] are used.

Remark 4.1 *For instance, a convex hamiltonian fulfills the condition*

$$H(\boldsymbol{z}_1) - H(\boldsymbol{z}_0) < DH(\boldsymbol{z}_1) \cdot [\boldsymbol{z}^h]_0; \tag{31}$$

see Apostol *[2]. Therefore, according to equation (27) a convex hamiltonian leads to a decay of the algorithmic hamiltonian H_{k+1}.*

Part II
The Circular Pendulum

The first considered natural system is a planar circular pendulum consisting of a particle of mass m suspended by a massless rod of length l and moving in a constant gravitational field $\mathbf{F} = m\,\mathbf{g}$, where $\mathbf{g}$ denotes the gravitational acceleration vector; see Figure 2. The generalized coordinate q of this system with $n_{dof} = 1$ degree is the clockwise rotation angle.
We apply the dG(0) and dG(1) method to determine linear motions (harmonic oscillations) and arbitrary (nonlinear) motions. We are particularly interested in algorithmic conservation properties. With this in mind, we investigate the conservation of the hamiltonian H, ie the total energy of the system, and the total angular momentum $\mathbf{L}$.

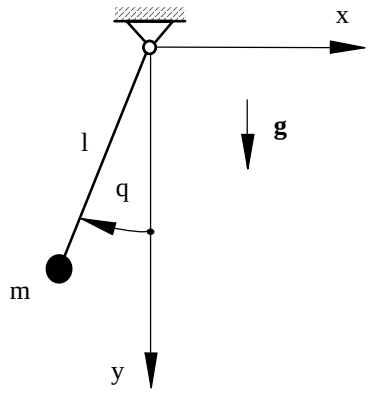

Figure 2: The planar circular pendulum.

5 The conservation of total angular momentum

Here we introduce the law of conservation of total angular momentum of only one particle according to Goldstein [14]. We consider the motion of a particle of mass m in the three-dimensional euclidean space $\mathcal{E}^3$ relating to an inertial cartesian coordinate system with the origin $\mathcal{O}$.
The total angular momentum, denoted by $\mathbf{L}$, is defined as

$$\mathbf{L} = \mathbf{r} \times \mathbf{P}, \tag{32}$$

where $\mathbf{r}$ and $\mathbf{P} = m\,\dot{\mathbf{r}}$ denote the radius vector of the particle with respect to O and the total linear momentum respectively. The total torque about O, we define as

$$\mathbf{N} = \mathbf{r} \times \mathbf{F}, \tag{33}$$

where $\mathbf{F} = \dot{\mathbf{P}}$ is the total force (Newton's Second Law of Motion). Therefore, we may write the total torgue as

$$\mathbf{N} = \mathbf{r} \times \frac{d}{dt} (m \dot{\mathbf{r}}) . \tag{34}$$

On the other hand, the product rule of differentiation implies

$$\frac{d}{dt} (\mathbf{r} \times m \dot{\mathbf{r}}) = \dot{\mathbf{r}} \times m \dot{\mathbf{r}} + \mathbf{r} \times \frac{d}{dt} (m \dot{\mathbf{r}}) . \tag{35}$$

The first term on the right vanishes on grounds of the cross product of two parallel vectors. In consequence of the identity (35), according to equation (34), we may write

$$\mathbf{N} = \frac{d}{dt} (\mathbf{r} \times m \dot{\mathbf{r}}) \equiv \dot{\mathbf{L}}. \tag{36}$$

Owing to equation (36), we establish the following

Theorem 5.1 *If the total torgue* $\boldsymbol{N}$ *vanishes then the total angular momentum* $\boldsymbol{L}$ *is conserved.* □

6 A time finite element formulation for the harmonic oscillator

Here we investigate the algorithmic conservation properties of the dG(0) and dG(1) method at the motion of the circular pendulum for small amplitudes (harmonic oscillations). Harmonic oscillations occur for a linear restoring force $Q = -c\,q$ with $c = m\,g\,l$, where g is the gravitational acceleration. Hence it follows that the potential $V(q)$ takes the form

$$V(q) = \frac{1}{2}\,c\,q^2. \tag{37}$$

The total kinetic energy of the particle is $T = \frac{1}{2}\,I\,\dot{q}^2$, with $I = m\,l^2$ the moment of inertia so that the lagrangian L is

$$L(q, \dot{q}) \equiv T(\dot{q}) - V(q) = \frac{1}{2}\,I\,\dot{q}^2 - \frac{1}{2}\,c\,q^2. \tag{38}$$

However, to obtain the time-stepping schemes we need the hamiltonian in symplectic notation. According to equation (5) we get the generalized momentum p as

$$p \equiv \partial_{\dot{q}} L = I\,\dot{q}. \tag{39}$$

Next we substitute in the total kinetic energy T the generalized momentum p for the generalized velocity $\dot{q}$ such that the hamiltonian H, being equal to the total energy of the system, takes the form

$$H(q, p) \equiv T(p) + V(q) = \frac{1}{2\,I}\,p^2 + \frac{1}{2}\,c\,q^2. \tag{40}$$

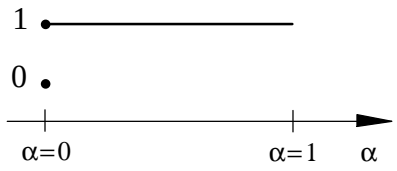

Figure 3: The master element I_α of the dG(0) method.

We see that the total kinetic energy T and the potential V are quadratic forms so that the hamiltonian H takes a quadratic form in symplectic notation. With $\mathbf{z} = [q,\, p]^T$ equation (40) yields

$$H = \frac{1}{2}\,\mathbf{z}^T\,\mathbf{H}\,\mathbf{z}, \tag{41}$$

where $\mathbf{H}$ is the following $2n_{dof} \times 2n_{dof}$ matrix

$$\mathbf{H} = \begin{bmatrix} c & 0 \\ 0 & 1/I \end{bmatrix}. \tag{42}$$

According to Zurmühl & Falk [35] we obtain the Jacobian matrix $DH(\mathbf{z})$ owing to equation (41) with the differentiation rule of quadratic forms:

$$DH(\mathbf{z}) = \mathbf{H}\,\mathbf{z}. \tag{43}$$

6.1 Constant time finite elements

We apply the algebraic equations (22) to get the time-stepping scheme for constant time finite elements (k=0), where $\mathbf{z}^h = \mathbf{z}_1$ is the trial function; also see Figure 3. For $k = 0$, we get only one equation because the indices are $I = J = 1$:

$$\int_0^1 M_1 M_1' d\alpha\, \mathbf{z}_1 - h_n \int_0^1 M_1 \mathbf{J} DH(\mathbf{z}^h) d\alpha + [\mathbf{z}^h]_0 = \mathbf{0}. \tag{44}$$

According to Table 1 the single nodal shape function is $M_1 = 1$. Hence, the derivative of M_1 with respect to α is zero. Accordingly, the first integral in equation (44) vanishes so that the time-stepping scheme may be written as:

$$\mathbf{z}_1 - \mathbf{z}_0 - h_n \int_0^1 \mathbf{J} DH(\mathbf{z}^h) d\alpha = \mathbf{0}. \tag{45}$$

We refer to equation (45) as the general dG(0) method for Hamilton's canonical equations.

6.1.1 Exact quadrature

With regard to equation (43) and taking into account $\mathbf{z}^h = \mathbf{z}_1$ according to equation (18), the time-stepping scheme may be written as

$$(\mathbf{1} - h_n \, \mathbf{JH}) \, \mathbf{z}_1 = \mathbf{z}_0, \tag{46}$$

where $\mathbf{1}$ denotes the $2n_{dof} \times 2n_{dof}$ identity matrix. Therefore, the time-stepping scheme takes the shape of a system of linear algebraic equations which can be directly solved with the given initial condition $\mathbf{z}_0$.

Remark 6.1 *The form of equation (45) is equivalent to the form which we obtain with the general cG(1) method (cf* Betsch & Steinmann *[8]):*

$$\boldsymbol{z}_2 - \boldsymbol{z}_1 - h_n \int_0^1 \boldsymbol{J} DH(\boldsymbol{z}^h) d\alpha = \boldsymbol{0}. \tag{47}$$

The difference lies in the trial function so that the time-stepping scheme generated by the cG(1) method with an exactly evaluated integral is given by

$$\left(\boldsymbol{1} - \frac{1}{2} h_n \, \boldsymbol{JH} \right) \boldsymbol{z}_2 - \left(\boldsymbol{1} + \frac{1}{2} h_n \, \boldsymbol{JH} \right) \boldsymbol{z}_1 = \boldsymbol{0}, \tag{48}$$

where $\boldsymbol{z}_2$ and $\boldsymbol{z}_1$ denote the nodal values of the linear trial function at $\alpha = 1$ and $\alpha = 0$ respectively.

This linear algebraic system is used to solve by direct methods based on Gaussian elimination; see eg Eriksson et al. [12]. In view of the solution of nonlinear algebraic systems, we implemented the Newton-Raphson method; see Table 2. The application of the Newton-Raphson method to a linear algebraic system does not prove disadvantageous for the cost of computing because the Newton-Raphson method solves in each iteration step the linearized system by a Gaussian elimination. Therefore, the Newton-Raphson method need one iteration for solving equation (46).

Numerical Example 6.1 *We take a length of the rod so that a harmonic solution with a period $T = 5$ occurs. Furthermore, let be the mass $m = 2$ and the gravitational acceleration $g = 9.81$. As initial condition, we take the vector $\boldsymbol{z}(t = 0) = [-0.1, 0]^T$. Figure 4 shows the course of the rotation angle $q = q(t)$ for a time step size $h_n = 0.1$ ($dt = 0.1$). We see that the dG(0) method leads to an asymptotic annihilation of the amplitude of the rotation angle. Thus with respect to a damped harmonic oscillator, we can conclude that the energy decays. This behavior is called algorithmic damping or numerical dissipation. The bullets on the solid line of the dG(0) method denote the nodes on each subinterval I_n, ie the nodes 0 and 1 with respect to the master element I_α; see Figure 3. The dotted line represents the reference curve which is computed with the continuous Galerkin method with linear trial functions (cG(1) method). On grounds of the continuous trial functions, the cG(1) method has also in the master element one unknown node. According to* Betsch & Steinmann *[7, 8, 9] the cG(k) method is energy conserving. Therefore, the amplitude is constant. Of course, the asymptotic annihilation also affects the amplitude of the generalized momentum p computed with the dG(1) method; see Figure 5.*

Given: initial condition $\mathbf{z}_0$, time step size h_n and residual tolerance $\epsilon = 10^{-13}$ set iteration counter $l = 1$
Find: nodal unknown $\mathbf{z}_1$
(a) compute residual vector $\mathbf{R}^{(l)} = (\mathbf{1} - h_n \mathbf{JH})\, \mathbf{z}_1^{(l)} - \mathbf{z}_0$ if $\|\mathbf{R}^{(l)}\| > \epsilon$ goto (b) else goto (c) (b) compute tangent $\mathbf{K}_T^{(l)} \equiv \partial_{\mathbf{z}_1} \mathbf{R}(\mathbf{z}_1^{(l)}) = (\mathbf{1} - h_n \mathbf{JH})$ solve for increment $\Delta\, \mathbf{z}_1^{(l)}$ $\Delta\, \mathbf{z}_1^{(l)} = -\left(\mathbf{K}_T^{(l)}\right)^{-1} \mathbf{R}^{(l)}$ update the nodal unknown $\mathbf{z}_1^{(l+1)} = \mathbf{z}_1^{(l)} + \Delta\, \mathbf{z}_1^{(l)}$ goto (a) with $l = l + 1$ (c) end.

Table 2: Newton-Raphson method to solve the dG(0) time-stepping scheme for linear motions.

6.1.2 The use of specific quadrature rules

We concern for two reasons quadrature rules within the scope of the discontinuous Galerkin finite element method: In general, it can be difficult to evaluate the integrals exactly such that quadrature rules are often used to compute finite integrals approximately. Second, with quadrature rules used for computation of the integrals in the dG(k) methods, we obtain implicit multi-level one-step schemes; for example, according to Lasaint & Raviart [27] the discrete dG(k) method is equivalent to a specific implicit Runge-Kutta method. In view of the second reason, this subsection deals with the influence of quadrature rules on the dG(0) method for the harmonic oscillator. Owing to equation (45), the general dG(0) method is given by

$$\mathbf{z}_1 - \mathbf{z}_0 - h_n \int_0^1 \mathbf{J} DH(\mathbf{z}^h) d\alpha = \mathbf{0}. \tag{49}$$

Employing equation (43) and the trial function $\mathbf{z}^h = \mathbf{z}_1$, we get

$$\mathbf{z}_1 - \mathbf{z}_0 - h_n\, \mathbf{J}\, \mathbf{H}\, \mathbf{z}_1 \int_0^1 d\alpha = \mathbf{0}. \tag{50}$$

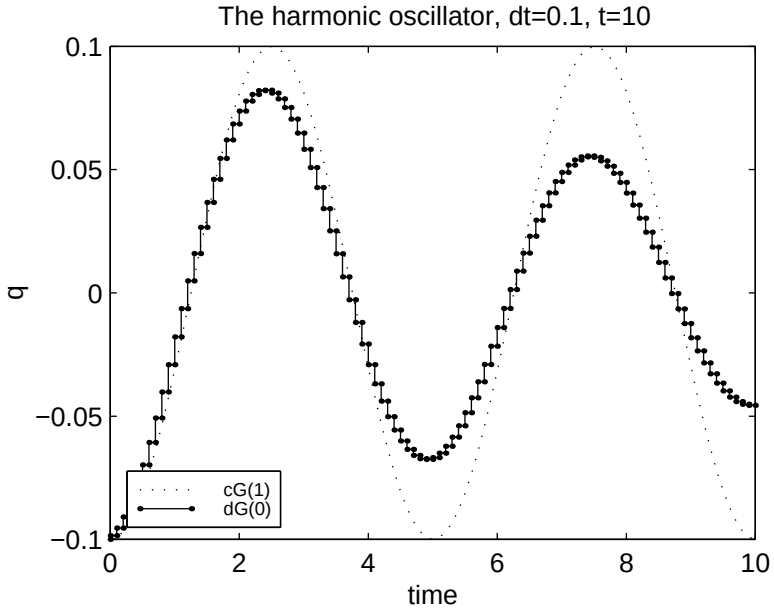

Figure 4: Rotation angle $q = q(t)$ of a harmonic oscillator with a period $T = 5$, mass $m = 2$ and gravitational acceleration $g = 9.81$. Computed with the dG(0) method with $h_n = 0.1$.

According to Isaacson & Keller [21] we approximate the integral with so-called interpolating quadrature rules defined as

$$\int_0^1 f(\alpha)d\alpha \approx \sum_{l=1}^{N_q} f(\alpha_l)\, w_l, \tag{51}$$

such that equation (50) takes the form

$$\mathbf{z}_1 - \mathbf{z}_0 - h_n\, \mathbf{J}\, \mathbf{H}\, \mathbf{z}_1 \sum_{l=1}^{N_q} w_l = \mathbf{0}, \tag{52}$$

where N_q denotes the number of quadrature points, and w_l and α_l denote the weights and abscissae for I_α respectively. When the quadrature rule fulfills the condition

$$\sum_{l=1}^{N_q} w_l = 1, \tag{53}$$

the time-stepping scheme (52) is identical with the scheme (46) emanating from exact quadrature in the previous subsection. In fact, this condition is fulfilled by all quadrature rules which are interpolated. In this connection, we investigate the midpoint rule, the trapezoidal rule and Gaussian quadrature rules. Therefore, we also obtain with this quadrature rules the time-stepping scheme (46).

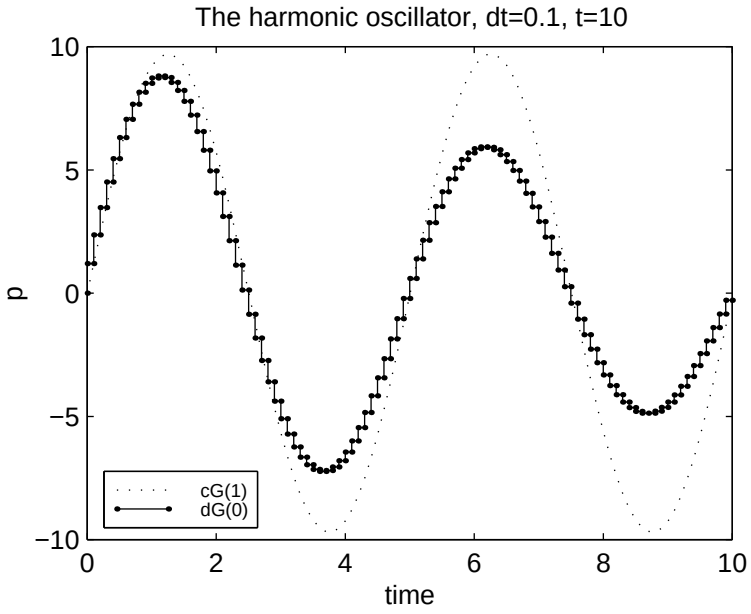

Figure 5: Generalized momentum $p = p(t)$ of a harmonic oscillator with a period $T = 5$, mass $m = 2$ and gravitational acceleration $g = 9.81$. Computed with the dG(0) method with $h_n = 0.1$.

6.2 Linear time finite elements

The application of the equations (22) with $k = 1$ leads to the dG(1) time-stepping scheme for the harmonic oscillator. Here we obtain the following two linear nodal shape functions (cf Table 1): $M_1 = 1 - \alpha$ and $M_2 = \alpha$. Therefore, the trial function $\mathbf{z}^h$ is as follows:

$$\mathbf{z}^h(\alpha) = (1 - \alpha)\ \mathbf{z}_1 + \alpha\, \mathbf{z}_2. \tag{54}$$

The trial function is a linear function in the nodes 1 and 2; cf Figure 1. The time-stepping scheme consists of two algebraic equations. Choosing the index $I = 1, 2$, we get

$$\int_0^1 M_1 M_1' d\alpha\, \mathbf{z}_1 + \int_0^1 M_1 M_2' d\alpha\, \mathbf{z}_2 - h_n \int_0^1 M_1 \mathbf{J} DH(\mathbf{z}^h) d\alpha + [\mathbf{z}^h]_0 = \mathbf{0}, \tag{55}$$

$$\int_0^1 M_2 M_1' d\alpha\, \mathbf{z}_1 + \int_0^1 M_2 M_2' d\alpha\, \mathbf{z}_2 - h_n \int_0^1 M_2 \mathbf{J} DH(\mathbf{z}^h) d\alpha = \mathbf{0}. \tag{56}$$

With regard to the derivatives of the nodal shape functions with respect to α, $M_1' = -1$ and $M_2' = 1$, the first two integrals will be integrated exactly such that the equations (55) and (56) yield the general dG(1) method for Hamilton's canonical equations:

$$\frac{1}{2}\, \mathbf{z}_2 + \frac{1}{2}\, \mathbf{z}_1 - \mathbf{z}_0 - h_n \int_0^1 M_1 \mathbf{J} DH(\mathbf{z}^h) d\alpha = \mathbf{0}, \tag{57}$$

$$\frac{1}{2}\, \mathbf{z}_2 - \frac{1}{2}\, \mathbf{z}_1 - h_n \int_0^1 M_2 \mathbf{J} DH(\mathbf{z}^h) d\alpha = \mathbf{0}. \tag{58}$$

Remark 6.2 *The form of the equations (57) and (58) of the general dG(1) method for the canonical equations of Hamilton and the corresponding equations of the general cG(2) method only differ in the coefficients of the nodal values (see* Betsch & Steinmann *[7, 9]):*

$$\frac{1}{6}\, \boldsymbol{z}_3 + \frac{2}{3}\, \boldsymbol{z}_2 - \frac{5}{6}\, \boldsymbol{z}_1 - h_n \int_0^1 \tilde{M}_1 \boldsymbol{J} DH(\boldsymbol{z}^h) d\alpha = \boldsymbol{0}, \tag{59}$$

$$\frac{5}{6}\, \boldsymbol{z}_3 - \frac{2}{3}\, \boldsymbol{z}_2 - \frac{1}{6}\, \boldsymbol{z}_1 - h_n \int_0^1 \tilde{M}_2 \boldsymbol{J} DH(\boldsymbol{z}^h) d\alpha = \boldsymbol{0}, \tag{60}$$

where $\boldsymbol{z}^h$ is the corresponding trial function of the cG(2) method plus the reduced shape functions $\tilde{M}_1 = 1 - \alpha$ and $\tilde{M}_2 = \alpha$.

6.2.1 Exact quadrature

Owing to the linear form of equation (43), the employment of the trial function (54) leads to the possibility of an exact evaluation of the integrals. Therefore, the time-stepping scheme takes the following form:

$$\frac{1}{2} \left(\mathbf{1} - \frac{1}{3}\, h_n\, \mathbf{J}\, \mathbf{H} \right) \mathbf{z}_2 + \frac{1}{2} \left(\mathbf{1} - \frac{2}{3}\, h_n\, \mathbf{J}\, \mathbf{H} \right) \mathbf{z}_1 - \mathbf{z}_0 = \mathbf{0}, \tag{61}$$

$$\frac{1}{2} \left(\mathbf{1} - \frac{2}{3}\, h_n\, \mathbf{J}\, \mathbf{H} \right) \mathbf{z}_2 - \frac{1}{2} \left(\mathbf{1} + \frac{1}{3}\, h_n\, \mathbf{J}\, \mathbf{H} \right) \mathbf{z}_1 = \mathbf{0}. \tag{62}$$

Given: initial condition $\mathbf{z}_0$, time step size h_n and residual tolerance $\epsilon = 10^{-13}$ set iteration counter $l = 1$
Find: nodal unknowns $\mathbf{z}_1$ and $\mathbf{z}_2$
(a) compute residual vector $\mathbf{R}^{(l)} = \mathbf{R}(\mathbf{x}^{(l)})$ if $\|\mathbf{R}^{(l)}\| > \epsilon$ goto (b) else goto (c) (b) compute tangent $\mathbf{K}_T^{(l)} = \mathbf{K}_T(\mathbf{x}^{(l)})$ solve for increment $\Delta\,\mathbf{x}^{(l)}$ $\Delta\,\mathbf{x}^{(l)} = -\left(\mathbf{K}_T^{(l)}\right)^{-1}\mathbf{R}^{(l)}$ update the nodal unknowns $\mathbf{x}^{(l+1)} = \mathbf{x}^{(l)} + \Delta\,\mathbf{x}^{(l)}$ goto (a) with $l = l + 1$ (c) end.

Table 3: Newton-Raphson method to solve the time-stepping scheme generated by the dG(1) method.

We also apply the Newton-Raphson method to solve the time-stepping scheme (61), (62). Therefore, we have to determine the residual vector $\mathbf{R}(\mathbf{x})$ which reads:

$$\mathbf{R}(\mathbf{x}) \equiv \frac{1}{2}\begin{bmatrix} \mathbf{1} - \frac{2}{3}\,h_n\,\mathbf{J}\,\mathbf{H} & \mathbf{1} - \frac{1}{3}\,h_n\,\mathbf{J}\,\mathbf{H} \\ -\mathbf{1} - \frac{1}{3}\,h_n\,\mathbf{J}\,\mathbf{H} & \mathbf{1} - \frac{2}{3}\,h_n\,\mathbf{J}\,\mathbf{H} \end{bmatrix}\mathbf{x} - \begin{bmatrix} \mathbf{z}_0 \\ \mathbf{0} \end{bmatrix} = \begin{bmatrix} \mathbf{0} \\ \mathbf{0} \end{bmatrix}, \tag{63}$$

where $\mathbf{x} = [\mathbf{z}_1^T\,\mathbf{z}_2^T]^T$ is the unknown vector. Accordingly, the tangent $\mathbf{K}_T = \partial_{\mathbf{x}}\mathbf{R}(\mathbf{x})$ takes the following shape:

$$\mathbf{K}_T = \frac{1}{2}\begin{bmatrix} \mathbf{1} - \frac{2}{3}\,h_n\,\mathbf{J}\,\mathbf{H} & \mathbf{1} - \frac{1}{3}\,h_n\,\mathbf{J}\,\mathbf{H} \\ -\mathbf{1} - \frac{1}{3}\,h_n\,\mathbf{J}\,\mathbf{H} & \mathbf{1} - \frac{2}{3}\,h_n\,\mathbf{J}\,\mathbf{H} \end{bmatrix}. \tag{64}$$

We summarize the Newton-Raphson method for the time-stepping scheme generated by the dG(1) method for the harmonic oscillator in Table 3.

Numerical Example 6.2 *To give a direct comparison of the dG(0) and dG(1) method, we compute in this example the same harmonic oscillator as in Example 6.1. For this reason, we choose again the length of the rod so that an oscillation with a period $T = 5$ occurs. Further, the mass is $m = 2$ and the gravitational acceleration is $g = 9.81$. The initial condition is the matrix $\boldsymbol{z}(t = 0) = [-0.1, 0]^T$. The reference solution is provided by the cG(2) method with quadratic trial functions and thus two unknown nodes, too. In Figure 6, the phase plane of the harmonic oscillator is shown only for three time steps*

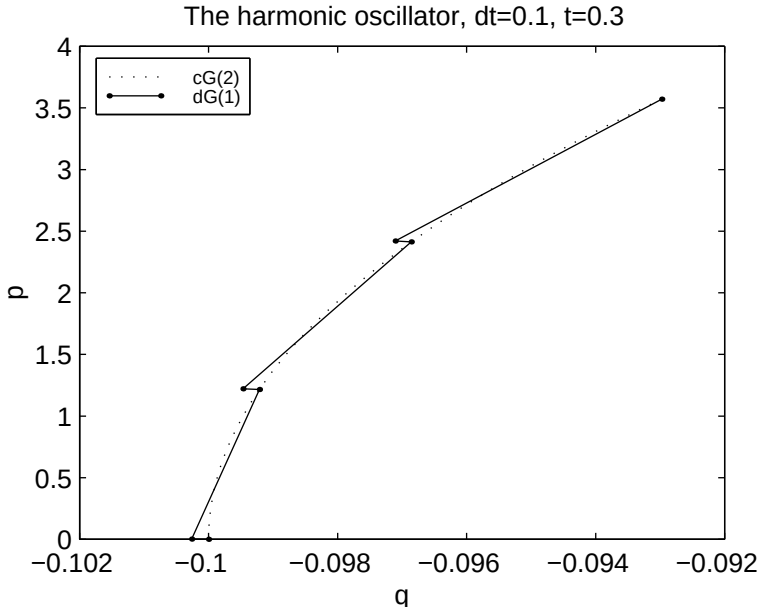

Figure 6: Phase plane of a harmonic oscillator with a period $T = 5$, mass $m = 2$ and gravitational acceleration $g = 9.81$. Computed with the dG(1) method with $h_n = 0.1$.

with a time step size $h_n = 0.1$ ($dt = 0.1$). In this brief time interval, we are able to see the jumps. In addition, we are able to see that in each subinterval the amount of $[p^h]_0$ is smaller than the amount of $[q^h]_0$. Figure 7 depicts the calculated phase plain corresponding to one complete period ($T = 5$). We see that in each subinterval the jump $[\boldsymbol{z}^h]_0$ has a minor amount. For the harmonic oscillator at hand, only considering a very long time interval demonstrates the algorithmic damping of the dG(1) method.

6.2.2 The use of specific quadrature rules

Here we investigate the dG(1) method (57), (58) for the harmonic oscillator with application of interpolating quadrature rules. For example, we have implemented the midpoint rule, trapezoidal rule and Gaussian quadrature rules.
The trial function (54) employed in equation (43) yields

$$DH(\mathbf{z}^h) = \mathbf{H}\,(M_1\,\mathbf{z}_1 + M_2\,\mathbf{z}_2)\,. \tag{65}$$

Thus the expansion of the integral of equation (57) results in

$$\int_0^1 M_1 \mathbf{J} DH(\mathbf{z}^h) d\alpha = \mathbf{JH}\left(\int_0^1 M_1^2(\alpha) d\alpha\,\mathbf{z}_1 + \int_0^1 M_1\,M_2 d\alpha\,\mathbf{z}_2\right). \tag{66}$$

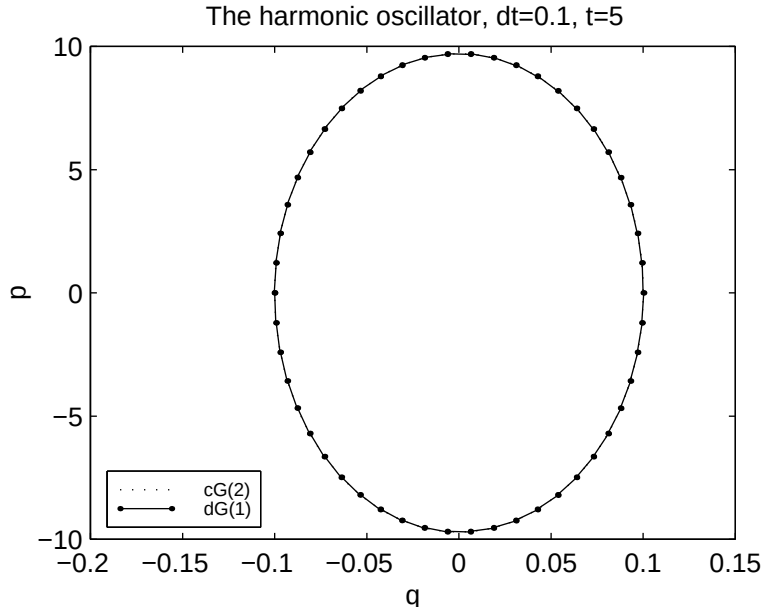

Figure 7: Phase plane of a harmonic oscillator with a period $T = 5$, mass $m = 2$ and gravitational acceleration $g = 9.81$. Computed with the dG(1) method with $h_n = 0.1$.

Therefore, the interpolating quadrature formula (51) leads to the following expression:

$$\int_0^1 M_1 \mathbf{J} DH(\mathbf{z}^h) d\alpha \approx \mathbf{JH} \left(\beta_{11}\, \mathbf{z}_1 + \beta_{12}\, \mathbf{z}_2\right), \tag{67}$$

where

$$\beta_{ij} = \sum_{l=1}^{N_q} M_i(\alpha_l)\, M_j(\alpha_l)\, w_l, \qquad i, j \in \{1, \ldots, k+1\}. \tag{68}$$

In the same way, we approximate the integral of equation (58) by the quadrature formula (51) and obtain

$$\int_0^1 M_2 \mathbf{J} DH(\mathbf{z}^h) d\alpha \approx \mathbf{JH} \left(\beta_{21}\, \mathbf{z}_1 + \beta_{22}\, \mathbf{z}_2\right), \tag{69}$$

where $\beta_{12} \equiv \beta_{21}$. Owing to equations (67), (69) the time-stepping scheme take the shape

$$\left(\frac{1}{2}\,\mathbf{1} - \beta_{12}\, h_n\, \mathbf{JH}\right) \mathbf{z}_2 + \left(\frac{1}{2}\,\mathbf{1} - \beta_{11}\, h_n\, \mathbf{JH}\right) \mathbf{z}_1 - \mathbf{z}_0 = \mathbf{0}, \tag{70}$$

$$\left(\frac{1}{2}\,\mathbf{1} - \beta_{22}\, h_n\, \mathbf{JH}\right) \mathbf{z}_2 - \left(\frac{1}{2}\,\mathbf{1} + \beta_{12}\, h_n\, \mathbf{JH}\right) \mathbf{z}_1 = \mathbf{0}. \tag{71}$$

To apply the Newton-Raphson method, we have to determine the residual vector $\mathbf{R}(\mathbf{x})$ with $\mathbf{x} = [\mathbf{z}_1^T\ \mathbf{z}_2^T]^T$. Accordingly, the residual vector of the time-stepping scheme can be

	β_{11}	β_{12}	β_{22}
midpoint rule	1/4	1/4	1/4
trapezoidal rule	1/2	0	1/2
two Gaussian points	1	-1/2	1
three to five Gaussian points	1/3	1/6	1/3

Table 4: Coefficients β_{ij} for a numerical quadrature within the dG(1) method.

written as

$$\mathbf{R}(\mathbf{x}) = \frac{1}{2}\begin{bmatrix} \mathbf{1} - 2\,\beta_{11}\,h_n\,\mathbf{JH} & \mathbf{1} - 2\,\beta_{12}\,h_n\,\mathbf{JH} \\ -\mathbf{1} - 2\,\beta_{12}\,h_n\,\mathbf{JH} & \mathbf{1} - 2\,\beta_{22}\,h_n\,\mathbf{JH} \end{bmatrix}\mathbf{x} - \begin{bmatrix} \mathbf{z}_0 \\ \mathbf{0} \end{bmatrix}. \tag{72}$$

Hence, the corresponding tangent $\mathbf{K}_T \equiv \partial_{\mathbf{X}}\mathbf{R}$ takes the form

$$\mathbf{K}_T = \begin{bmatrix} \mathbf{1} - 2\,\beta_{11}\,h_n\,\mathbf{JH} & \mathbf{1} - 2\,\beta_{12}\,h_n\,\mathbf{JH} \\ -\mathbf{1} - 2\,\beta_{12}\,h_n\,\mathbf{JH} & \mathbf{1} - 2\,\beta_{22}\,h_n\,\mathbf{JH} \end{bmatrix}. \tag{73}$$

We refer to Table 4 for the β_{ij} corresponding to the midpoint rule ($N_q = 1$), trapezoidal rule ($N_q = 2$) and Gaussian rules with $N_q = 2,\ldots,5$ quadrature points. The time-stepping scheme emanating from the *midpoint rule* takes the form

$$\left(\frac{1}{2}\,\mathbf{1} - \frac{1}{4}\,h_n\,\mathbf{JH}\right)\,\mathbf{z}_2 + \left(\frac{1}{2}\,\mathbf{1} - \frac{1}{4}\,h_n\,\mathbf{JH}\right)\,\mathbf{z}_1 - \mathbf{z}_0 = \mathbf{0}, \tag{74}$$

$$\left(\frac{1}{2}\,\mathbf{1} - \frac{1}{4}\,h_n\,\mathbf{JH}\right)\,\mathbf{z}_2 - \left(\frac{1}{2}\,\mathbf{1} + \frac{1}{4}\,h_n\,\mathbf{JH}\right)\,\mathbf{z}_1 = \mathbf{0}. \tag{75}$$

Subtraction of the equations (74), (75) yields

$$\mathbf{z}_1 = \mathbf{z}_0. \tag{76}$$

Therefore, the midpoint rule leads to a continuous solution because the jump $[\mathbf{z}^h]_0$ vanishes. On the other hand, addition of the equations (74), (75) yields

$$\left(\mathbf{1} - \frac{1}{2}\,h_n\,\mathbf{JH}\right)\,\mathbf{z}_2 - \frac{1}{2}\,h_n\,\mathbf{JH}\,\mathbf{z}_1 - \mathbf{z}_0 = \mathbf{0}. \tag{77}$$

Referring to equation (76), equation (77) may be also written in the form

$$\left(\mathbf{1} - \frac{1}{2}\,h_n\,\mathbf{JH}\right)\,\mathbf{z}_2 - \left(\mathbf{1} + \frac{1}{2}\,h_n\,\mathbf{JH}\right)\,\mathbf{z}_1 = \mathbf{0}. \tag{78}$$

This is the time-stepping scheme generated by the cG(1) method for the harmonic oscillator with exactly computed integral. Cf equation (48). Owing to the fact that with equation (76) the trial functions of the dG(1) method and the cG(1) method are also identical, the midpoint rule applied on the dG(1) method leads to the cG(1) method. Hence, in the case of the harmonic oscillator, the cG(1) method is a special case of the discrete dG(1) method; cf Figure 8.

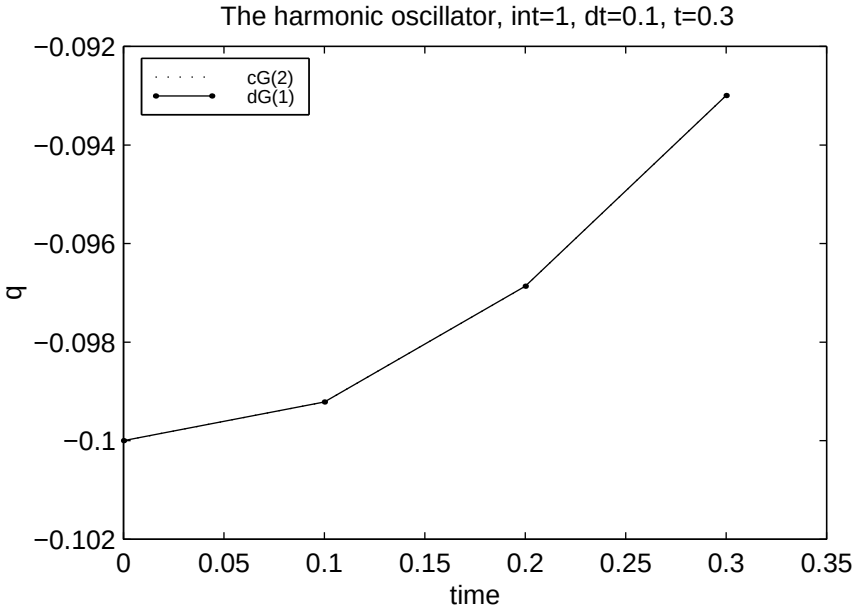

Figure 8: Rotation angle $q = q(t)$ of a harmonic oscillator with a period $T = 5$, mass $m = 2$ and gravitational acceleration $g = 9.81$. Computed with the dG(1) method with midpoint rule ($N_q = 1$) and by a time step size $h_n = 0.1$.

Remark 6.3 *Applying the midpoint rule to the cG(2) method leads to the discrete cG(1) method. We are able to proof this by considering the equations (59) and (60). First we add equation (59) and equation (60), using the midpoint rule and obtain*

$$\boldsymbol{z}_3 - \boldsymbol{z}_1 - h_n \, \boldsymbol{J} DH(\boldsymbol{z}^h(\frac{1}{2})) = \boldsymbol{0}, \tag{79}$$

owing to the identity $\tilde{M}_1 + \tilde{M}_2 = 1$. *Furthermore, a subtraction of the equations (59), (60) and subsequently applying the midpoint rule leads to*

$$-\frac{1}{2}\,\boldsymbol{z}_3 + \boldsymbol{z}_2 - \frac{1}{2}\,\boldsymbol{z}_1 = \boldsymbol{0}. \tag{80}$$

The trial function of the cG(2) method reads $\boldsymbol{z}^h = \sum_{i=1}^{3} M_i \, \boldsymbol{z}_i$, *with the nodal shape function for the case* $k = 2$ *according to Table 1. Taking into account equation (80), the trial function takes the form*

$$\boldsymbol{z}^h(\frac{1}{2}) = \frac{1}{2}\,(\boldsymbol{z}_1 + \boldsymbol{z}_3)\,. \tag{81}$$

The linear trial function (81) in connection with equation (79) describes the cG(1) method according to equation (48), of which the integral is approximated by the midpoint rule. Note that for this reason the dotted line of the cG(2) method is covered by the solid line of the dG(1) method in Figure 8.

Remark 6.4 *Referring to* Betsch & Steinmann *[9] the cG(1) method preserves the total energy at each time step. Therefore, we expect algorithmic energy conservation for the dG(1) method with midpoint rule, what we also proof in Section 7.*

Now let us consider the *trapezoidal rule*. Referring to Table 4, the time-stepping scheme reads

$$\frac{1}{2}\,\mathbf{z}_2 + \frac{1}{2}\,\left(\mathbf{1} - h_n\,\mathbf{JH}\right)\,\mathbf{z}_1 - \mathbf{z}_0 = \mathbf{0}, \tag{82}$$

$$\frac{1}{2}\,\left(\mathbf{1} - h_n\,\mathbf{JH}\right)\,\mathbf{z}_2 - \frac{1}{2}\,\mathbf{z}_1 = \mathbf{0}. \tag{83}$$

We add equation (82) and equation (83) and obtain

$$\mathbf{z}_2 - \mathbf{z}_0 - h_n\,\mathbf{JH}\,\frac{1}{2}\,\left(\mathbf{z}_1 + \mathbf{z}_2\right) = \mathbf{0}. \tag{84}$$

Furthermore, a subtraction yields

$$\mathbf{z}_1 - \mathbf{z}_0 - h_n\,\mathbf{JH}\,\frac{1}{2}\,\left(\mathbf{z}_1 - \mathbf{z}_2\right) = \mathbf{0}. \tag{85}$$

According to Hughes [18] equation (84) would be identical with the so-called trapezoidal rule (or Crank-Nicholson) algorithm (or average acceleration method in structural dynamics) if $\mathbf{z}_0 = \mathbf{z}_1$, ie the solution is continuous. On the other hand, with regard to equation (85) the solution can only become continuous if $\mathbf{z}_1 = \mathbf{z}_2$ which corresponds to an equilibrium point.
The *Gaussian rules* with $N_q = 3, \ldots, 5$ lead to the time-stepping scheme which coincides with exact quadrature.

7 The algorithmic total energy of the harmonic oscillator

In this section we examine under which conditions constant and linear time finite elements, ie the dG(0) and dG(1) method, obey the law of conservation of total energy of the harmonic oscillator. We know from Section 2 that for natural systems the hamiltonian H is the total energy of the system. Further, the hamiltonian H is constant for all times if H does not depend explicitly on time. Therefore, within the scope of the finite element formulation, we investigate the algorithmic hamiltonian H_{k+1} at the last node of the master element. Note that we refer to H_{k+1} as the hamiltonian at the $k+1$ node of the master element I_α of the dG(k) method. According to equation (41) the algorithmic hamiltonian H_{k+1} of a harmonic oscillator is

$$H_{k+1} = \frac{1}{2}\,\mathbf{z}_{k+1}^T\,\mathbf{H}\,\mathbf{z}_{k+1}. \tag{86}$$

Through an elimination of the nodal values corresponding to the internal nodes of I_α, we may bring each time-stepping scheme generated by the dG(k) method for the harmonic oscillator into the form

$$\mathbf{z}_{k+1} = \mathbf{A}_k \, \mathbf{z}_0, \tag{87}$$

where the $2n_{dof} \times 2n_{dof}$ matrix $\mathbf{A}_k$ denotes the amplification matrix of the dG(k) method. According to RICHTMYER & MORTON [31] we refer to (87) as the two-level scheme of the dG(k) method. Furthermore, referring to CADZOW & MARTENS [10] or GANTMACHER [13], we are able to substitute the so-called Lagrange-Sylvester's interpolation polynomial of $\mathbf{A}_k$ for the matrix $\mathbf{A}_k$ itself. If the eigenvalues λ_i, $i = 1, \ldots, N_\lambda$, of $\mathbf{A}_k$ are distinct, we have to substitute such that

$$\mathbf{z}_{k+1} = \left(\sum_{i=1}^{N_\lambda} \mathbf{A}_{k,i} \, \lambda_i \right) \mathbf{z}_0, \tag{88}$$

where simple distinct eigenvalues imply $N_\lambda = 2n_{dof}$. The $2n_{dof} \times 2n_{dof}$ matrix $\mathbf{A}_{k,i}$ is called the ith constituent matrix of the Lagrange-Sylvester's interpolation polynomial of $\mathbf{A}_k$ and takes for distinct eigenvalues λ_i the form

$$\mathbf{A}_{k,i} \;=\; \prod_{\substack{j=1 \\ j \neq i}}^{N_\lambda} \frac{\mathbf{A}_k - \lambda_j \mathbf{1}}{\lambda_i - \lambda_j}, \quad 1 \leq i \leq N_\lambda. \tag{89}$$

Remark 7.1 *In general, the Lagrange-Sylvester's interpolation polynomial defines a function f for arguments in form of square matrices $\boldsymbol{A}$ with the relation*

$$f(\boldsymbol{A}) = \sum_{i=1}^{N_\lambda} \boldsymbol{A}_i \, f(\lambda_i).$$

Therefore, the identity function implies:

$$\boldsymbol{A} = \sum_{i=1}^{N_\lambda} \lambda_i \, \boldsymbol{A}_i,$$

with the simple distinct eigenvalues λ_i, $i = 1, \ldots, N_\lambda$. The Lagrange-Sylvester's interpolation polynomial goes back to SYLVESTER *[34].*

We obtain with two distinct eigenvalues ($N_\lambda = 2$) the following expression for the hamiltonian H_{k+1} after employing equation (88) in equation (86):

$$H_{k+1} = \frac{1}{2} \, \mathbf{z}_0^T \left(\mathbf{A}_{k,1} \, \lambda_1 + \mathbf{A}_{k,2} \, \lambda_2 \right)^T \mathbf{H} \left(\mathbf{A}_{k,1} \, \lambda_1 + \mathbf{A}_{k,2} \, \lambda_2 \right) \mathbf{z}_0. \tag{90}$$

The expansion of expression (90) yields

$$H_{k+1} \;=\; \frac{1}{2} \, \rho^2 \, \mathbf{z}_0^T \left(\sum_{\substack{i=1 \\ j \neq i}}^{2} \mathbf{A}_{k,i}^T \, \mathbf{H} \, \mathbf{A}_{k,j} \right) \mathbf{z}_0 + \frac{1}{2} \, \mathbf{z}_0^T \left(\sum_{i=1}^{2} \lambda_i^2 \mathbf{A}_{k,i}^T \, \mathbf{H} \, \mathbf{A}_{k,i} \right) \mathbf{z}_0, \tag{91}$$

with $j \in \{1,2\}$, where ρ denotes the spectral radius $\rho(\mathbf{A}_k) \equiv \max\{|\lambda_i|\} = \sqrt{\lambda_1 \lambda_2}$ because the eigenvalues λ_1 and λ_2 are complex conjugate.
The reason why we have introduced the representation (88) of the time-stepping scheme will become apparent in the applications to the dG(0) and dG(1) method in the subsections below.

7.1 Constant time finite elements

Here we consider the dG(0) method for the harmonic oscillator and apply the Lagrange-Sylvester's interpolation polynomial to the amplification matrix $\mathbf{A}_0$ to get the algorithmic hamiltonian H_1. According to the equations (42), (46) the amplification matrix $\mathbf{A}_0$ takes the following shape:

$$\mathbf{A}_0 = \frac{1}{1+\Omega^2} \begin{bmatrix} 1 & h_n/I \\ -h_n\, c & 1 \end{bmatrix}, \tag{92}$$

where according to Hughes & Liu [19] $\Omega = h_n\, \omega$ is called the sampling frequency and $\omega = \sqrt{c/I}$ denotes the eigenfrequency of the harmonic oscillator with the moment of inertia I. Determination of the eigenvalues λ_1 and λ_2 of $\mathbf{A}_0$ yields

$$\lambda_1 = \frac{1}{1 - i\,\Omega}, \qquad \lambda_2 = \frac{1}{1 + i\,\Omega}, \tag{93}$$

where i denotes the imaginary unit. Therefore, we get from equation (89) the constituent matrices of the amplification matrix $\mathbf{A}_0$:

$$\mathbf{A}_{0,1} = \frac{1}{2} \begin{bmatrix} 1 & 1/(i\,\omega\, I) \\ i\,\omega\, I & 1 \end{bmatrix}, \qquad \mathbf{A}_{0,2} = \frac{1}{2} \begin{bmatrix} 1 & -1/(i\,\omega\, I) \\ -i\,\omega\, I & 1 \end{bmatrix}. \tag{94}$$

Now we are able to determine the algorithmic hamiltonian. Owing to the equations in (94), we obtain

$$\mathbf{A}_{k,i}^T\, \mathbf{H}\, \mathbf{A}_{k,i} = \mathbf{O}_2, \tag{95}$$

with $i \in \{1,2\}$, where $\mathbf{O}_2$ generally denotes the $2n_{dof} \times 2n_{dof}$ zero matrix, and

$$\sum_{\substack{i=1 \\ j \neq i}}^{2} \mathbf{A}_{k,i}^T\, \mathbf{H}\, \mathbf{A}_{k,j} = \mathbf{H}, \tag{96}$$

with $j \in \{1,2\}$. Employing equation (95) and (96) in equation (91) yields

$$H_1 = \frac{1}{2}\, \rho^2\, \mathbf{z}_0^T \mathbf{H}\, \mathbf{z}_0 = \rho^2\, H_0, \tag{97}$$

where H_0 denotes the hamiltonian of the initial node 0; see Figure 3. Hence the difference of the algorithmic hamiltonian at node 1 and node 0 is

$$H_1 - H_0 = \left(\rho^2 - 1\right)\, H_0. \tag{98}$$

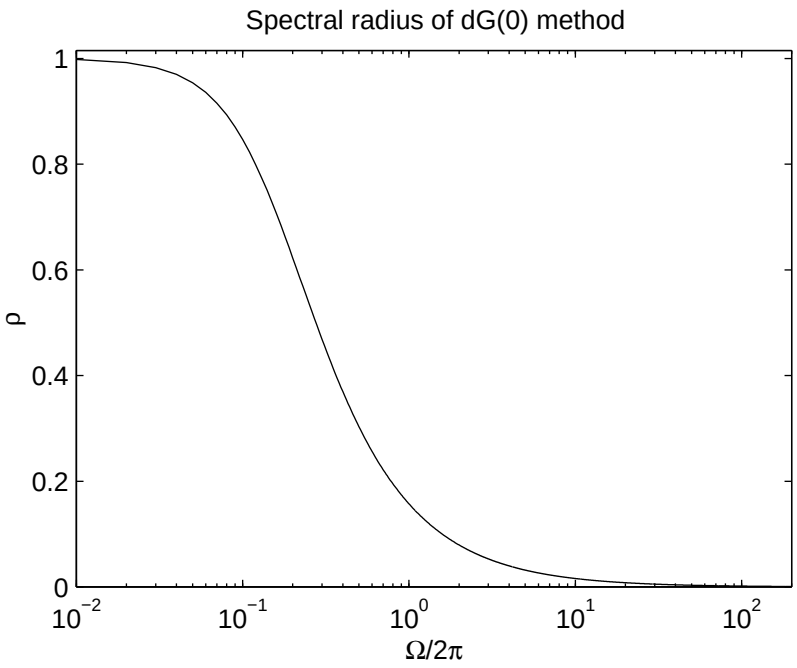

Figure 9: Spectral radius of the dG(0) method.

Thus for a positive definite matrix $\mathbf{H}$ the energy is preserved in the sense that $H_1 = H_0$ if $\rho^2 = 1$ but we obtain energy decay and growth for $\rho^2 < 1$ and $\rho^2 > 1$ respectively .

$$\begin{cases} \rho^2 < 1, & \text{energy decay} \\ \rho^2 = 1, & \text{energy conservation} \\ \rho^2 > 1, & \text{energy growth} \end{cases}$$

The squared spectral radius of the amplification matrix $\mathbf{A}_0$ is given by

$$\rho^2 = \frac{1}{1+\Omega^2}. \tag{99}$$

Since the denominator is larger than the numerator for all sampling frequencies $\Omega \neq 0$, the squared spectral radius ρ^2 is less than one; also see Figure 9 and HULBERT [20]. Only for infinitesimal time steps ($h_n = 0$) the energy is preserved. Figure 9 shows a numerical dissipation already in the region of low sampling frequencies. Accordingly, we notice an early starting high-frequency dissipation for the dG(0) method.
Since the time-stepping schemes emanating from the quadrature rules examined in Subsection 6.1.2 are identical with the scheme resulting from exact quadrature, we also get the squared spectral radius (99).

Numerical Example 7.1 *We show in Figure 10 the course of the total energy of the harmonic oscillator in Example 6.1 for one period with a time step size* $h_n = 0.1$. *One*

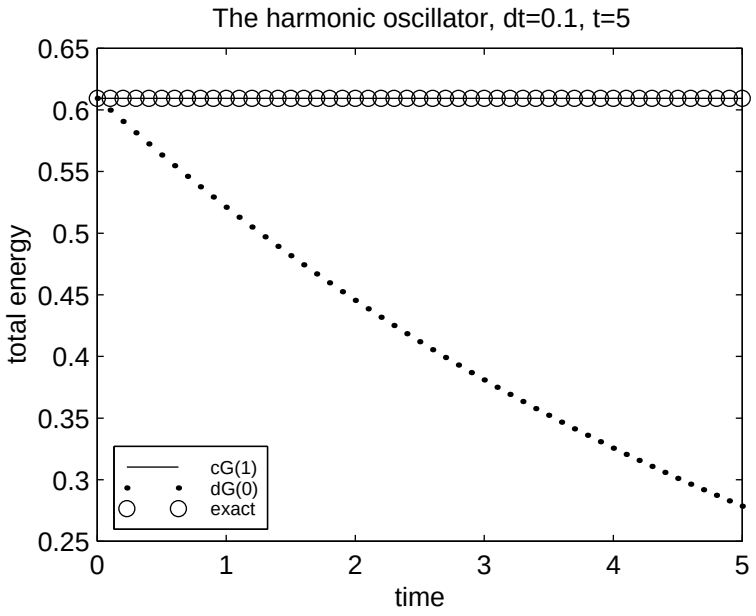

Figure 10: Total energy $E = E(t)$ of a harmonic oscillator with a period $T = 5$, mass $m = 2$ and gravitational acceleration $g = 9.81$. Computed with the dG(0) method with $h_n = 0.1$.

sees the energy decay of the dG(0) method for each time finite element on account of the squared spectral radius (99). Furthermore, the cG(1) method corroborates the algorithmic energy conservation according to Betsch & Steinmann *[7, 8, 9].*

7.2 Linear time finite elements

In this section we proceed along the lines of Subsection 7.1 to obtain the behavior of the algorithmic hamiltonian H_2 for the harmonic oscillator computed with linear time finite elements ($k = 1$). We investigate as well the time-stepping scheme emanating from exact quadrature as the schemes which we obained by applying specific quadrature rules.

7.2.1 Time-stepping scheme associated with exact quadrature

We consider the time-stepping scheme (61), (62) generated by the dG(1) method with exactly evaluated integrals.

$$\begin{aligned} \frac{1}{2}\left(\mathbf{1} - \frac{1}{3}\,h_n\,\mathbf{J}\,\mathbf{H}\right)\,\mathbf{z}_2 + \frac{1}{2}\left(\mathbf{1} - \frac{2}{3}\,h_n\,\mathbf{J}\,\mathbf{H}\right)\,\mathbf{z}_1 - \mathbf{z}_0 &= \mathbf{0}, \\ \frac{1}{2}\left(\mathbf{1} - \frac{2}{3}\,h_n\,\mathbf{J}\,\mathbf{H}\right)\,\mathbf{z}_2 - \frac{1}{2}\left(\mathbf{1} + \frac{1}{3}\,h_n\,\mathbf{J}\,\mathbf{H}\right)\,\mathbf{z}_1 &= \mathbf{0}. \end{aligned}$$

We now eliminate the nodal value $\mathbf{z}_1$ to get the two-level scheme of the dG(1) method according to equation (87). Therefore, the time-stepping scheme may be written as

$$\mathbf{z}_2 = 2\,\left(\mathbf{B}_- + \mathbf{C}\,\mathbf{B}_+^{-1}\mathbf{C}\right)^{-1}\,\mathbf{z}_0, \tag{100}$$

with the matrices

$$\mathbf{B}_+ = \mathbf{1} + \frac{1}{3}\,h_n\,\mathbf{JH}, \qquad \mathbf{B}_- = \mathbf{1} - \frac{1}{3}\,h_n\,\mathbf{JH}, \tag{101}$$

$$\mathbf{C} = \mathbf{1} - \frac{2}{3}\,h_n\,\mathbf{JH}. \tag{102}$$

Accordingly, taking into account equation (42) the amplification matrix $\mathbf{A}_1$ for the harmonic oscillator takes the following shape (also see Hulbert [20] and Ruge [32]):

$$\mathbf{A}_1 = \frac{-2}{\Omega^4 + 4\,\Omega^2 + 36}\,\begin{bmatrix} 7\,\Omega^2 - 18 & (\Omega^2 - 18)\,h_n/I \\ -(\Omega^2 - 18)\,h_n\,c & 7\,\Omega^2 - 18 \end{bmatrix}. \tag{103}$$

Furthermore, the eigenvalues λ_i, i=1, 2, of the amplification matrix $\mathbf{A}_1$ are as follows:

$$\lambda_1 = -2\,\frac{7\,\Omega^2 - 18 - i\,\Omega\,(\Omega^2 - 18)}{\Omega^4 + 4\,\Omega^2 + 36}, \qquad \lambda_2 = -2\,\frac{7\,\Omega^2 - 18 + i\,\Omega\,(\Omega^2 - 18)}{\Omega^4 + 4\,\Omega^2 + 36}, \tag{104}$$

where i denotes the imaginary unit. Owing to equation (89), the constituent matrices are as follows:

$$\mathbf{A}_{1,1} = \frac{1}{2}\,\begin{bmatrix} 1 & -1/(i\,\omega\,I) \\ -i\,\omega\,I & 1 \end{bmatrix}, \qquad \mathbf{A}_{1,2} = \frac{1}{2}\,\begin{bmatrix} 1 & 1/(i\,\omega\,I) \\ i\,\omega\,I & 1 \end{bmatrix}. \tag{105}$$

This constituent matrices fulfill the equations (95) and (96) such that the algorithmic hamiltonian H_2 is

$$H_2 = \frac{1}{2}\,\rho^2\,\mathbf{z}_0^T\mathbf{H}\,\mathbf{z}_0 = \rho^2\,H_0, \tag{106}$$

and thus takes the same form as H_1. Accordingly, the behavior of the algorithmic hamiltonian H_2 is also determined by the squared spectral radius ρ^2 in the following sense:

$$\begin{cases} \rho^2 < 1, & \text{energy decay} \\ \rho^2 = 1, & \text{energy conservation} \\ \rho^2 > 1, & \text{energy growth} \end{cases}$$

The squared spectral radius of the amplification matrix $\mathbf{A}_1$ is

$$\rho^2 = \frac{4\,\Omega^2 + 36}{\Omega^4 + 4\,\Omega^2 + 36}. \tag{107}$$

Hence for exact computation of the integrals the energy decays because for all sampling frequencies $\Omega \neq 0$ is the denominator of ρ^2 bigger than the numerator of ρ^2 and thus $\rho^2 < 1$. We generally obtain energy conservation at $\Omega = 0$, but we only get a sampling frequency $\Omega = 0$ for infinitesimal time steps which means a time step size $h_n = 0$.

Numerical Example 7.2 *Figure 11 shows the total energy of the harmonic oscillator in Example 6.1 for each time step with a time step size $h_n = 0.1$. The course describes the energy decay of the dG(1) method owing to the squared spectral radius (107) for one period. The cG(2) method also corroborates the algorithmic energy conservation according to* Betsch & Steinmann *[7, 9].*

7.2.2 Time-stepping schemes associated with specific quadrature rules

We now consider the time-stepping scheme (70), (71) with approximated integrals resulting from the application of interpolating quadrature rules.

$$\begin{aligned} \left(\frac{1}{2}\,\mathbf{1} - \beta_{12}\,h_n\,\mathbf{JH}\right)\,\mathbf{z}_2 + \left(\frac{1}{2}\,\mathbf{1} - \beta_{11}\,h_n\,\mathbf{JH}\right)\,\mathbf{z}_1 - \mathbf{z}_0 &= \mathbf{0}, \\ \left(\frac{1}{2}\,\mathbf{1} - \beta_{22}\,h_n\,\mathbf{JH}\right)\,\mathbf{z}_2 - \left(\frac{1}{2}\,\mathbf{1} + \beta_{12}\,h_n\,\mathbf{JH}\right)\,\mathbf{z}_1 &= \mathbf{0}. \end{aligned}$$

Elimination of the nodal value $\mathbf{z}_1$ leads to a two-level scheme according to equation (87). In analogy to the time-stepping scheme with exactly evaluated integrals, we may write

$$\mathbf{z}_2 = 2\,\left(\mathbf{B}_{12} + \mathbf{B}_{11}\,\mathbf{B}_{12}^{-1}\mathbf{B}_{22}\right)^{-1}\,\mathbf{z}_0, \tag{108}$$

with the matrices

$$\mathbf{B}_{ij} = \mathbf{1} - 2\,\beta_{ij}\,h_n\,\mathbf{JH}, \tag{109}$$

for $i, j \in \{1, 2\}$. On account of the complicated terms, we omit to represent the amplification matrix and eigenvalues explicitly. The constituent matrices are identical with the matrices (105) of the time-stepping scheme emanating from exact quadrature. Hence, we have

$$H_{2,q} = \frac{1}{2}\,\rho_q^2\,\mathbf{z}_0^T\mathbf{H}\,\mathbf{z}_0 = \rho_q^2\,H_0, \tag{110}$$

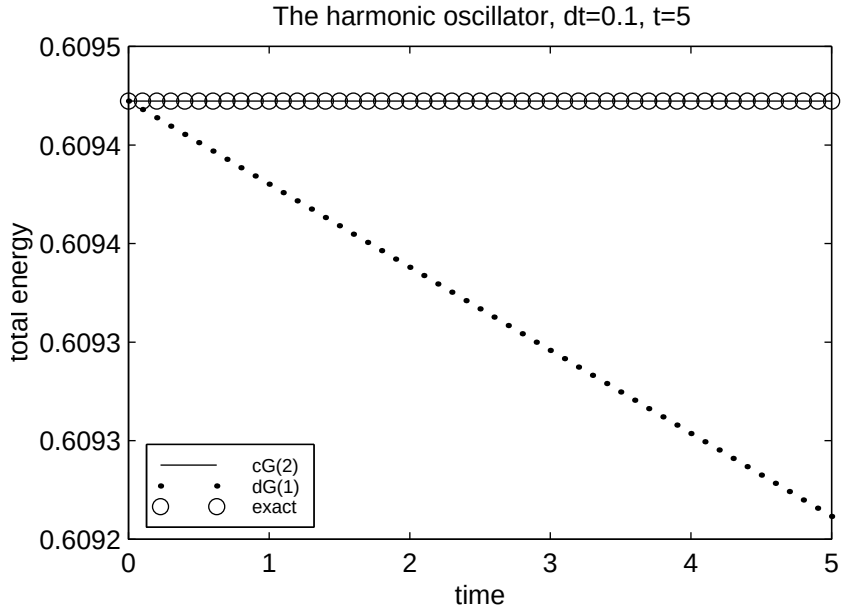

Figure 11: Total energy $E = E(t)$ of a harmonic oscillator with a period $T = 5$, mass $m = 2$ and gravitational acceleration $g = 9.81$. Computed with the dG(1) method with $h_n = 0.1$.

where the index q denotes the quadrature rule. We obtain the following squared spectral radius for arbitrary number of quadrature points:

$$\rho_q^2 = \frac{1 + 4\,\beta_{12}^2\,\Omega^2}{1 + 4\,\beta_{12}^2\,\Omega^2 + (\beta_{22} - \beta_{11})^2\,\Omega^2 + 4\,(\beta_{12}^2 - \beta_{11}\,\beta_{22})^2\,\Omega^4}. \tag{111}$$

We see that only for $\beta_{11} = \beta_{12} = \beta_{22}$ one obtains $\rho_q^2 = 1$ for arbitrary sampling frequencies, ie the energy is preserved. In the other cases the energy decays because the squared spectral radius is less than one (unless for the case $\Omega = 0$ where the energy is generally preserved).

We consider the midpoint rule, the trapezoidal rule and Gaussian quadrature rules with $N_q = 2, \ldots, 5$ quadrature points. We obtain for the *midpoint rule* $\beta_{11} = \beta_{12} = \beta_{22} = 1/4$; cf Table 4. Therefore, $\rho_{mid}^2 = 1$, ie the midpoint rule preserves the total energy of the dG(1) method; see Figure 12. The conservation of the total energy of the dG(1) method associated with the midpoint rule also follows from the fact that the resulting time-stepping scheme is identical to the cG(1) method; cf Subsection 6.2.2. Therefore, taking into account equation (76), it looks as if a continuous solution is connected with algorithmic total energy conservation in the linear regime.

The *trapezoidal rule* ($N_q = 2$) leads to $\beta_{11} = \beta_{22} = 1/2$ and $\beta_{12} = 0$ so that the squared spectral radius takes the form

$$\rho_{trp}^2 = \frac{4}{\Omega^4 + 4}, \tag{112}$$

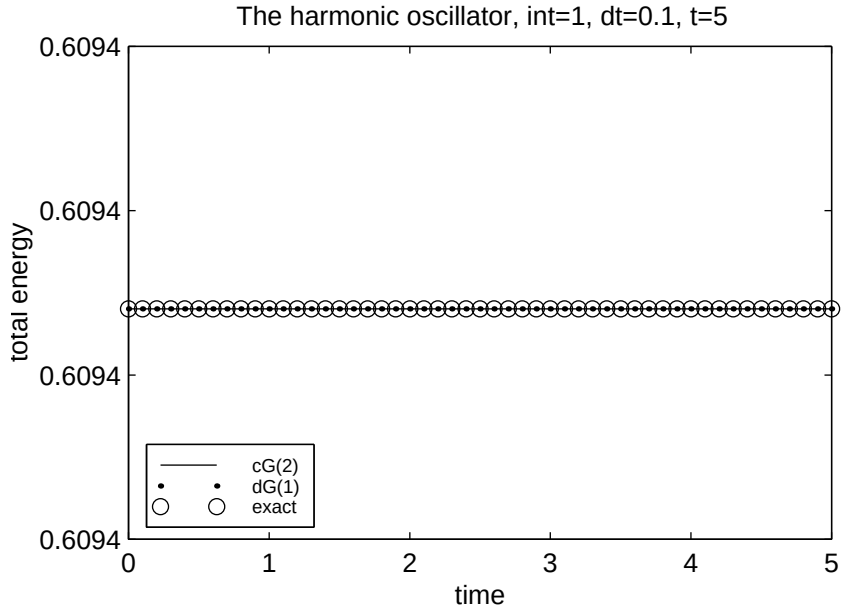

Figure 12: Total energy $E = E(t)$ of a harmonic oscillator with a period $T = 5$, mass $m = 2$ and gravitational acceleration $g = 9.81$. Computed with the dG(1) method with midpoint rule ($N_q = 1$) and with a time step size $h_n = 0.1$.

and implies an energy decay for $\Omega \neq 0$. *Two Gaussian quadrature points* result in $\beta_{11} = \beta_{22} = 1$ and $\beta_{12} = -1/2$. Hence the squared spectral radius is given by

$$\rho_{2gp}^2 = \frac{4\,\Omega^2 + 4}{9\,\Omega^4 + 4\,\Omega^2 + 4}. \tag{113}$$

The Gaussian quadrature rules with *three to five quadrature points* yield $\beta_{11} = \beta_{22} = 1/3$ and $\beta_{12} = 1/6$ which we also obtain with exact quadrature. Accordingly, the squared spectral radius is as follows:

$$\rho_{3g5}^2 = \frac{4\,\Omega^2 + 36}{\Omega^4 + 4\,\Omega^2 + 36}. \tag{114}$$

Figure 13 shows a comparison of the spectral radii of the dG(1) method associated with specific quadrature rules and the exactly integrated dG(0) method; cf HULBERT [20]. In Figure 13, we are able to see that the quadrature rule influences the frequency region in which the asymptotic annihilation begins. Therefore, as well the degree k of the finite elements in time as the applied quadrature affects the low-frequency dissipation. Further, we see that with two quadradure points the dG(1) method has a faster annihilation as the dG(0) method in the following sense. From $\Omega^2 = 0.8$ upward lies the spectral radius

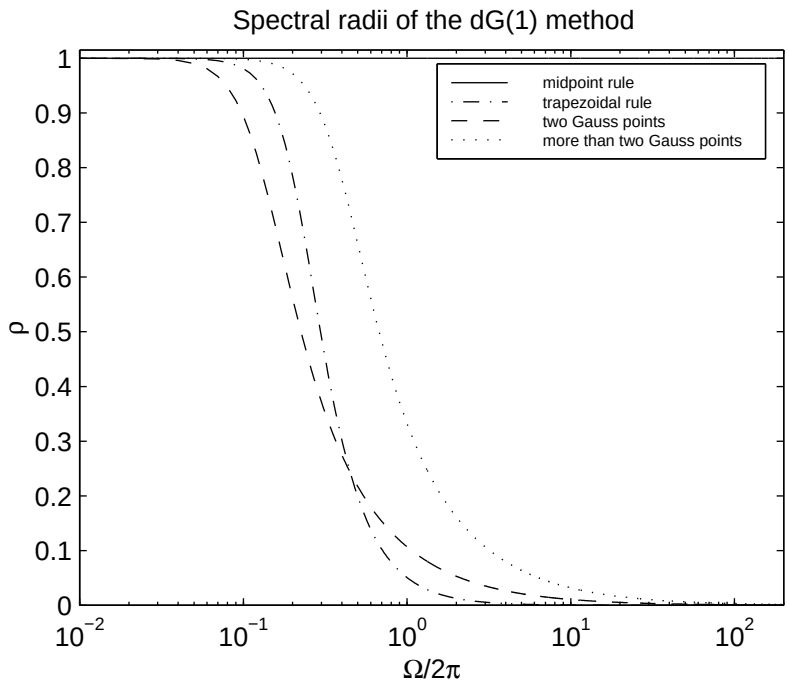

Figure 13: Spectral radii of the dG(1) method associated with specific quadrature rules.

of two Gaussian quadrature points under that of the dG(0) method. The spectral radius of the trapezoidal rule is for $\Omega^2 > 4$ less than the spectral radius of dG(0). The fastest annihilation occurs for $0 \leq \Omega^2 \leq 0.8$ with the dG(0) method, for $0.8 \leq \Omega^2 \leq 8$ with two Gaussian quadrature points and from $\Omega^2 = 8$ upward with the trapezoidal rule. The slowest annihilation of the dG(1) method occurs with three to five Gaussian quadrature points because here is the spectral radius identical with the spectral radius of the time-stepping scheme generated by the exactly integrated dG(1) method.

8 A time finite element formulation for the circular pendulum for arbitrary motions

This section is devoted to the circular pendulum for arbitrary motions, ie we have to consider the nonlinear potential $V = -c\,\cos(q)$, with $c = m\,g\,l$. The total kinetic energy T of the particle can be taken from the harmonic oscillator:

$$T = \frac{1}{2}\,I\,\dot{q}^2, \tag{115}$$

where $I = m\,l^2$ is the moment of inertia. Therefore, the lagrangian L is

$$L(q,\dot{q}) \equiv T(\dot{q}) - V(q) = \frac{1}{2}\,I\,\dot{q}^2 - V(q). \tag{116}$$

Hence it follows that the generalized momentum p reads again

$$p = I\,\dot{q}. \tag{117}$$

The substitution of the generalized momentum p for the generalized velocity $\dot{q}$ leads to the hamiltonian H of the system:

$$H(q,p) \equiv T(p) + V(q) = \frac{1}{2\,I}\,p^2 + V(q). \tag{118}$$

To determine the time-stepping schemes, we require the Jacobian matrix $DH(\mathbf{z})$. With respect to the nonlinearity of the hamiltonian (118), we have to use the Jacobian matrix to get $DH(\mathbf{z})$. Accordingly, the Jacobian matrix takes the shape

$$DH(\mathbf{z}) \equiv \begin{bmatrix} \partial_q H(q,p) \\ \partial_p H(q,p) \end{bmatrix} = \begin{bmatrix} dV/dq \\ p/I \end{bmatrix}. \tag{119}$$

8.1 Constant time finite elements

We use the general dG(0) method (45) to obtain the time-stepping scheme for constant trial functions $\mathbf{z}^h = \mathbf{z}_1$ according to equation (18):

$$\mathbf{z}_1 - \mathbf{z}_0 - h_n \int_0^1 \mathbf{J} DH(\mathbf{z}^h) d\alpha = \mathbf{0}.$$

Employing equation (119) and the trial function $\mathbf{z}^h = [q_1, p_1]^T$ leads to the time-stepping scheme in the following form:

$$\mathbf{z}_1 - \mathbf{z}_0 - h_n \int_0^1 \mathbf{J} \begin{bmatrix} dV(q_1)/dq \\ p_1/I \end{bmatrix} d\alpha = \mathbf{0}. \tag{120}$$

On grounds of the constant trial function, we do not have to distinguish between exact quadrature and the use of interpolating quadrature rules; see Subsection 6.1.2. Hence for constant time finite elements the time-stepping scheme reads

$$\mathbf{z}_1 - \mathbf{z}_0 - h_n\,\mathbf{J} \begin{bmatrix} dV(q_1)/dq \\ p_1/I \end{bmatrix} = \mathbf{0}. \tag{121}$$

Given: initial condition $\mathbf{z}_0$, time step size h_n and residual tolerance $\epsilon = 10^{-13}$ set iteration counter $l = 1$
Find: nodal unknown $\mathbf{z}_1$
(a) compute residual vector $\mathbf{R}^{(l)} = \mathbf{z}_1^{(l)} - \mathbf{z}_0 - h_n \mathbf{J} \begin{bmatrix} dV(q_1^{(l)})/dq \\ p_1^{(l)}/I \end{bmatrix}$ if $\|\mathbf{R}^{(l)}\| > \epsilon$ goto (b) else goto (c) (b) compute tangent $\mathbf{K}_T^{(l)} \equiv \partial_{\mathbf{z}_1} \mathbf{R}(\mathbf{z}_1^{(l)}) = \mathbf{1} - h_n \mathbf{J} \begin{bmatrix} d^2V(q_1^{(l)})/dq^2 & 0 \\ 0 & 1/I \end{bmatrix}$ solve for increment $\Delta \mathbf{z}_1^{(l)}$ $\Delta \mathbf{z}_1^{(l)} = -\left(\mathbf{K}_T^{(l)}\right)^{-1} \mathbf{R}^{(l)}$ update the nodal unknown $\mathbf{z}_1^{(l+1)} = \mathbf{z}_1^{(l)} + \Delta \mathbf{z}_1^{(l)}$ goto (a) with $l = l + 1$ (c) end.

Table 5: Newton-Raphson method to solve the time-stepping scheme generated by the dG(0) method for nonlinear motions of the circular pendulum.

The time-stepping scheme (121) consists of nonlinear algebraic equations which have to be solved by an iterative method. Again, we have implemented the Newton-Raphson method. Therefore, we have to determine the residual vector $\mathbf{R}(\mathbf{z}_1)$ and the corresponding tangent $\mathbf{K}_T$. The residual vector is given by

$$\mathbf{R}(\mathbf{z}_1) = \mathbf{z}_1 - \mathbf{z}_0 - h_n \mathbf{J} \begin{bmatrix} dV(q_1)/dq \\ p_1/I \end{bmatrix}. \tag{122}$$

The tangent $\mathbf{K}_T$ is the Jacobi matrix of the residual vector (122):

$$\mathbf{K}_T \equiv \partial_{\mathbf{z}_1} \mathbf{R}(\mathbf{z}_1) = \mathbf{1} - h_n \mathbf{J} \begin{bmatrix} d^2V(q_1)/dq^2 & 0 \\ 0 & 1/I \end{bmatrix}. \tag{123}$$

The realization of the Newton-Raphson method is shown in Table 5.

Numerical Example 8.1 *Let the initial condition be* $\boldsymbol{z}(t=0) = [-\pi/2, 0]^T$. *We compute the motion of a circular pendulum with a rod of length* $l = 1$ *and a particle of mass* $m = 5$. *Further, we choose a gravitational acceleration of* $g = 9.81$. *Figure 14 represents the rotation angle of the pendulum computed with a time step size* $h_n = 0.1$

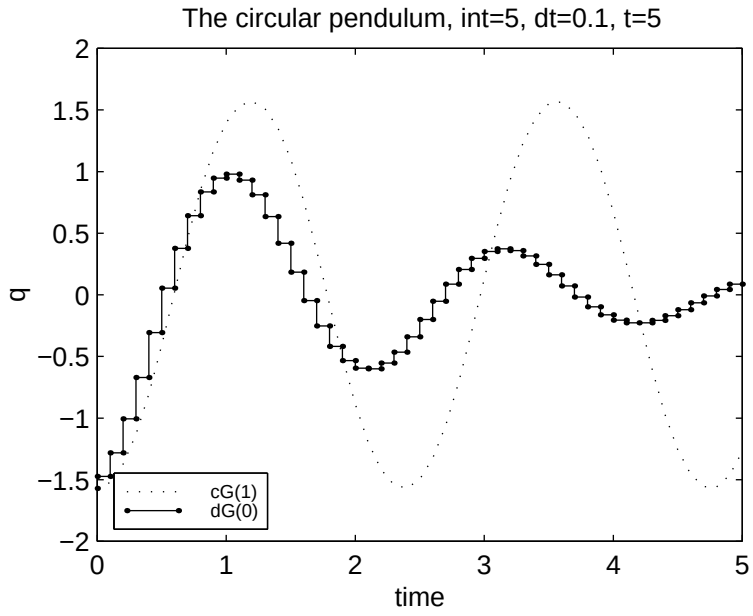

Figure 14: Rotation angle $q = q(t)$ of a circular pendulum with a rod of length $l = 1$, a particle of mass $m = 5$ and gravitational acceleration $g = 9.81$. Computed with the dG(0) method with $h_n = 0.1$.

($dt = 0.1$). The dotted line gives the reference course computed with the cG(1) method with five Gaussian quadrature points ($int = 5$). We choose five Gaussian quadrature points because owing to Betsch & Steinmann *[7] increasing the order of the applied Gaussian rule will increase the energy preservation of the cG(k) method. Figure 14 also shows the algorithmic damping of the dG(0) method in the nonlinear case. Furthermore, for example from equation (121) it is obvious that for a smaller time step size h_n the jump $[\boldsymbol{z}^h]_0 \equiv \boldsymbol{z}_1 - \boldsymbol{z}_0$ will be smaller so that the algorithmic damping will decrease; see Figure 15 with a time step size $h_n = 0.01$ ($dt = 0.01$). Figure 16 shows the jumps in the course of the total energy of the circular pendulum. We see that the dG(0) method approximates the total energy with a step function, owing to the constant finite elements in time, which is attracted to $V(t = \infty) = -mgl$ on account of the algorithmic damping. The dotted line depicts the course of the cG(1) method with linear time finite elements. We are able to corroborate the algorithmic energy conserving in the sense that $E(t_n) = E(t_{n-1})$.*

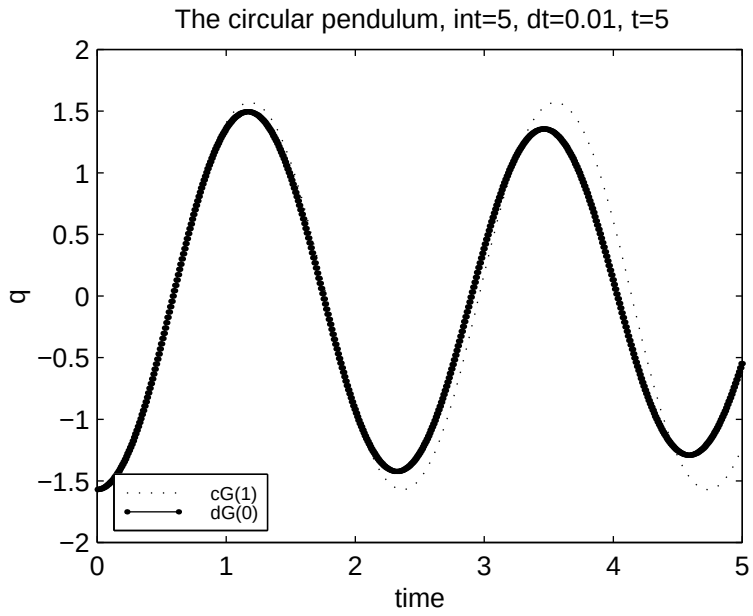

Figure 15: Rotation angle $q = q(t)$ of a circular pendulum with a rod of length $l = 1$, a particle of mass $m = 5$ and gravitational acceleration $g = 9.81$. Computed with the dG(0) method with $h_n = 0.01$.

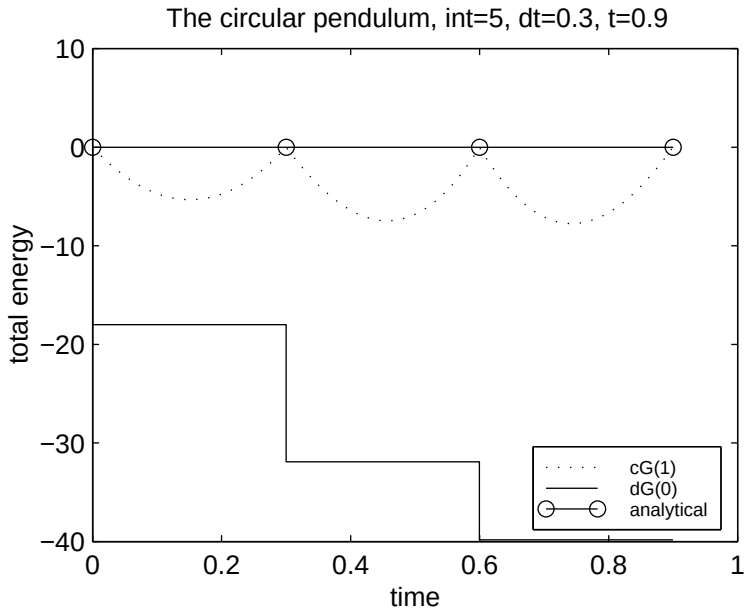

Figure 16: Approximated course $E = E(\mathbf{z}^h(\alpha(t)))$ of the total energy of a circular pendulum with a rod of length $l = 1$, a particle of mass $m = 5$ and gravitational acceleration $g = 9.81$. Computed with the dG(0) method with $h_n = 0.3$.

8.2 Linear time finite elements

In this section we elaborate on linear time finite elements ($k = 1$) for the circular pendulum. The general dG(1) method, given by the equations (57), (58), takes the form

$$\frac{1}{2}\,\mathbf{z}_2 + \frac{1}{2}\,\mathbf{z}_1 - \mathbf{z}_0 - h_n \int_0^1 M_1 \mathbf{J} DH(\mathbf{z}^h) d\alpha = \mathbf{0},$$
$$\frac{1}{2}\,\mathbf{z}_2 - \frac{1}{2}\,\mathbf{z}_1 - h_n \int_0^1 M_2 \mathbf{J} DH(\mathbf{z}^h) d\alpha = \mathbf{0},$$

where $M_1 = 1 - \alpha$ and $M_2 = \alpha$ are the nodal shape functions; cf Table 1. According to equation (119) $DH(\mathbf{z})$ is the Jacobian matrix of the hamiltonian H with respect to $\mathbf{z}$. Taking into account the trial function $\mathbf{z}^h \equiv [q^h,\, p^h]^T$ one obtains

$$DH(\mathbf{z}^h) = \begin{bmatrix} dV(q^h)/dq \\ p^h/I \end{bmatrix}. \tag{124}$$

This time-stepping scheme is nonlinear owing to the appearance of the potential V. Therefore, we have to solve this algebraic system of equations iteratively, eg by the Newton-Raphson method. Here the residual vector $\mathbf{R}(\mathbf{x})$ takes the shape of the following $4n_{dof} \times 1$ hyper matrix:

$$\mathbf{R}(\mathbf{x}) = \frac{1}{2}\begin{bmatrix} \mathbf{1} & \mathbf{1} \\ -\mathbf{1} & \mathbf{1} \end{bmatrix} \mathbf{x} - \begin{bmatrix} \mathbf{1} \\ \mathbf{0} \end{bmatrix} \mathbf{z}_0 - h_n \int_0^1 \begin{bmatrix} M_1(\alpha)\,\mathbf{1} \\ M_2(\alpha)\,\mathbf{1} \end{bmatrix} \mathbf{J} DH(\mathbf{z}^h(\alpha)) d\alpha, \tag{125}$$

where $\mathbf{x} = [\mathbf{z}_1^T\ \mathbf{z}_2^T]^T$. The tangent $\mathbf{K}_T = \partial_{\mathbf{X}} \mathbf{R}(\mathbf{x})$ of the residual vector (125) for the Newton-Raphson method (see Table 3) takes the shape

$$\mathbf{K}_T = \frac{1}{2}\begin{bmatrix} \mathbf{1} & \mathbf{1} \\ -\mathbf{1} & \mathbf{1} \end{bmatrix} - h_n \int_0^1 \begin{bmatrix} M_1\,\mathbf{1} \\ M_2\,\mathbf{1} \end{bmatrix} \begin{bmatrix} \partial_{\mathbf{z}_1}\mathbf{z}^h & \partial_{\mathbf{z}_2}\mathbf{z}^h \end{bmatrix} \begin{bmatrix} \mathbf{J}\mathcal{H}_H^h & \mathbf{O}_2 \\ \mathbf{O}_2 & \mathbf{J}\mathcal{H}_H^h \end{bmatrix} d\alpha, \tag{126}$$

where $\mathcal{H}_H^h \equiv D^2 H(\mathbf{z}^h)$ denotes the $2n_{dof} \times 2n_{dof}$ Hessian matrix of the hamiltonian H. Hence $\mathcal{H}_H^h$ takes the form

$$\mathcal{H}_H^h = \begin{bmatrix} d^2V(q^h)/dq^2 & 0 \\ 0 & 1/I \end{bmatrix}. \tag{127}$$

The trial function $\mathbf{z}^h$ for linear time finite elements is $\mathbf{z}^h = M_1\,\mathbf{z}_1 + M_2\,\mathbf{z}_2$ so that the partial derivatives in equation (126) yield

$$\partial_{\mathbf{z}_1}\mathbf{z}^h = M_1\,\mathbf{1} \quad \text{and} \quad \partial_{\mathbf{z}_2}\mathbf{z}^h = M_2\,\mathbf{1}. \tag{128}$$

To solve the nonlinear residual vector (125), we have to approximate the integral with an interpolating quadrature rule in the manner of equation (51):

$$\mathbf{R}(\mathbf{x}) \approx \frac{1}{2}\begin{bmatrix} \mathbf{1} & \mathbf{1} \\ -\mathbf{1} & \mathbf{1} \end{bmatrix} \mathbf{x} - \begin{bmatrix} \mathbf{1} \\ \mathbf{0} \end{bmatrix} \mathbf{z}_0 - h_n \sum_{l=1}^{N_q} \begin{bmatrix} M_1(\alpha_l)\,\mathbf{1} \\ M_2(\alpha_l)\,\mathbf{1} \end{bmatrix} \mathbf{J} DH(\mathbf{z}^h(\alpha_l)) w_l. \tag{129}$$

We have to also approximate the integral in the tangent such that

$$\mathbf{K}_T \approx \frac{1}{2}\begin{bmatrix} \mathbf{1} & \mathbf{1} \\ -\mathbf{1} & \mathbf{1} \end{bmatrix} - h_n \sum_{l=1}^{N_q} \begin{bmatrix} M_{1,l}\,\mathbf{1} \\ M_{2,l}\,\mathbf{1} \end{bmatrix} \begin{bmatrix} M_{1,l}\,\mathbf{1} & M_{2,l}\,\mathbf{1} \end{bmatrix} \begin{bmatrix} \mathbf{J}\mathcal{H}^h_{H,l} & \mathbf{O}_2 \\ \mathbf{O}_2 & \mathbf{J}\mathcal{H}^h_{H,l} \end{bmatrix} w_l, \quad (130)$$

where the index l denotes the evaluation at the abscissae α_l.

Numerical Example 8.2 *We consider the pendulum of Example 8.1. Therefore, the initial condition is the matrix* $\boldsymbol{z}(t=0) = [-\pi/2,\, 0]^T$*, the length of the rod is* $l = 1$ *and the particle has a mass of* $m = 5$*. Moreover, we choose a gravitational acceleration of* $g = 9.81$*. Figure 17 depicts the rotation angle of the pendulum computed with a time step size* $h_n = 0.1$ *(*$dt = 0.1$*). The dotted line gives the reference solution computed with the cG(2) method again. We used for both methods five Gaussian quadrature points (*$int = 5$*). We do not see a difference between the both methods in Figure 17, ie negligible algorithmic damping of the dG(1) method and very small jumps. To see the jumps, we have to consider a shorter time intervall; see Figure 18. We are able to also see that the initial condition is not exactly fulfilled by the dG(1) method. We used five Gaussian quadrature points but alredy two Gaussian quadrature points yield identical results; cf* Betsch & Steinmann *[9]. The trapezoidal rule leads to larger jumps; see Figure 19. The midpoint rule is an exception again because Figure 20 shows that the jumps also vanish in the nonlinear case. Figure 21 shows the jumps in the course of the total energy approximated by linear time finite elements. We see that the total energy computed by the dG(1) method decays on account of the algorithmic damping. The dotted line depicts the course of the cG(2) method with quadratic time finite elements, which corroborates the algorithmic energy conserving in the sense that* $E(t_n) = E(t_{n-1})$*.*

Remember, we obtained in Subsection 6.2.2 the result that the time-stepping scheme generated by the dG(1) method for the harmonic oscillator in connection with the midpoint rule leads to a continuous solution and further to the time-stepping scheme generated by the cG(1) method with exactly evaluated integrals. Hence we formulate the following

Theorem 8.1 *The general dG(1) method in connection with the midpoint rule leads to the discrete cG(1) method with a continuous solution.*

Proof. We consider the equations (57), (58):

$$\begin{aligned} \frac{1}{2}\,\mathbf{z}_2 + \frac{1}{2}\,\mathbf{z}_1 - \mathbf{z}_0 - h_n \int_0^1 M_1 \mathbf{J} DH(\mathbf{z}^h) d\alpha = \mathbf{0}, \\ \frac{1}{2}\,\mathbf{z}_2 - \frac{1}{2}\,\mathbf{z}_1 - h_n \int_0^1 M_2 \mathbf{J} DH(\mathbf{z}^h) d\alpha = \mathbf{0}. \end{aligned}$$

Addition of equation (57) and equation (58) yields

$$\mathbf{z}_2 - \mathbf{z}_0 - h_n \int_0^1 (M_1 + M_2)\,\mathbf{J} DH(\mathbf{z}^h) d\alpha = \mathbf{0}, \quad (131)$$

and on the other hand, a subtraction of the equations (57), (58) results in

$$\mathbf{z}_1 - \mathbf{z}_0 + h_n \int_0^1 (M_2 - M_1)\,\mathbf{J} DH(\mathbf{z}^h) d\alpha = \mathbf{0}. \quad (132)$$

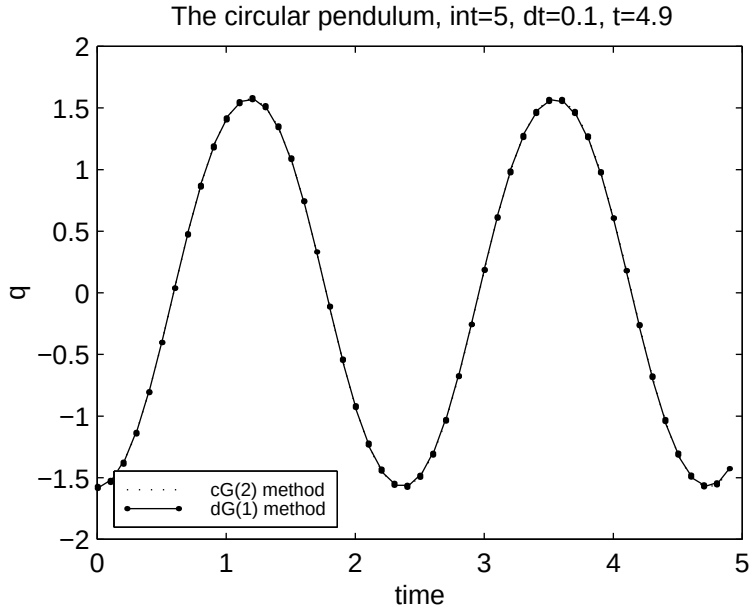

Figure 17: Rotation angle $q = q(t)$ of a circular pendulum with a rod of length $l = 1$, a particle of mass $m = 5$ and gravitational acceleration $g = 9.81$. Computed with the dG(1) method with $h_n = 0.1$ and five Gaussian quadrature points.

We get with the nodal shape functions $M_1 = 1 - \alpha$ and $M_2 = \alpha$

$$M_1 + M_2 = 1, \tag{133}$$
$$M_2 - M_1 = 2\,\alpha - 1. \tag{134}$$

We now introduce the quadrature rule. The midpoint rule approximation of $\int_0^1 f(\alpha)d\alpha$ is $f(\alpha = 1/2)$ such that we obtain a discrete dG(1) method given by

$$\mathbf{z}_2 - \mathbf{z}_0 - h_n\,\mathbf{J}DH(\mathbf{z}^h(\frac{1}{2})) = \mathbf{0}, \tag{135}$$
$$\mathbf{z}_1 - \mathbf{z}_0 = \mathbf{0}. \tag{136}$$

Therefore, the solution, obtained by the midpoint rule, is continuous. This result is corroborated by the numerical calculations; see Figure 20. Employing equation (136) in equation (135) leads to

$$\mathbf{z}_2 - \mathbf{z}_1 - h_n\,\mathbf{J}DH(\mathbf{z}^h(\frac{1}{2})) = \mathbf{0}. \tag{137}$$

Equation (137) is identical with the cG(1) method (47) of which the integral is approximated by the midpoint rule. Accordingly, the dG(1) method can be converted into the cG(1) method by the midpoint rule. □

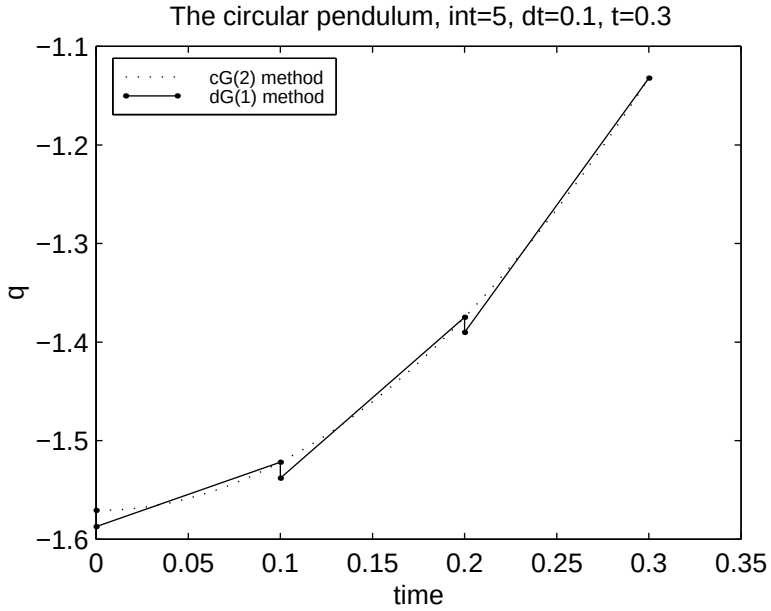

Figure 18: Rotation angle $q = q(t)$ of a circular pendulum with a rod of length $l = 1$, a particle of mass $m = 5$ and gravitational acceleration $g = 9.81$. Computed with the dG(1) method with $h_n = 0.1$ and five Gaussian quadrature points.

Remark 8.1 *In contrast to the harmonic oscillator, we do not expect energy conservation with the time-stepping scheme (137) because according to* Betsch & Steinmann *[9] it is well-known that the midpoint rule does not preserve the energy in the nonlinear regime. Figure 22 corroborates our presumption.*

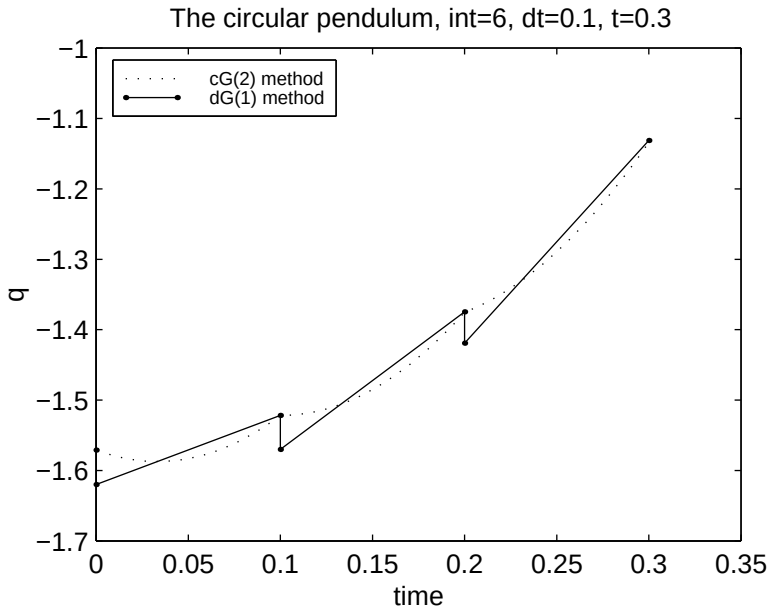

Figure 19: Rotation angle $q = q(t)$ of a circular pendulum with a rod of length $l = 1$, a particle of mass $m = 5$ and gravitational acceleration $g = 9.81$. Computed with the dG(1) method with $h_n = 0.1$ and trapezoidal rule ($N_q = 2$).

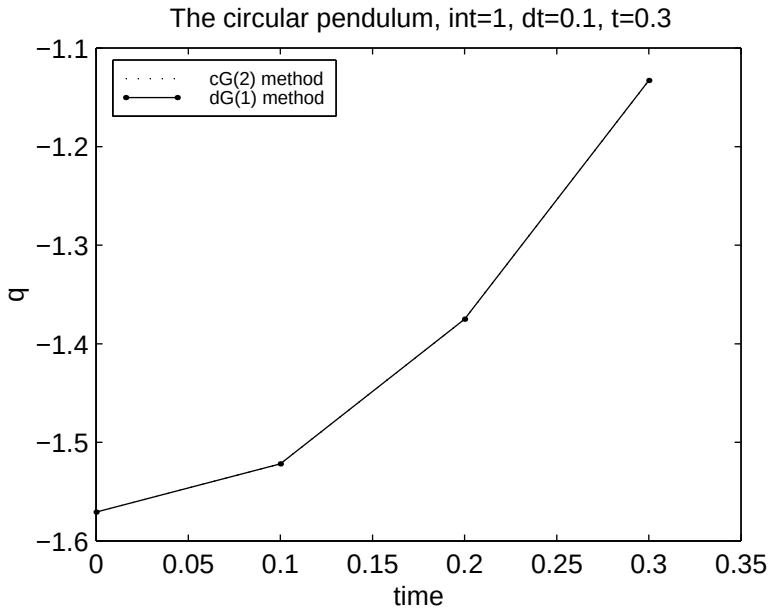

Figure 20: Rotation angle $q = q(t)$ of a circular pendulum with a rod of length $l = 1$, a particle of mass $m = 5$ and gravitational acceleration $g = 9.81$. Computed with the dG(1) method with $h_n = 0.1$ and midpoint rule ($N_q = 1$).

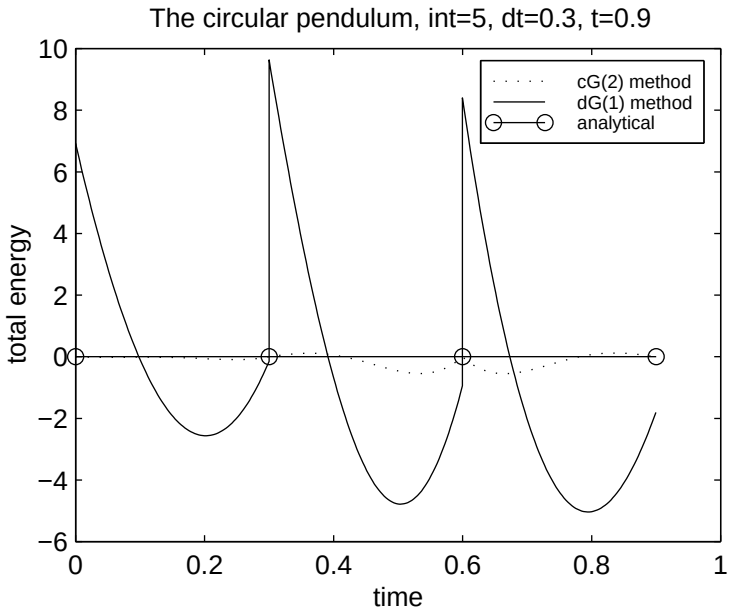

Figure 21: Approximated course $E = E(\mathbf{z}^h(\alpha(t)))$ of the total energy of a circular pendulum with a rod of length $l = 1$, a particle of mass $m = 5$ and gravitational acceleration $g = 9.81$. Computed with the dG(1) method with $h_n = 0.3$.

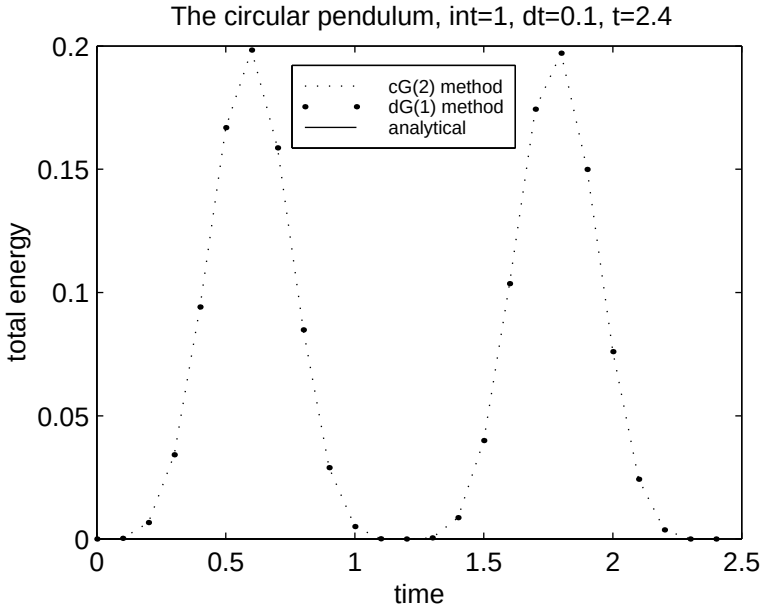

Figure 22: Total energy $E = E(t)$ of a circular pendulum with a rod of length $l = 1$, a particle of mass $m = 5$ and gravitational acceleration $g = 9.81$. Computed with the dG(1) method with $h_n = 0.1$ and midpoint rule ($N_q = 1$).

9 The algorithmic total angular momentum of the circular pendulum

Here we examine the algorithmic total angular momentum $\mathbf{L}_{k+1}$ of the circular pendulum. Note that we refer to $\mathbf{L}_{k+1}$ as the total angular momentum at the $k+1$ node of the master element I_α of the dG(k) method. We deal with constant ($k = 0$) and linear ($k = 1$) time finite elements.
We have established in Section 5 that the total angular momentum $\mathbf{L}$ is preserved only if the total torgue $\mathbf{N}$ vanishes. Owing to the definition (33) of the total torgue, $\mathbf{N}$ vanishes if (i) the total force $\mathbf{F}$ vanishes, ie the gravitational acceleration vector has to vanish or (ii) the total force and the radius vector $\mathbf{r}$ of the particle are linearly dependent vectors, ie the rotation angle q has to amount to $q = \nu\,\pi$, for $\nu = 0, 1, 2, \ldots$; see eg Apostol [2]. Since the generalized coordinate q denotes the rotation angle, we present the radius vector $\mathbf{r}$ in polar coordinates such that we obtain

$$\mathbf{r} = l\,\mathbf{u}_r, \tag{138}$$

where $\|\mathbf{r}\| \equiv r = l$ the length of the rod of the circular pendulum. The vector $\mathbf{u}_r$ denotes the unit vector which reflects the direction of the coordinate r; see Figure 23.

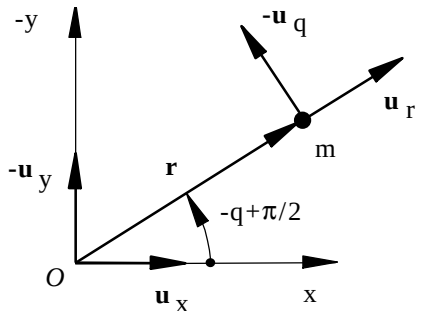

Figure 23: Polar coordinates for the circular pendulum; see eg Apostol [2].

To determine the total angular momentum $\mathbf{L}$ owing to definition (32), we have to calculate the total linear momentum $\mathbf{P} = m\,\dot{\mathbf{r}}$, where m is the mass of the particle. Referring to the radius vector (138), we obtain

$$\mathbf{P} \equiv m\,l\,\frac{d\mathbf{u}_r}{dt} = m\,l\,\partial_q\mathbf{u}_r\,\frac{dq}{dt} = m\,l\,\dot{q}\,\partial_q\mathbf{u}_r. \tag{139}$$

According to Apostol [2] and taking Figure 23 into consideration, the unit vector $\mathbf{u}_r$ is given by

$$\mathbf{u}_r = \sin q\,\mathbf{u}_x - \cos q\,\mathbf{u}_y. \tag{140}$$

We now determine the partial derivative of the unit vector $\mathbf{u}_r$ with respect to the generalized coordinate q:

$$\partial_q \mathbf{u}_r = \cos q\, \mathbf{u}_x + \sin q\, \mathbf{u}_y \equiv -\mathbf{u}_q, \tag{141}$$

where $\mathbf{u}_q$ is also an unit vector, perpendicular to $\mathbf{u}_r$ (see Figure 23), which is defined as

$$\mathbf{u}_q = -\cos q\, \mathbf{u}_x - \sin q\, \mathbf{u}_y. \tag{142}$$

Therefore, the total linear momentum $\mathbf{P}$ is as follows:

$$\mathbf{P} = m\, l\, \dot{q}\, (-\mathbf{u}_q)\,. \tag{143}$$

The total angular momentum $\mathbf{L}$ is defined as the cross product of the radius vector (138) and the total linear momentum (143) such that

$$\mathbf{L} \equiv l\, \mathbf{u}_r \times m\, l\, \dot{q}\, (-\mathbf{u}_q) = -m\, l^2\, \dot{q}\, \mathbf{u}_z = -I\, \dot{q}\, \mathbf{u}_z, \tag{144}$$

where the unit vector $\mathbf{u}_z$ reflects the direction of the z-axis which passes through the origin O and the paper plane, perpendicular to the xy-plane (right-handed coordinate system), and $I = m\, l^2$ denotes the moment of inertia. Taking into account equation (117), we are able to relate the total angular momentum $\mathbf{L}$ to the generalized momentum p:

$$\mathbf{L} = -p\, \mathbf{u}_z. \tag{145}$$

Hence it follows that the generalized momentum p has the magnitude of the total angular momentum $\mathbf{L}$. Since the direction of $\mathbf{L}$ is constant, we only have to consider the behavior of the generalized momentum p.

9.1 Constant time finite elements

First we investigate the generalized momentum of the general dG(0) method (120) for constant time finite elements which reads

$$\mathbf{z}_1 - \mathbf{z}_0 - h_n \int_0^1 \mathbf{J} \begin{bmatrix} dV(q_1)/dq \\ p_1/I \end{bmatrix} d\alpha = \mathbf{0}.$$

To let vanishes the total torgue on the particle, we have to neglect the gravitational acceleration g. Therefore, the potential constant $c = m\, g\, l$ is zero and the potential V vanishes. Accordingly, we obtain

$$\mathbf{z}_1 - \mathbf{z}_0 - h_n \int_0^1 \mathbf{J} \begin{bmatrix} 0 \\ p_1/I \end{bmatrix} d\alpha = \mathbf{0}. \tag{146}$$

Now we can write the integrand in an other form and get

$$\mathbf{z}_1 - \mathbf{z}_0 - h_n \int_0^1 \begin{bmatrix} p_1/I \\ 0 \end{bmatrix} d\alpha = \mathbf{0}. \tag{147}$$

On account of the constant trial function $\mathbf{z}^h = [q_1,\ p_1]^T$, we do not have to make a distinction between the exactly evaluated integral and the use of interpolating quadrature rules; see Subsection 6.1.2. Therefore, it is sufficient to consider the time-stepping scheme which results from equation (147) by exact evaluation of the integral:

$$\mathbf{z}_1 - \mathbf{z}_0 - h_n \begin{bmatrix} p_1/I \\ 0 \end{bmatrix} = \mathbf{0}. \tag{148}$$

To investigate only the generalized momentum $p^h = p_1$, we devolve upon the representation of scalar equations:

$$q_1 - q_0 - \frac{h_n}{I}\, p_1 = 0, \tag{149}$$

$$p_1 - p_0 = 0. \tag{150}$$

It is immediate from equation (150) that the generalized momentum is preserved on each time step. Therefore, the time-stepping scheme obeys the law of conservation of total angular momentum $\mathbf{L}$ according to Theorem 5.1 in the sense that

$$\mathbf{L}_1 = \mathbf{L}_0, \tag{151}$$

where $\mathbf{L}_0$ denotes the total angular momentum at the initial node 0 of the master element I_α.

9.2 Linear time finite elements

In this subsection we examine whether linear time finite elements ($k = 1$) also preserve the generalized momentum and the total angular mometum in the case of vanishing gravitational acceleration ($g = 0$). However, we have to distinguish between employing exact quadrature and using quadrature rules in the dG(1) method.
We consider the general dG(1) method (57), (58) for arbitrary motions of the circular pendulum which is given by

$$\frac{1}{2}\,\mathbf{z}_2 + \frac{1}{2}\,\mathbf{z}_1 - \mathbf{z}_0 - h_n \int_0^1 M_1 \mathbf{J} \begin{bmatrix} dV(q^h)/dq \\ p^h/I \end{bmatrix} d\alpha = \mathbf{0},$$

$$\frac{1}{2}\,\mathbf{z}_2 - \frac{1}{2}\,\mathbf{z}_1 - h_n \int_0^1 M_2 \mathbf{J} \begin{bmatrix} dV(q^h)/dq \\ p^h/I \end{bmatrix} d\alpha = \mathbf{0},$$

where we have used equation (124). The nodal shape functions are $M_1 = 1 - \alpha$ and $M_2 = \alpha$. The scalar trial functions take the shape:

$$q^h(\alpha) = M_1(\alpha)\, q_1 + M_2(\alpha)\, q_2, \tag{152}$$

$$p^h(\alpha) = M_1(\alpha)\, p_1 + M_2(\alpha)\, p_2. \tag{153}$$

The vanishing gravitational acceleration g leads to a potential $V = 0$ so that the dG(1) method takes the form

$$\frac{1}{2}\,\mathbf{z}_2 + \frac{1}{2}\,\mathbf{z}_1 - \mathbf{z}_0 - h_n \int_0^1 M_1 \begin{bmatrix} p^h/I \\ 0 \end{bmatrix} d\alpha = \mathbf{0}, \tag{154}$$

$$\frac{1}{2}\,\mathbf{z}_2 - \frac{1}{2}\,\mathbf{z}_1 - h_n \int_0^1 M_2 \begin{bmatrix} p^h/I \\ 0 \end{bmatrix} d\alpha = \mathbf{0}. \tag{155}$$

Now we give up the symplectic notation and write the dG(1) method by means of scalar equations and obtain

$$\frac{1}{2}\,q_2 + \frac{1}{2}\,q_1 - q_0 - \frac{h_n}{I} \int_0^1 M_1\, p^h d\alpha = 0, \tag{156}$$

$$\frac{1}{2}\,p_2 + \frac{1}{2}\,p_1 - p_0 - h_n \int_0^1 0\, d\alpha = 0, \tag{157}$$

$$\frac{1}{2}\,q_2 - \frac{1}{2}\,q_1 - \frac{h_n}{I} \int_0^1 M_2\, p^h d\alpha = 0, \tag{158}$$

$$\frac{1}{2}\,p_2 - \frac{1}{2}\,p_1 - h_n \int_0^1 0\, d\alpha = 0. \tag{159}$$

Since interpolating quadrature rules evaluate integrals of constant integrands exactly (cf Subsection 6.1.2), we can also write

$$\frac{1}{2}\,q_2 + \frac{1}{2}\,q_1 - q_0 - \frac{h_n}{I} \int_0^1 M_1\, p^h d\alpha = 0, \tag{160}$$

$$\frac{1}{2}\,p_2 + \frac{1}{2}\,p_1 - p_0 = 0, \tag{161}$$

$$\frac{1}{2}\,q_2 - \frac{1}{2}\,q_1 - \frac{h_n}{I} \int_0^1 M_2\, p^h d\alpha = 0, \tag{162}$$

$$\frac{1}{2}\,p_2 - \frac{1}{2}\,p_1 = 0. \tag{163}$$

From the addition of equation (161) and equation (163) it follows

$$p_2 - p_0 = 0. \tag{164}$$

Therefore, regardless of the kind of quadrature being employed, the generalized momentum is conserved for each time step size. On account of the relation (145) linear time finite elements also obey the law of conservation of total angular momentum at each time step:

$$\mathbf{L}_2 = \mathbf{L}_0. \tag{165}$$

10 The algorithmic total energy conservation of the circular pendulum for arbitrary motions with linear time finite elements

In the present section we show how algorithmic total energy conservation for arbitrary motions of the circular pendulum can be obtained with linear time finite elements by a nonstandard quadrature rule.
According to Theorem 8.1 the application of the midpoint rule to the general dG(1) method leads to the discrete cG(1) method of which the integrals are approximated by the midpoint rule. We know from Remark 8.1 in connection with Figure 22 that the resulting time-stepping scheme do not preserve the total energy. However, according to Betsch & Steinmann [7] it is possible to gain algorithmic total energy conservation with the discrete cG(1) method emanating from the so-called modified midpoint rule. In contrast to the standard midpoint rule the modified midpoint rule is weighted such that an arbitrary integral is approximated with

$$\int_0^1 f(\alpha)d\alpha \approx \kappa\, f(\frac{1}{2}), \tag{166}$$

where κ is determined by a condition. We consider the discrete dG(1) method (137) which follows from the proof of Theorem 8.1:

$$\mathbf{z}_2 - \mathbf{z}_0 - h_n\, \mathbf{J} DH(\mathbf{z}^h(\frac{1}{2})) = \mathbf{0}.$$

We have immediately employed equation (136) which reads $\mathbf{z}_1 = \mathbf{z}_0$. However, we leave the symplectic notation and take the explizit representation of the scheme (137). For that purpose, we employ the Jacobian matrix (124) of the hamiltonian. Thus the explizit representation takes the shape:

$$q_2 - q_0 - \frac{h_n}{I}\, p^h(\frac{1}{2}) = 0, \tag{167}$$

$$p_2 - p_0 - h_n\, Q(q^h(1/2)) = 0, \tag{168}$$

where $I = m\, l^2$ and $Q = -dV/dq$ designates the moment of inertia and the generalized force respectively. Now we have to transform the time-stepping scheme according to equation (166) to consider the modified midpoint rule instead of the standard midpoint rule, which means we have to introduce a weight for each integral:

$$q_2 - q_0 - \frac{h_n}{I}\, \kappa_p\, p^h(\frac{1}{2}) = 0, \tag{169}$$

$$p_2 - p_0 - h_n\, \kappa_q\, Q(q^h(1/2)) = 0. \tag{170}$$

The introduction of this weights retains a continuous solution. This states the following

Theorem 10.1 *The general dG(1) method in connection with the modified midpoint rule leads to the discrete cG(1) method with a continuous solution.*

Proof. We consider the general dG(1) method (57), (58):

$$\frac{1}{2}\,\mathbf{z}_2 + \frac{1}{2}\,\mathbf{z}_1 - \mathbf{z}_0 - h_n \int_0^1 M_1 \mathbf{J} DH(\mathbf{z}^h) d\alpha = \mathbf{0},$$
$$\frac{1}{2}\,\mathbf{z}_2 - \frac{1}{2}\,\mathbf{z}_1 - h_n \int_0^1 M_2 \mathbf{J} DH(\mathbf{z}^h) d\alpha = \mathbf{0}.$$

Addition of equation (57) and equation (58) leads to

$$\mathbf{z}_2 - \mathbf{z}_0 - h_n \int_0^1 (M_1 + M_2)\, \mathbf{J} DH(\mathbf{z}^h) d\alpha = \mathbf{0}, \tag{171}$$

and a subtraction of the equations (57), (58) gains

$$\mathbf{z}_1 - \mathbf{z}_0 + h_n \int_0^1 (M_2 - M_1)\, \mathbf{J} DH(\mathbf{z}^h) d\alpha = \mathbf{0}. \tag{172}$$

We obtain with the nodal shape functions $M_1 = 1-\alpha$ and $M_2 = \alpha$ the following relations:

$$M_1 + M_2 = 1, \tag{173}$$
$$M_2 - M_1 = 2\,\alpha - 1. \tag{174}$$

Using the modified midpoint rule according to equation (166) yields a discrete dG(1) method which reads

$$\mathbf{z}_2 - \mathbf{z}_0 - h_n\, \mathbf{K}\mathbf{J} DH(\mathbf{z}^h(\frac{1}{2})) = \mathbf{0}, \tag{175}$$
$$\mathbf{z}_1 - \mathbf{z}_0 = \mathbf{0}, \tag{176}$$

where

$$\mathbf{K} = \begin{bmatrix} \kappa_p \mathbf{I} & \mathbf{O} \\ \mathbf{O} & \kappa_q \mathbf{I} \end{bmatrix}. \tag{177}$$

Therefore, the solution is also continuous by applying the modified midpoint rule. On the other hand, employing equation (176) in equation (175) leads to

$$\mathbf{z}_2 - \mathbf{z}_1 - h_n\, \mathbf{K}\mathbf{J} DH(\mathbf{z}^h(\frac{1}{2})) = \mathbf{0}. \tag{178}$$

Note that equation (178) is identical with the cG(1) method (47) of which the integral is approximated by the modified midpoint rule. Hence, the dG(1) method can be transformed into the discrete cG(1) method emanating from the modified midpoint rule. □
Obviously, the scheme in (169), (170) is the explicit representation of equation (175). According to Betsch & Steinmann [7], the condition for energy conservation is the exact fulfillment of the Fundamental Theorem of Calculus for the kinetic energy $T = T(p^h)$ which reads

$$T_2 - T_1 = \int_0^1 \partial_p T(p^h) \left(p^h\right)' d\alpha \equiv \int_0^1 \partial_p H(p^h) \left(p^h\right)' d\alpha, \tag{179}$$

as well as for the potential $V = V(q^h)$:

$$V_2 - V_1 = \int_0^1 \partial_q V(q^h) \left(q^h\right)' \, d\alpha \equiv \int_0^1 \partial_q H(q^h) \left(q^h\right)' \, d\alpha, \tag{180}$$

where the prime indicates differentiation with respect to α. Taking into account the equation (119) and the trial function $\mathbf{z}^h \equiv [q^h,\, p^h]^T$, the equations (179) and (180) take the form:

$$T_2 - T_1 = \int_0^1 \frac{1}{I}\, p^h \left(p^h\right)' \, d\alpha, \tag{181}$$

$$V_2 - V_1 = \int_0^1 \frac{dV(q^h)}{dq} \left(q^h\right)' \, d\alpha. \tag{182}$$

Now we consider the explizit trial functions. First we employ $p^h = \sum_{i=1}^2 M_i\, p_i$ in equation (181):

$$T_2 - T_1 = \int_0^1 \frac{1}{I} \left(\sum_{i=1}^2 M_i(\alpha)\, p_i \right) (p_2 - p_1) \, d\alpha, \tag{183}$$

where $M_1 = 1-\alpha$ and $M_2 = \alpha$. We aim at fulfilling the equation (183) with the modifiied midpoint rule according to equation (166). Therefore, we obtain

$$T_2 - T_1 = \frac{\kappa_p}{2\, I} \, (p_1 + p_2)\, (p_2 - p_1)\,. \tag{184}$$

The expansion of equation (184) yields

$$T_2 - T_1 = \kappa_p \left(\frac{1}{2\, I}\, p_2^2 - \frac{1}{2\, I}\, p_1^2 \right). \tag{185}$$

In consideration of the hamiltonian $H = T + V$ in equation (118), we are able to simplify the right side of equation (185) as follows:

$$T_2 - T_1 = \kappa_p \, (T_2 - T_1)\,. \tag{186}$$

Hence it follows that the Fundamental Theorem of Calculus for the kinetic energy is satisfied for the weight $\kappa_p = 1$, which means the standard midpoint rule.
Now we employ the trial function $q^h = \sum_{i=1}^2 M_i\, q_i$ in equation (182) and obtain

$$V_2 - V_1 = \int_0^1 \frac{dV(q^h(\alpha))}{dq} \, (q_2 - q_1) \, d\alpha. \tag{187}$$

Applying the modified midpoint rule according to equation (166) to equation (187) yields

$$V_2 - V_1 = \kappa_q \, \frac{dV(q^h(1/2))}{dq} \, (q_2 - q_1)\,. \tag{188}$$

Accordingly, we obtain the following weight if we consider that the solution is continuous:

$$\kappa_q = -\frac{\tilde{Q}}{Q(q^h(1/2))}, \tag{189}$$

with

$$\tilde{Q} = \frac{V_2 - V_0}{q_2 - q_0}. \tag{190}$$

The calculated weights of the modified midpoint rule yields the following time-stepping scheme:

$$q_2 - q_0 - \frac{h_n}{2\,I}\,(p_0 + p_2) = 0, \tag{191}$$

$$p_2 - p_0 + h_n\,\tilde{Q} = 0. \tag{192}$$

The time-stepping scheme (191), (192) is identical with the scheme in Betsch & Steinmann [9] which is generated by the cG(1) method with exact quadrature. Furthermore, owing to the time-stepping scheme (191), (192) we are able to formulate the following

Theorem 10.2 *The modified midpoint rule conserves the algorithmic total energy of the circular pendulum for linear time finite elements.*

Proof. We consider the time-stepping scheme (191), (192). Taking into account the identity (190), equation (192) multiplied by $(q_2 - q_0)$ reads

$$(p_2 - p_0)\,(q_2 - q_0) + h_n\,(V_2 - V_0) = 0. \tag{193}$$

Employing equation (191), equation (193) yields

$$\frac{h_n}{2\,I}\,(p_2 - p_0)\,(p_0 + p_2) + h_n\,(V_2 - V_0) = 0. \tag{194}$$

Expanding equation (194) gains

$$h_n\left(\frac{1}{2\,I}\,p_2^2 - \frac{1}{2\,I}\,p_0^2\right) + h_n\,(V_2 - V_0) = 0. \tag{195}$$

With regard to the hamiltonian $H = T + V$ of the circular pendulum in equation (118), for a non-vanishing time step size h_n the equation (195) leads to

$$H_2 - H_0 = 0. \tag{196}$$

□

To solve the time-stepping scheme (191), (192) by applying the Newton-Raphson method, which is depicted in Table 6, we need the residual

$$R(q_2) = \frac{2\,I}{h_n}\,(q_2 - q_0) - 2\,p_0 + h_n\tilde{Q}. \tag{197}$$

The tangent $K_T = \partial_{q_2} R(q_2)$ takes the form

$$K_T = \frac{2\,I}{h_n} + h_n\,\partial_{q_2}\tilde{Q}. \tag{198}$$

Given: initial conditions q_0 and p_0, time step size h_n and residual tolerance $\epsilon = 10^{-13}$ set iteration counter $l = 1$
Find: nodal unknown q_2 and p_2
(a) initialization $q_2^{(l)} = q_0 + h_n/(2\,I)\,\left(p_0 + p_2^{(l)}\right)$ (b) compute residual $R^{(l)} = R(q_2^{(l)})$ if $\|R^{(l)}\| > \epsilon$ goto (c) else goto (d) (c) compute tangent $K_T^{(l)} = K_T(q_2^{(l)})$ solve for increment $\Delta\, q_2^{(l)}$ $\Delta\, q_2^{(l)} = -\left(K_T^{(l)}\right)^{-1} R^{(l)}$ update the nodal unknowns $q_2^{(l+1)} = q_2^{(l)} + \Delta\, q_2^{(l)}$ goto (b) with $l = l + 1$ (d) update generalized momentum $p_2^{(l)} = (2\,I)/h_n\,\left(q_2^{(l)} - q_0\right) - p_0$ (e) end.

Table 6: Newton-Raphson method to solve the time-stepping scheme generated by the dG(1) method with modified midpoint rule for the circular pendulum.

We calculate $\partial_{q_2}\tilde{Q}$ with the derivative formula for a quotient of two functions:

$$\partial_{q_2}\tilde{Q} = \frac{dV(q_2)/dq - \tilde{Q}}{q_2 - q_0}. \tag{199}$$

Employing equation (199) in equation (198), the tangent reads

$$K_T = \frac{2\,I}{h_n} - h_n\,\frac{Q_2 + \tilde{Q}}{q_2 - q_0}, \tag{200}$$

with the generalized force

$$Q_2 = -\frac{dV(q_2)}{dq}. \tag{201}$$

Numerical Example 10.1 *We compute the total energy of a circular pendulum with the modified midpoint rule. Let the initial condition be* $\boldsymbol{z} = [-\pi/2,\, 1]^T$. *The particle*

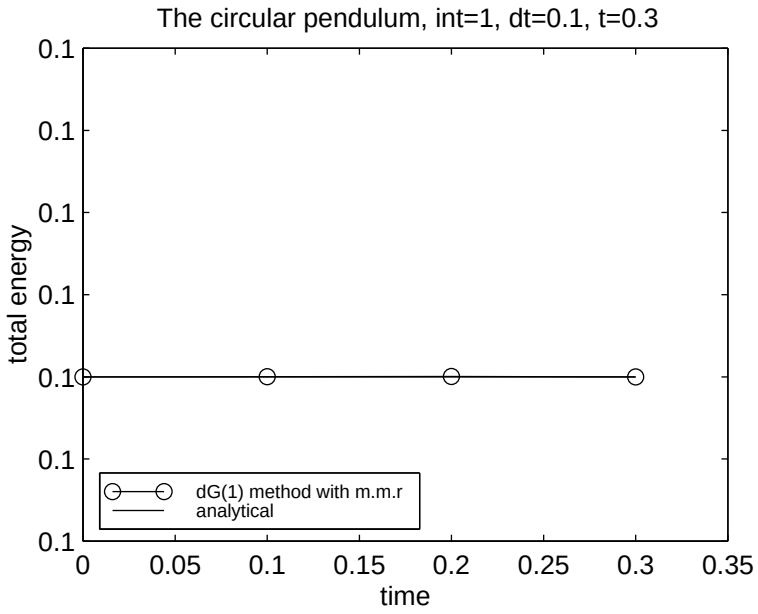

Figure 24: Total energy $E = E(t)$ of a circular pendulum with a rod of length $l = 1$, a particle of mass $m = 5$ and gravitational acceleration $g = 9.81$. Computed with the dG(1) method with the modified midpoint rule and by a time step size $h_n = 0.1$.

has the mass $m = 5$ *and the length of the rod is* $l = 1$. *Further, we take a gravitational acceleration* $g = 9.81$. *Figure 24 bear out the algorithmic conservation of the total energy. Figure 25 give a comparison of the discrete dG(1) method emanating from the modified midpoint rule with the discrete dG(1) and cG(2) method emanating from the standard midpoint rule. According to Remark 6.3 the dG(1) and cG(2) method lead to identical schemes by applying the standard midpoint rule; therefore, in this case the total energies of both methods are identical. Referring to* Betsch & Steinmann *[9] it is well-known that the standard midpoint rule does not conserves the total energy in the nonlinear regime, what is corroborated in Figure 25.*

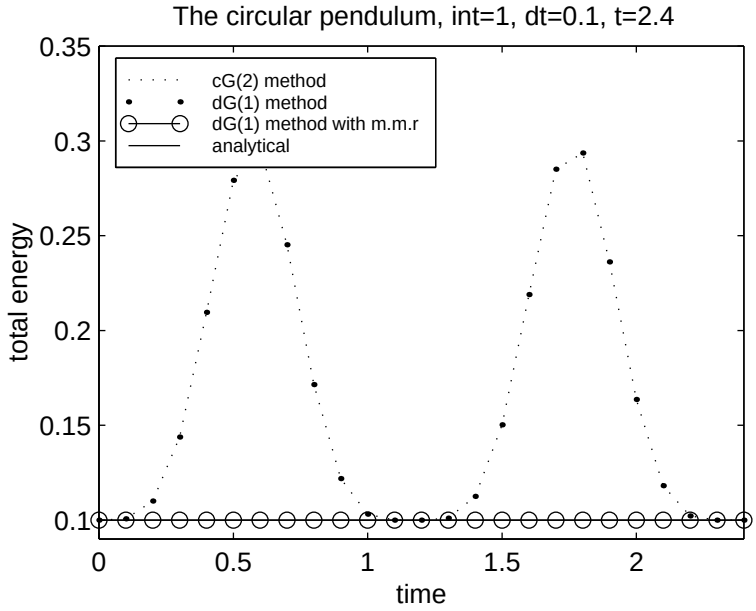

Figure 25: Total energy $E = E(t)$ of a circular pendulum with a rod of length $l = 1$, a particle of mass $m = 5$ and gravitational acceleration $g = 9.81$. Computed with the dG(1) method with the modified midpoint rule and by a time step size $h_n = 0.1$.

Part III
The Two-Body Central Force Problem

This part of the paper in hand is concerned with the motion of two particles m_1 and m_2 which takes place in the three-dimensional euclidean space $\mathcal{E}^3$. We introduce an inertial cartesian coordinate system (x, y, z) with the origin O; see Figure 26. The two particles move under the influence of a central force field. Such a natural system is said to be closed. For more details, we refer to ARNOLD [3], GOLDSTEIN [14] and KUYPERS [25].

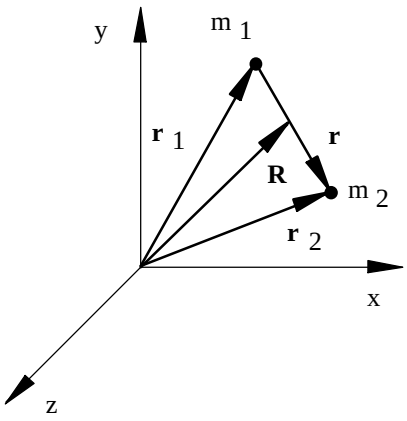

Figure 26: System of two particles in the three-dimensional euclidean space $\mathcal{E}^3$.

We compute the system by applying constant ($k = 0$) and linear ($k = 1$) finite elements in time corresponding to the dG method. We consider both a linear and a nonlinear central force. The goal is the investigation of the conservation laws which means the total energy and the total angular momentum $\mathbf{L}$.

11 The reduction to an equivalent one-body problem

First we summarize the derivation of the equations of motion of the two particles. Newton's second law of motion implies for a closed system of two particles

$$m_1 \ddot{\mathbf{r}}_1 = \mathbf{F}_{12}, \tag{202}$$
$$m_2 \ddot{\mathbf{r}}_2 = \mathbf{F}_{21}, \tag{203}$$

where r_i, $i = 1, 2$, denotes the radius vector of the ith particle (see Figure 26) and the force of interaction $\mathbf{F}_{ij}$, $j = 1, 2$, denotes a force vector in the direction from the ith to the jth particle. Furthermore, the weak law of action and reaction implies that $\mathbf{F}_{ij}$ and $\mathbf{F}_{ji}$ are equal and opposite:

$$\mathbf{F}_{ij} = -\mathbf{F}_{ji}. \tag{204}$$

Therefore, the equations (202), (203) may be written as

$$m_1 \, \ddot{\mathbf{r}}_1 = -\mathbf{F}, \tag{205}$$

$$m_2 \, \ddot{\mathbf{r}}_2 = \mathbf{F}, \tag{206}$$

where $\mathbf{F} \equiv \mathbf{F}_{21}$ denotes the total force. Owing to the nature of an euclidean space the total force $\mathbf{F}$ is able to depend only on the difference vector $\mathbf{r} \equiv \mathbf{r}_2 - \mathbf{r}_1$ and the time derivative $\dot{\mathbf{r}}$. In the present thesis, we exclusively consider natural systems such that an explizit dependence on time t does not appear:

$$\mathbf{F} = f(\mathbf{r}, \dot{\mathbf{r}}) \, \mathbf{u}_r, \tag{207}$$

where $\mathbf{u}_r = \mathbf{r}/r$ denotes the unit vector in direction of $\mathbf{r}$ and $r \equiv \|\mathbf{r}\|$ denotes the magnitude of $\mathbf{r}$ with respect to the euclidean norm. The scalar function f denotes the magnitude of the total force $\mathbf{F}$. Obviously, the total force $\mathbf{F}$ is co-linear with the vector $\mathbf{r}$. Since the total force depends on the difference vector $\mathbf{r}$, we introduce the components of the difference vector as new coordinates of the motion. Addition of equation (205) and equation (206) leads to

$$m_1 \, \ddot{\mathbf{r}}_1 + m_2 \, \ddot{\mathbf{r}}_2 = \mathbf{0}, \tag{208}$$

where $\mathbf{0}$ denotes a 3×1 zero matrix. Considering the definition of the radius vector $\mathbf{R}$ to the center of mass of n_p particles

$$\mathbf{R} = \frac{\sum_{i=1}^{n_p} m_i \, \mathbf{r}_i}{\sum_{i=1}^{n_p} m_i}, \tag{209}$$

the equation (208) takes the following form:

$$\ddot{\mathbf{R}} = \mathbf{0}. \tag{210}$$

Therefore, it is apparent that the center of mass is either at rest or moving uniformly. We now subtract equation (205) from (206) and obtain

$$\mu \, \ddot{\mathbf{r}} = \mathbf{F}, \tag{211}$$

where

$$\mu = \frac{m_1 \, m_2}{m_1 + m_2} \tag{212}$$

denotes the reduced mass. Thus we have substituted the components of the difference vector $\mathbf{r}$ and the components of the radius vector $\mathbf{R}$ for the components of the radii vectors $\mathbf{r}_1$ and $\mathbf{r}_2$ as coordinates of the motion. The new equations of motion (210),

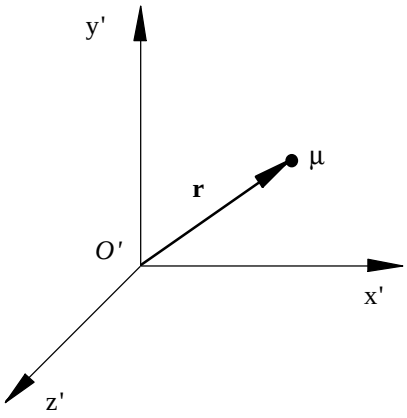

Figure 27: The reduced mass μ in the three-dimensional euclidean space $\mathcal{E}'^3$.

(211) are uncoupled so that two independent motions occur: the motion of the center of mass $\mathbf{R}$ of the two particles m_1 and m_2 (the inertial motion) and the motion of the reduced mass μ at a distance $\mathbf{r}$ from a fixed center of force (the relative motion).
The subsequent discussion deals only with the motion of the reduced mass μ. Let $\mathcal{E}'^3$ be a three-dimensional euclidean space, including an inertial cartesian coordinate system (x', y', z') with the origin O' in which the difference vector $\mathbf{r}$ denotes the radius vector of the reduced mass μ with respect to O'; see Figure 27. Furthermore, the origin O' is also the center of the total force $\mathbf{F}$ of equation (211). Note that a force which directs to a point of an euclidean space is called a central force. The central force $\mathbf{F}$ can only take the form

$$\mathbf{F} = f(\mathbf{r})\,\mathbf{u}_r. \tag{213}$$

To aim at a natural system, we restrict to conservative central forces $\mathbf{F} = -\partial_{\mathbf{r}} V$ which can be derived from a potential V which exclusively depends on the magnitude $r = \|\mathbf{r}\|$ of the radius vector $\mathbf{r}$ so that

$$\mathbf{F} \equiv -\partial_{\mathbf{r}} V = -\frac{dV(r)}{dr}\,\mathbf{u}_r \equiv f(r)\,\mathbf{u}_r. \tag{214}$$

We now have the two-body problem reduced to the motion of the reduced mass μ in a three-dimensional euclidean space with the following nonlinear equation of motion:

$$\mu\,\ddot{\mathbf{r}} = -\frac{dV(\|\mathbf{r}\|)}{dr}\,\frac{\mathbf{r}}{\|\mathbf{r}\|}. \tag{215}$$

Furthermore, the reduced mass μ, moving relative to the origin of the euclidean space, preserves the total angular momentum $\mathbf{L} = \mathbf{r} \times \mathbf{P}$, where $\mathbf{P} = \mu\,\dot{\mathbf{r}}$ denotes the total linear momentum of the reduced mass. That ensues from Theorem 5.1 because the total torgue $\mathbf{N} = \mathbf{r} \times \mathbf{F}$ vanishes on account of equation (214). The direction of the total

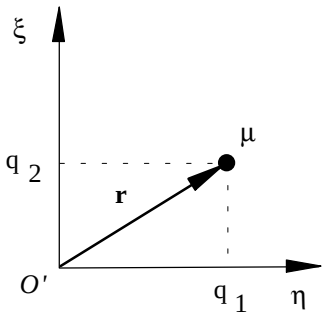

Figure 28: Euclidean plane of motion $\mathcal{E}_m^2 \subset \mathcal{E}'^3$ of the reduced mass μ.

angular momentum is perpendicular to the radius vector independently of time because the scalar product $\mathbf{r}\cdot\mathbf{L}$ vanishes. Hence the motion $\mathbf{r} = \mathbf{r}(t)$ of the reduced mass μ always lies in an euclidean plane $\mathcal{E}_m^2 \subset \mathcal{E}'^3$. Since the reduced mass has two degrees of freedom ($n_{dof} = 2$), we only need two generalized coordinates. In the subsequent discussion we consider the cartesian coordinates q_1 und q_2; see Figure 28.

12 The Hamiltonian formulation of the equivalent one-body problem

In this section we develop the Hamiltonian formulation of the one-body problem which represents the unknown relative motion of the two-body problem. The problem is as follows: the reduced mass is moving in an euclidean plane $\mathcal{E}_m^2 \subset \mathcal{E}'^3$ with two degrees of freedom. The motion is influenced by a conservative central force

$$\mathbf{F} = -\frac{dV(\|\mathbf{r}\|)}{dr}\,\frac{\mathbf{r}}{\|\mathbf{r}\|}, \tag{216}$$

with respect to the origin O', where $\mathbf{r}$ and $V(\|\mathbf{r}\|)$ denotes the radius vector of the reduced mass and the potential of the central force respectively.
The total kinetic energy T of this natural system is

$$T = \frac{1}{2}\,\mu\,\dot{\mathbf{r}}^2. \tag{217}$$

We express the radius vector $\mathbf{r}$ in the (η,ξ) coordinate system in the way

$$\mathbf{r} = q_1\,\mathbf{u}_\eta + q_2\,\mathbf{u}_\xi, \tag{218}$$

where the unit vectors $\mathbf{u}_\eta$ and $\mathbf{u}_\xi$ reflect the direction of the η-axis and the ξ-axis respectively. Since (η,ξ) is an inertial system, the velocity vector of the reduced mass is as follows:

$$\dot{\mathbf{r}} = \dot{q}_1\,\mathbf{u}_\eta + \dot{q}_2\,\mathbf{u}_\xi. \tag{219}$$

Thus the matrix representation of the velocity vector with respect to the basis $\{\mathbf{u}_\eta, \mathbf{u}_\xi\}$ is given by

$$\dot{\mathbf{q}} = \begin{bmatrix} \dot{q}_1 \\ \dot{q}_2 \end{bmatrix}, \tag{220}$$

where we refer to $\dot{\mathbf{q}}$ as the generalized velocity vector. According to equation (217), the total kinetic energy takes the shape

$$T = \frac{1}{2}\,\mu\,\dot{\mathbf{q}}^T\mathbf{I}\,\dot{\mathbf{q}}. \tag{221}$$

The matrix representation with respect to the basis $\{\mathbf{u}_\eta, \mathbf{u}_\xi\}$ also represents the transformation from the radius vector $\mathbf{r}$ to the generalized coordinate vector

$$\mathbf{q} = \begin{bmatrix} q_1 \\ q_2 \end{bmatrix}. \tag{222}$$

Hence it follows that the potential V may be expressed as $V = V(\sqrt{\mathbf{q}^T\mathbf{q}})$ so that the lagrangian $L(\mathbf{q}, \dot{\mathbf{q}})$ takes the form

$$L(\mathbf{q}, \dot{\mathbf{q}}) = \frac{1}{2}\,\mu\,\dot{\mathbf{q}}^T\mathbf{I}\,\dot{\mathbf{q}} - V(\sqrt{\mathbf{q}^T\mathbf{q}}). \tag{223}$$

To obtain the hamiltonian H, we have to determine the generalized momentum vector $\mathbf{p} = [p_1,\, p_2]^T$. Referring to definition (5), we get

$$\mathbf{p} \equiv \partial_{\dot{\mathbf{q}}} L = \mu\,\dot{\mathbf{q}}, \tag{224}$$

considering the differentiation rule of quadratic forms owing to Zurmühl & Falk [35]. Introducing the generalized momentum vector $\mathbf{p}$ in the total kinetic energy (221) leads to

$$H(\mathbf{q}, \mathbf{p}) = \frac{1}{2\,\mu}\,\mathbf{p}^T\mathbf{I}\,\mathbf{p} + V(\sqrt{\mathbf{q}^T\mathbf{q}}). \tag{225}$$

13 A time finite element formulation for the isotropic harmonic oscillator

At first we consider Hooke's central force law which implies a linear restoring force associated with each degree of freedom (isotropic case). According to Goldstein [14] the Hooke's central force $\mathbf{F}$ results in closed orbits for all bound particles. The potential V of the central force $\mathbf{F}$ is given by

$$V = -\frac{1}{2}\,c\,\|\mathbf{r}\|^2, \tag{226}$$

with $c < 0$ and expressing the euclidean norm by the generalized coordinate vector $\mathbf{q}$, we obtain

$$V = -\frac{1}{2}\,c\,\mathbf{q}^T\mathbf{I}\,\mathbf{q}. \tag{227}$$

We gain the hamiltonian H of Hooke's law by equation (225)

$$H(\mathbf{q}, \mathbf{p}) = \frac{1}{2\,\mu}\,\mathbf{p}^T\mathbf{I}\,\mathbf{p} - \frac{1}{2}\,c\,\mathbf{q}^T\mathbf{I}\,\mathbf{q}. \tag{228}$$

To use the dG(k) method (22), we have to introduce the symplectic notation in the hamiltonian H. On account of the quadratic form of the total kinetic energy T and the potential V, we also obtain a quadratic form of the hamiltonian H in symplectic notation. With $\mathbf{z} = [\mathbf{q},\, \mathbf{p}]^T$ we have

$$H = \frac{1}{2}\,\mathbf{z}^T\mathbf{H}\,\mathbf{z}, \tag{229}$$

where owing to $n_{dof} = 2$, $\mathbf{H}$ is a 4×4 matrix of the shape

$$\mathbf{H} = \begin{bmatrix} -c\,\mathbf{I} & \mathbf{O} \\ \mathbf{O} & 1/\mu\,\mathbf{I} \end{bmatrix}. \tag{230}$$

Using the derivative formula for quadratic forms (see eg Zurmühl & Falk [35]), we get the Jacobian matrix $DH(\mathbf{z})$ owing to equation (229) as follows:

$$DH(\mathbf{z}) = \mathbf{H}\,\mathbf{z}. \tag{231}$$

13.1 Constant time finite elements

In this subsection we examine a finite element formulation for constant time elements. Apart from the matrix dimensions, the hamiltonian (229) is analogously to the hamiltonian (41) of the harmonic oscillator which is based upon the circular pendulum. Therefore, we will gain time-stepping schemes which have the form of Subsection 6.1 and we do not have to distinguish between exact quadrature and interpolating quadrature rules; see Subsection 6.1.2.
Referring to equation (46), the time-stepping scheme emanating from exact quadrature of the dG(0) method (45) reads

$$(\mathbf{1} - h_n\,\mathbf{JH})\;\mathbf{z}_1 = \mathbf{z}_0.$$

Analogous to Subsection 6.1.1, this time-stepping scheme will be solved by the Newton-Raphson method according to Table 2.

Numerical Example 13.1 *We compute the orbit of the reduced mass $\mu = 2$. The total energy E of the reduced mass and the potential constant c are $E = 0.25$ and $c = -0.25$ respectively. Owing to this values, the orbit has to be circular. We determine the initial condition $\boldsymbol{z}(t = 0)$ according to* Gross *[15]. The used initial condition leads to a circular orbit only for the energy conserving cG(1) method; see Figure 29. On account of the asymptotic annihilation, the dG(0) method computes a spiral orbit. Note that for a clear presentation only the nodal points corresponding to the dG(0) method have been plotted in Figure 29.*

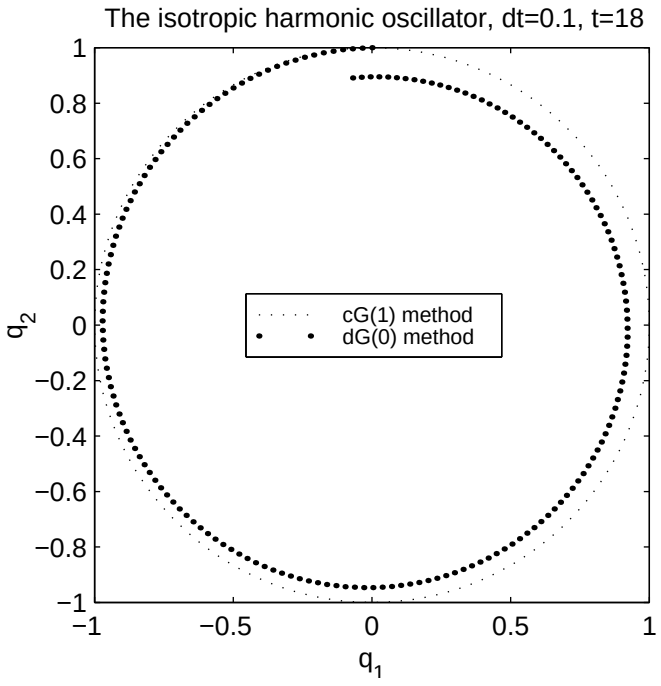

Figure 29: Orbit of an isotropic harmonic oscillator with the reduced mass $\mu = 2$, total energy $E = 0.25$ and potential constant $c = -0.25$. Computed with the dG(0) method with $h_n = 0.1$.

13.2 Linear time finite elements

Next we examine a finite element formulation for linear time finite elements. Linear finite elements in time also yield time-stepping schemes which are equivalent to the corresponding schemes for the harmonic oscillator; see Subsection 6.2. The dG(1) method for Hooke's law is equivalent to equations (57), (58) which reads

$$\begin{aligned}\frac{1}{2}\,\mathbf{z}_2 + \frac{1}{2}\,\mathbf{z}_1 - \mathbf{z}_0 - h_n \int_0^1 M_1 \mathbf{J} DH(\mathbf{z}^h) d\alpha = \mathbf{0},\\ \frac{1}{2}\,\mathbf{z}_2 - \frac{1}{2}\,\mathbf{z}_1 - h_n \int_0^1 M_2 \mathbf{J} DH(\mathbf{z}^h) d\alpha = \mathbf{0}.\end{aligned}$$

The linear trial function $\mathbf{z}^h(\alpha) = (1-\alpha)\ \mathbf{z}_1 + \alpha\,\mathbf{z}_2$ requires a distinction between exact quadrature and the use of quadrature rules.

13.2.1 Exact quadrature

The exact evaluation of the two integrals in the equations (57), (58) lead to the time-stepping scheme (61), (62) which reads:

$$\begin{aligned}\frac{1}{2}\left(\mathbf{1} - \frac{1}{3}\,h_n\,\mathbf{J}\,\mathbf{H}\right)\,\mathbf{z}_2 + \frac{1}{2}\left(\mathbf{1} - \frac{2}{3}\,h_n\,\mathbf{J}\,\mathbf{H}\right)\,\mathbf{z}_1 - \mathbf{z}_0 = \mathbf{0},\\ \frac{1}{2}\left(\mathbf{1} - \frac{2}{3}\,h_n\,\mathbf{J}\,\mathbf{H}\right)\,\mathbf{z}_2 - \frac{1}{2}\left(\mathbf{1} + \frac{1}{3}\,h_n\,\mathbf{J}\,\mathbf{H}\right)\,\mathbf{z}_1 = \mathbf{0}.\end{aligned}$$

We determine the numerical solution by applying the Newton-Raphson method as described in Table 3, where the residual vector $\mathbf{R}$ and the tangent $\mathbf{K}_T$ is given by the equivalent equations (63) and (64) respectively.

Numerical Example 13.2 *Now we compare the dG(0) method with the dG(1) method by computing the same oscillator as in Example 13.1. That means: mass $\mu = 2$, a total energy $E = 0.25$ and a potential constant $c = -0.25$. Figure 30 shows the orbit of the oscillator computed with the dG(1) and the energy preserving cG(2) method. In contrast to the orbit of the dG(0) method in Figure 29, the dG(1) method does not reveal a perceptible asymptotic annihilation in the same time interval. The algorithmic damping of the dG(1) method with exactly evaluated integrals is for the isotropic harmonic oscillator very small. Cf the phase plane of the harmonic oscillator in Figure 7. Analogous to the harmonic oscillator, we see the jumps of dG(1) method in a brief time interval; see Figure 31.*

13.2.2 The use of specific quadrature rules

Let us evaluate the integrals of the equivalent equations (57), (58) by interpolating quadrature rules. Owing to the form of the Jacobian matrix $DH(\mathbf{z})$ in equation (231), the time-stepping schemes generated by the dG(1) method for the isotropic harmonic

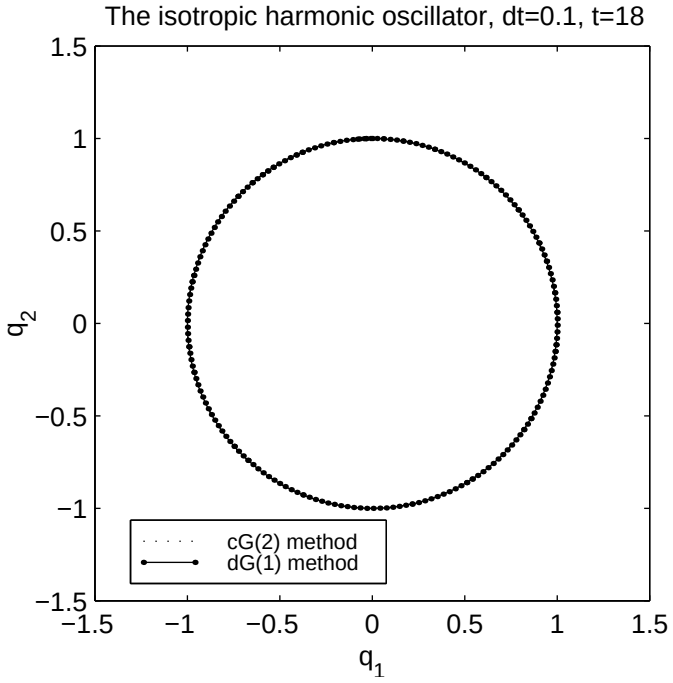

Figure 30: Orbit of an isotropic harmonic oscillator with the reduced mass $\mu = 2$, total energy $E = 0.25$ and potential constant $c = -0.25$. Computed with the dG(1) method with $h_n = 0.1$.

oscillator take the shape of the schemes in Subsection 6.2.2 which read

$$\left(\frac{1}{2}\,\mathbf{1} - \beta_{12}\,h_n\,\mathbf{JH}\right)\,\mathbf{z}_2 + \left(\frac{1}{2}\,\mathbf{1} - \beta_{11}\,h_n\,\mathbf{JH}\right)\,\mathbf{z}_1 - \mathbf{z}_0 = \mathbf{0},$$
$$\left(\frac{1}{2}\,\mathbf{1} - \beta_{22}\,h_n\,\mathbf{JH}\right)\,\mathbf{z}_2 - \left(\frac{1}{2}\,\mathbf{1} + \beta_{12}\,h_n\,\mathbf{JH}\right)\,\mathbf{z}_1 = \mathbf{0}.$$

We refer to Table 4 for the coefficients β_{ij} of the considered quadrature rules. On grounds of the equivalence of the time-stepping schemes for the harmonic and the isotropic harmonic oscillator, we gain the results of Subsection 6.2.2.

Numerical Example 13.3 *For a brief demonstration of this equivalence, we compute by the midpoint rule the orbit of the same oscillator as in Example 13.1, ie mass $\mu = 2$, total energy $E = 0.25$ and potential constant $c = -0.25$. According to Subsection 6.2.2 we expect for the dG(1) method a continuous orbit and nodal values which are identical with the nodal values of the cG(2) method. Figure 32 shows the expected result.*

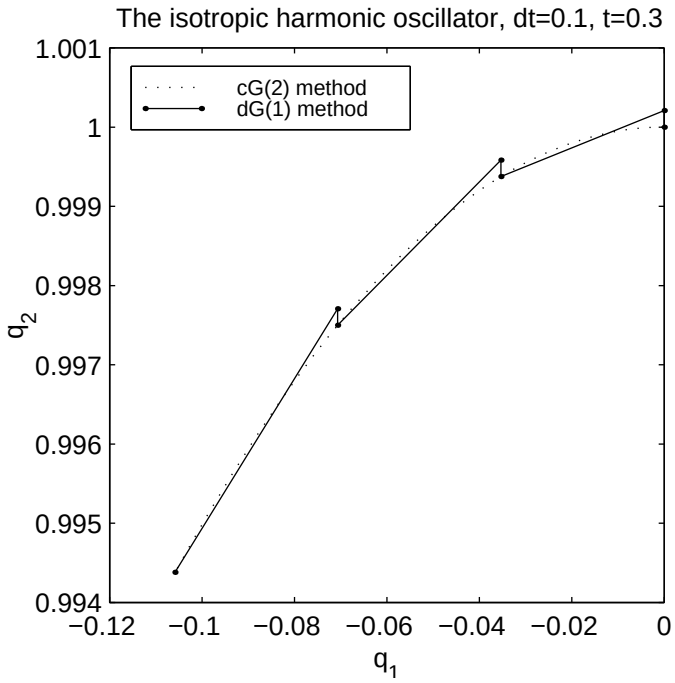

Figure 31: Orbit of an isotropic harmonic oscillator with the reduced mass $\mu = 2$, total energy $E = 0.25$ and potential constant $c = -0.25$. Computed with the dG(1) method with $h_n = 0.1$.

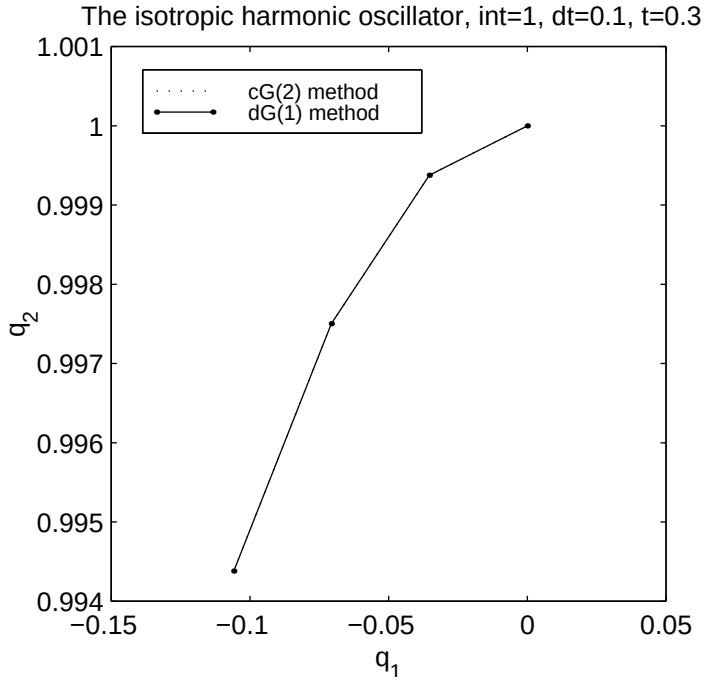

Figure 32: Orbit of an isotropic harmonic oscillator with the reduced mass $\mu = 2$, total energy $E = 0.25$ and potential constant $c = -0.25$. Computed with the dG(1) method with midpoint rule ($N_q = 1$) and by a time step size $h_n = 0.1$.

14 The algorithmic total energy of the isotropic harmonic oscillator

This section determines the behavior of the algorithmic total energy of the isotropic harmonic oscillator by the Lagrange-Sylvester's interpolation polynomial which we have introduced for the harmonic oscillator in Section 7. Since the time-stepping schemes for both oscillators only differ by the matrix dimensions, the way of calculating the algorithmic hamiltonian H_{k+1} is identical.

14.1 Constant time finite elements

First we consider the dG(0) method with constant time finite elements. Owing to the equations (230) and (45), the amplification matrix $\mathbf{A}_0$ is as follows:

$$\mathbf{A}_0 = \frac{1}{1+\Omega^2} \begin{bmatrix} \mathbf{I} & h_n/\mu\, \mathbf{I} \\ h_n\, c\, \mathbf{I} & \mathbf{I} \end{bmatrix}, \tag{232}$$

with the sampling frequency $\Omega = h_n\, \omega$ and the eigenfrequency $\omega = \sqrt{-c/\mu}$, $c < 0$. The eigenvalues of the amplification matrix (232) read

$$\lambda_1 = \lambda_3 = \frac{1}{1 - i\,\Omega}, \qquad \lambda_2 = \lambda_4 = \frac{1}{1 + i\,\Omega}, \tag{233}$$

where i denotes the imaginary unit. Accordingly, the amplification matrix (232) has multiple eigenvalues, ie the characteristic polynomial

$$P_c(\lambda) = \prod_{i=1}^{4} (\lambda - \lambda_i) \tag{234}$$

of $\mathbf{A}_0$ has multiple roots. But this characteristic polynomial which satisfies the characteristic equation $P_c(\lambda) = 0$ is not a polynomial of minimum degree. The polynomial $P_m(\lambda)$ of minimum degree which also fulfills the equation $P_m(\lambda) = 0$ is called the minimal polynomial (see eg Loomis & Sternberg [28]) and takes here the form

$$P_m(\lambda) = (\lambda - \lambda_1)\,(\lambda - \lambda_2)\,. \tag{235}$$

To show that the polynomial (235) holds for the condition $P_m(\lambda) = 0$, we may use the Cayley-Hamilton theorem owing to Lorenz [29]. The Cayley-Hamilton theorem states that $\mathbf{A}_0$ satisfies its own characteristic equation which means

$$P_c(\mathbf{A}_0) \equiv \prod_{i=1}^{4} (\mathbf{A}_0 - \lambda_i\, \mathbf{1}) = \mathbf{0}. \tag{236}$$

Since the minimal polynomial is a factor of the characteristic polynomial, the minimal polynomial has to also fulfill the condition $P_m(\mathbf{A}_0) = \mathbf{0}$. Because of $(\mathbf{A}_0 - \lambda_1\, \mathbf{1}) \neq \mathbf{0}$

but $(\mathbf{A}_0 - \lambda_1\,\mathbf{1})(\mathbf{A}_0 - \lambda_2\,\mathbf{1}) = \mathbf{0}$ is the polynomial (235) the minimal polynomial $P_m(\lambda)$ of the amplification matrix (232). According to GANTMACHER [13] we have to choose in the equations (88), (89) $N_\lambda = \deg(P_m) \equiv 2$, where $\deg(P_m)$ denotes the degree of the minimal polynomial. Therefore, we may continue in the way of Subsection 7.1 and calculate the constituent matrices owing to equation (89):

$$\mathbf{A}_{0,1} = \frac{1}{2}\begin{bmatrix} \mathbf{I} & -1/(i\,\omega\,\mu)\,\mathbf{I} \\ -i\,\omega\,\mu\,\mathbf{I} & \mathbf{I} \end{bmatrix}, \qquad \mathbf{A}_{0,2} = \frac{1}{2}\begin{bmatrix} \mathbf{I} & 1/(i\,\omega\,\mu)\,\mathbf{I} \\ i\,\omega\,\mu\,\mathbf{I} & \mathbf{I} \end{bmatrix}. \tag{237}$$

This constituent matrices also satisfy the conditions (95), (96) such that according to equation (97), we also come to the algorithmic hamiltonian

$$H_1 = \frac{1}{2}\,\rho^2\,\mathbf{z}_0^T\mathbf{H}\,\mathbf{z}_0 = \rho^2\,H_0. \tag{238}$$

Thus the behavior of the algorithmic hamiltonian H_1 of the dG(0) method depends for $H_0 \neq 0$ on the spectral radius ρ of the amplification matrix $\mathbf{A}_0$ as follows:

$$\begin{cases} \rho^2 < 1, & \text{energy decay} \\ \rho^2 = 1, & \text{energy conservation} \\ \rho^2 > 1, & \text{energy growth} \end{cases}$$

The squared spectral radius $\rho^2 = \lambda_1\lambda_2$ of the amplification matrix (232) yields

$$\rho^2 = \frac{1}{1+\Omega^2}, \tag{239}$$

where it is identical to the squared spectral radius (99) of the harmonic oscillator in Subsection 7.1. Hence we are able to refer to Figure 9 for a plot of the spectral radius. Equation (239) also implies that for all sampling frequencies $\Omega \neq 0$ the denominater is bigger than the numerator. Accordingly, the squared spectral radius is less than one for $\Omega \neq 0$ and we gain algorithmic energy decay; see Figure 33. We get for interpolating quadrature rules the same result because the time-stepping schemes are the same; see Subsection 13.1.

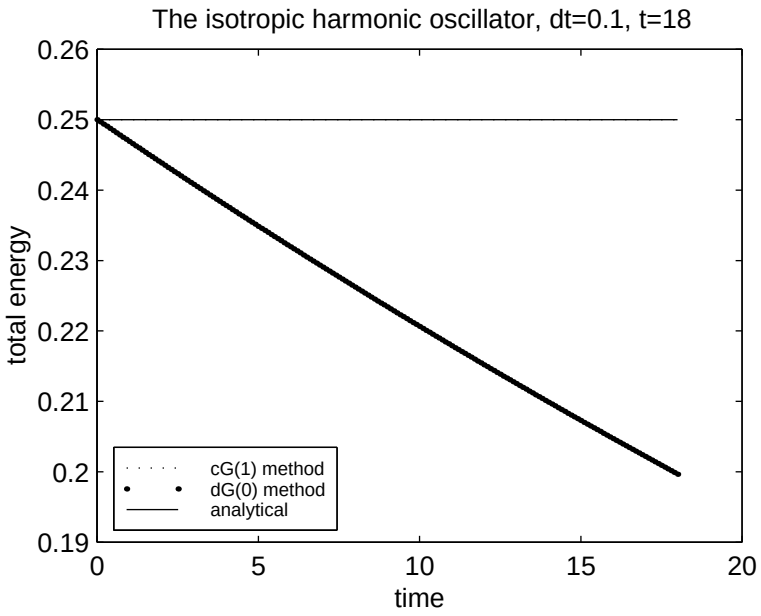

Figure 33: Total energy $E = E(t)$ of an isotropic harmonic oscillator with the reduced mass $\mu = 2$, total energy $E = 0.25$ and potential constant $c = -0.25$. Computed with the dG(0) method with $h_n = 0.1$.

14.2 Linear time finite elements

Next we investigate the algorithmic hamiltonian H_2 of the dG(1) method. In contrast to the dG(0) method in Subsection 14.1, we have to distinguish between exactly evaluated integrals and the use of quadrature rules. Through the equivalent time-stepping schemes, we will also get different matrices but an identical spectral radius as for the harmonic oscillator.

14.2.1 Time-stepping scheme associated with exact quadrature

The considered time-stepping scheme consists of the equations (61), (62) in conjunction with the matrix (230). The elimination of the internal node $\mathbf{z}_1$ leads to the two-level scheme (100), out of which we are able to identify the amplification matrix:

$$\mathbf{A}_1 = \frac{-2}{\Omega^4 + 4\,\Omega^2 + 36} \begin{bmatrix} (7\,\Omega^2 - 18)\,\mathbf{I} & h_n/\mu\,(\Omega^2 - 18)\,\mathbf{I} \\ h_n\,c\,(\Omega^2 - 18)\,\mathbf{I} & (7\,\Omega^2 - 18)\,\mathbf{I} \end{bmatrix}. \tag{240}$$

The eigenvalues of the amplification matrix (240) read

$$\lambda_1 = \lambda_3 = -2\,\frac{7\,\Omega^2 - 18 + i\,\Omega\,(\Omega^2 - 18)}{\Omega^4 + 4\,\Omega^2 + 36}, \tag{241}$$

$$\lambda_2 = \lambda_4 = -2\,\frac{7\,\Omega^2 - 18 - i\,\Omega\,(\Omega^2 - 18)}{\Omega^4 + 4\,\Omega^2 + 36}, \tag{242}$$

where i denotes the imaginary unit. According to equation (89) we determine the constituent matrices and obtain:

$$\mathbf{A}_{1,1} = \frac{1}{2} \begin{bmatrix} \mathbf{I} & 1/(i\,\omega\,\mu)\,\mathbf{I} \\ i\,\omega\,\mu\,\mathbf{I} & \mathbf{I} \end{bmatrix}, \qquad \mathbf{A}_{1,2} = \frac{1}{2} \begin{bmatrix} \mathbf{I} & -1/(i\,\omega\,\mu)\,\mathbf{I} \\ -i\,\omega\,\mu\,\mathbf{I} & \mathbf{I} \end{bmatrix}. \tag{243}$$

The constituent matrices (243) satisfy the conditions (95), (96). Accordingly, equation (106) is also valid for the isotropic harmonic oscillator:

$$H_2 = \frac{1}{2}\,\rho^2\,\mathbf{z}_0^T \mathbf{H}\,\mathbf{z}_0 = \rho^2\,H_0. \tag{244}$$

From equation (244) we are able to conclude:

$$\begin{cases} \rho^2 < 1, & \text{energy decay} \\ \rho^2 = 1, & \text{energy conservation} \\ \rho^2 > 1, & \text{energy growth} \end{cases}$$

The squared spectral radius ρ which determines the algorithmic hamiltonian H_2 results from the eigenvalues (241), (242). We get

$$\rho^2 = \frac{4\,\Omega^2 + 36}{\Omega^4 + 4\,\Omega^2 + 36}. \tag{245}$$

This spectral radius is identical to the spectral radius of the harmonic oscillator which is why we also gain energy decay for all sampling frequencies $\Omega \neq 0$; see Figure 34.

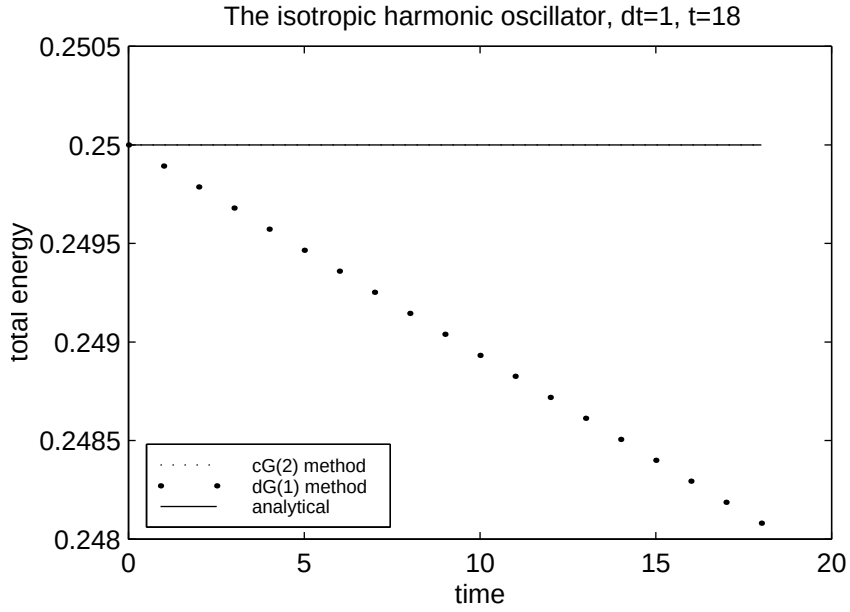

Figure 34: Total energy $E = E(t)$ of an isotropic harmonic oscillator with the reduced mass $\mu = 2$, total energy $E = 0.25$ and potential constant $c = -0.25$. Computed with the dG(1) method with $h_n = 1$.

14.2.2 Time-stepping schemes associated with specific quadrature rules

To consider quadrature rules, we are allowed to use the time-stepping scheme (70), (71) for the harmonic oscillator and take into account the definition of the vector $\mathbf{z}$ for the isotropic harmonic oscillator. Moreover, we employ equation (230) in the scheme. Because of the complicated terms, we renounce an explicit representation of the amplification matrix and of the eigenvalues. The constituent matrices are identical with the matrices (243). Therefore, the algorithmic hamiltonian which we obtain by interpolating quadrature rules takes the form of equation (110):

$$H_{2,q} = \frac{1}{2}\,\rho_q^2\,\mathbf{z}_0^T\mathbf{H}\,\mathbf{z}_0 = \rho_q^2\,H_0, \tag{246}$$

The following squared spectral radius is given for an arbitrary interpolating quadrature rule:

$$\rho_q^2 = \frac{1 + 4\,\beta_{12}^2\,\Omega^2}{1 + 4\,\beta_{12}^2\,\Omega^2 + \left(\beta_{22} - \beta_{11}\right)^2\Omega^2 + 4\left(\beta_{12}^2 - \beta_{11}\,\beta_{22}\right)^2\Omega^4}, \tag{247}$$

where we refer to Table 4 for the coefficients β_{ij} of the considered quadrature rules. We have already obtained the spectral radius (247) for the harmonic oscillator in Subsec-

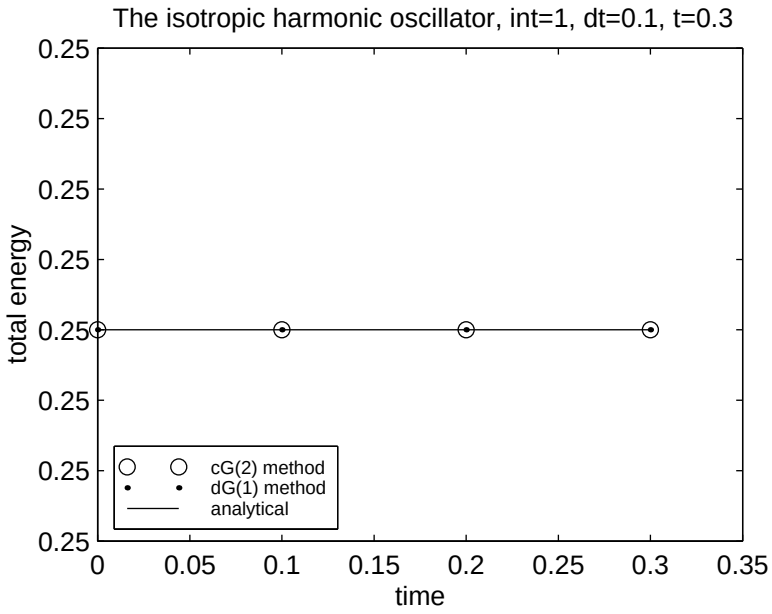

Figure 35: Total energy $E = E(t)$ of an isotropic harmonic oscillator with the reduced mass $\mu = 2$, total energy $E = 0.25$ and potential constant $c = -0.25$. Computed with the dG(1) method with midpoint rule ($N_q = 1$) and by a time step size $h_n = 0.1$.

tion 7.2.2. Therefore, we get the results given in Subsection 7.2.2 from the discussion of the spectral radius (247). For example, we gain energy conservation by the midpoint rule; see Figure 35.

15 The algorithmic total angular momentum of the isotropic harmonic oscillator

This section deals with the total angular momentum $\mathbf{L}$ of the reduced mass μ. We adhere to the planar Hamiltonian formulation with respect to the euclidean plane of motion $\mathcal{E}_m^2$ (see Figure 28) because according to Gross [15] we are able to determine the initial condition for the numerical examples easily.
We consider the equivalent one-body problem. Therefore, we are able to refer to Section 5 for the calculation of the total angular momentum. We describe the motion of the isotropic harmonic oscillator by means of the cartesian coordinates q_1 and q_2; see Figure 28. Thus the radius vector $\mathbf{r}$ of the reduced mass μ is given by

$$\mathbf{r} = q_1\,\mathbf{u}_\eta + q_2\,\mathbf{u}_\xi. \tag{248}$$

Accordingly, the total linear momentum $\mathbf{P} = \mu\,\dot{\mathbf{r}}$ result in

$$\mathbf{P} = \mu\,(\dot{q}_1\,\mathbf{u}_\eta + \dot{q}_2\,\mathbf{u}_\xi) \tag{249}$$

because the unit vectors $\mathbf{u}_\eta$,$\mathbf{u}_\xi$ are linear combinations of the inertial unit vectors of the euclidean space $\mathcal{E}'^3$. In the consequence of the equations (220), (224), the total linar momentum $\mathbf{P}$ may be written in the form

$$\mathbf{P} = p_1\,\mathbf{u}_\eta + p_2\,\mathbf{u}_\xi. \tag{250}$$

Furthermore, the matrix representation of the total linear momentum $\mathbf{P}$ with respect to the basis $\{\mathbf{u}_\eta, \mathbf{u}_\xi\}$ takes the form

$$\mathbf{P} = \begin{bmatrix} p_1 \\ p_2 \end{bmatrix}. \tag{251}$$

We see that the matrix representation of total linear momentum $\mathbf{P}$ is identical with the generalized momentum vector (224) of the reduced mass. Moreover, according to equation (222) the matrix representation of the radius vector $\mathbf{r}$ is identical with the generalized coordinate vector $\mathbf{q} = [q_1,\ q_2]^T$. Therefore, the definition (32) of the total angular momentum $\mathbf{L}$ yields

$$\begin{aligned} \mathbf{L} &= (q_1\,\mathbf{u}_\eta + q_2\,\mathbf{u}_\xi) \times (p_1\,\mathbf{u}_\eta + p_2\,\mathbf{u}_\xi) && (252)\\ &= q_1\,p_2\ (\mathbf{u}_\eta \times \mathbf{u}_\xi) + q_2\,p_1\ (\mathbf{u}_\xi \times \mathbf{u}_\eta) && (253)\\ \mathbf{L} &= (q_1\,p_2 - q_2\,p_1)\ \mathbf{u}_\zeta, && (254) \end{aligned}$$

where $\mathbf{u}_\zeta = \mathbf{u}_\eta \times \mathbf{u}_\xi$ denotes a new unit vector which is perpendicular to $\mathbf{u}_\eta$ and $\mathbf{u}_\xi$ such that a right-handed cartesian coordinate system (η, ξ, ζ) is introduced.
Next we define an operator $\bowtie$ to obtain a compact matrix representation of the total angular momentum by means of the generalized coordinate vector $\mathbf{q}$ and the generalized momentum vector $\mathbf{p}$. The matrix representation of the total angular momentum (254) with respect to the basis $\{\mathbf{u}_\eta, \mathbf{u}_\xi, \mathbf{u}_\zeta\}$ takes the shape:

$$\mathbf{L} = \begin{bmatrix} 0 \\ 0 \\ q_1\,p_2 - q_2\,p_1 \end{bmatrix}. \tag{255}$$

Owing to the fact that the matrix representations of the radius vector $\mathbf{r}$ and the total linear momentum $\mathbf{P}$ are equivalent to the generalized coordinate vector $\mathbf{q}$ and the generalized momentum vector $\mathbf{p}$ respectively, the matrix representation (255) of the total angular momentum also results from the cross product

$$\mathbf{L} = \begin{bmatrix} q_1 \\ q_2 \\ 0 \end{bmatrix} \times \begin{bmatrix} p_1 \\ p_2 \\ 0 \end{bmatrix}. \tag{256}$$

To use the 2×1 matrices $\mathbf{q}$ and $\mathbf{p}$ in a compact notation, we define an operator $\bowtie$ as follows:

$$\mathbf{q} \bowtie \mathbf{p} = \begin{bmatrix} \mathbf{q} \\ 0 \end{bmatrix} \times \begin{bmatrix} \mathbf{p} \\ 0 \end{bmatrix}. \tag{257}$$

The following calculations with the operator $\bowtie$ determine the directly following theorem of which the proofs are based upon theorems of the cross product; see eg APOSTOL [2].

Theorem 15.1 *For all* 2×1 *matrices* $\boldsymbol{a}$,$\boldsymbol{b}$,$\boldsymbol{c}$ *and for all real* a, *we have*

(i) $\boldsymbol{a} \bowtie \boldsymbol{b} = -(\boldsymbol{b} \bowtie \boldsymbol{a})$ *(skew symmetry),*

(ii) $\boldsymbol{a} \bowtie (\boldsymbol{b} + \boldsymbol{c}) = \boldsymbol{a} \bowtie \boldsymbol{b} + \boldsymbol{a} \bowtie \boldsymbol{c}$ *(distributive law),*

(iii) $(a\,\boldsymbol{a}) \bowtie \boldsymbol{b} = a\,(\boldsymbol{a} \bowtie \boldsymbol{b})$,

(iv) $\boldsymbol{a} \bowtie \boldsymbol{a} = [0,0,0]^T$,

(v) $\boldsymbol{0} \bowtie \boldsymbol{a} = [0,0,0]^T$, *where* $\boldsymbol{0}$ *designates the* 2×1 *zero matrix.*

Hence it follows that we are able to write the total angular momentum $\mathbf{L}$ in matrix form as follows:

$$\mathbf{L} = \mathbf{q} \bowtie \mathbf{p}. \tag{258}$$

Now let us consider the algorithmic total angular momentum $\mathbf{L}_{k+1}$, where the index $k+1$ denotes the value at the $k+1$ node of the master element I_α of the dG(k) method. Referring to equation (258), the algorithmic total angular momentum is given by

$$\mathbf{L}_{k+1} = \mathbf{q}_{k+1} \bowtie \mathbf{p}_{k+1}. \tag{259}$$

We aim at a representation which $\mathbf{L}_{k+1}$ presents only as a linear function of $\mathbf{L}_0$, where $\mathbf{L}_0 = \mathbf{q}_0 \bowtie \mathbf{p}_0$ denotes the algorithmic total angular momentum at the initial node 0 of the master element I_α. To obtain the generalized coordinate vector $\mathbf{q}_{k+1}$ and the generalized momentum vector $\mathbf{p}_{k+1}$ in dependence of the initial values $\mathbf{q}_0$ and $\mathbf{p}_0$, we consider the two-level scheme (87) of the dG(k) method. Again, we introduce Lagrange-Sylvester's interpolation polynomial of the amplification matrix $\mathbf{A}_k$ of the dG(k) method. The minimal polynomial of the isotropic harmonic oscillator has two distinct roots ($N_\lambda = 2$) so that we get the following two-level scheme:

$$\mathbf{z}_{k+1} = \sum_{i=1}^{2} \lambda_i\, \mathbf{A}_{k,i}\, \mathbf{z}_0, \tag{260}$$

where λ_i and $\mathbf{A}_{k,i}$ denotes the ith eigenvalue and the ith constituent matrix respectively. However, the determination of the algorithmic total angular momentum requires leaving the symplectic notation of the two-level scheme:

$$\begin{bmatrix} \mathbf{q}_{k+1} \\ \mathbf{p}_{k+1} \end{bmatrix} = \sum_{i=1}^{2} \lambda_i \begin{bmatrix} \mathbf{A}_{k,i}^{(1,1)} & \mathbf{A}_{k,i}^{(1,2)} \\ \mathbf{A}_{k,i}^{(2,1)} & \mathbf{A}_{k,i}^{(2,2)} \end{bmatrix} \begin{bmatrix} \mathbf{q}_0 \\ \mathbf{p}_0 \end{bmatrix}. \tag{261}$$

The matrices $\mathbf{A}_{k,i}^{(l,m)}$, $l, m \in \{1, 2\}$, denote the four $n_{dof} \times n_{dof}$ blocks of the $2n_{dof} \times 2n_{dof}$ constituent matrix $\mathbf{A}_{k,i}$. We consider the constituent matrices (237) and (243) for constant and linear time finite elements respectively, so that in this section $k \in \{0, 1\}$ and hence the blocks of the constituent matrices have the form

$$\mathbf{A}_{k,i}^{(l,m)} = a_{k,i}^{(l,m)} \, \mathbf{I}. \tag{262}$$

Thus expansion of the matrices on the right side and introduction of an explicit representation leads to the following two equations:

$$\mathbf{q}_{k+1} = \sum_{i=1}^{2} \lambda_i \, a_{k,i}^{(1,1)} \, \mathbf{q}_0 + \sum_{i=1}^{2} \lambda_i \, a_{k,i}^{(1,2)} \, \mathbf{p}_0, \tag{263}$$

$$\mathbf{p}_{k+1} = \sum_{i=1}^{2} \lambda_i \, a_{k,i}^{(2,1)} \, \mathbf{q}_0 + \sum_{i=1}^{2} \lambda_i \, a_{k,i}^{(2,2)} \, \mathbf{p}_0. \tag{264}$$

Employing the equations (263), (264) in the equation (259) leads to

$$\mathbf{L}_{k+1} = \left(\sum_{i=1}^{2} \lambda_i \, a_{k,i}^{(1,1)} \, \mathbf{q}_0 + \sum_{i=1}^{2} \lambda_i \, a_{k,i}^{(1,2)} \, \mathbf{p}_0 \right) \bowtie \left(\sum_{i=1}^{2} \lambda_i \, a_{k,i}^{(2,1)} \, \mathbf{q}_0 + \sum_{i=1}^{2} \lambda_i \, a_{k,i}^{(2,2)} \, \mathbf{p}_0 \right). \tag{265}$$

The Application of the properties (i), (ii) of Theorem 15.1 enables the expansion of the equation (265):

$$\mathbf{L}_{k+1} = \sum_{i=1}^{2} \lambda_i \, a_{k,i}^{(1,1)} \, \mathbf{q}_0 \bowtie \sum_{j=1}^{2} \lambda_j \, a_{k,j}^{(2,1)} \, \mathbf{q}_0 + \sum_{i=1}^{2} \lambda_i \, a_{k,i}^{(1,1)} \, \mathbf{q}_0 \bowtie \sum_{j=1}^{2} \lambda_j \, a_{k,j}^{(2,2)} \, \mathbf{p}_0 + \tag{266}$$

$$+ \sum_{i=1}^{2} \lambda_i \, a_{k,i}^{(1,2)} \, \mathbf{p}_0 \bowtie \sum_{j=1}^{2} \lambda_j \, a_{k,j}^{(2,1)} \, \mathbf{q}_0 + \sum_{i=1}^{2} \lambda_i \, a_{k,i}^{(1,2)} \, \mathbf{p}_0 \bowtie \sum_{j=1}^{2} \lambda_j \, a_{k,j}^{(2,2)} \, \mathbf{p}_0. \tag{267}$$

Using property (iii) of Theorem 15.1 results in

$$\mathbf{L}_{k+1} = \sum_{i,j=1}^{2} \left(\lambda_i \, \lambda_j \, a_{k,i}^{(1,1)} \, a_{k,j}^{(2,1)} \, \mathbf{q}_0 \bowtie \mathbf{q}_0 + \lambda_i \, \lambda_j \, a_{k,i}^{(1,1)} \, a_{k,j}^{(2,2)} \, \mathbf{q}_0 \bowtie \mathbf{p}_0 \right) + \tag{268}$$

$$+ \sum_{i,j=1}^{2} \left(\lambda_i \, \lambda_j \, a_{k,i}^{(1,2)} \, a_{k,j}^{(2,1)} \, \mathbf{p}_0 \bowtie \mathbf{q}_0 + \lambda_i \, \lambda_j \, a_{k,i}^{(1,2)} \, a_{k,j}^{(2,2)} \, \mathbf{p}_0 \bowtie \mathbf{p}_0 \right). \tag{269}$$

The properties (i) and (iv) of Theorem 15.1 make it possible to simplify as follows:

$$\mathbf{L}_{k+1} = \sum_{i,j=1}^{2} \lambda_i \, \lambda_j \, \left(a_{k,i}^{(1,1)} \, a_{k,j}^{(2,2)} - a_{k,i}^{(1,2)} \, a_{k,j}^{(2,1)} \right) \mathbf{L}_0. \tag{270}$$

The coefficients $a_{k,i}^{(l,m)}$ of the main diagonal blocks of the constituent matrices (237) and (243) are identical one half so that the condition $a_{k,i}^{(1,1)} = a_{k,j}^{(2,2)} = 1/2$ is fulfilled. Therefore, we obtain

$$\mathbf{L}_{k+1} = \sum_{i,j=1}^{2} \lambda_i \, \lambda_j \, \left(\frac{1}{4} - a_{k,i}^{(1,2)} \, a_{k,j}^{(2,1)} \right) \mathbf{L}_0. \tag{271}$$

Further, the coefficients of the off-diagonal blocks of the constituent matrices (237), (243) satisfy the identities $a_{k,i}^{(1,2)} \, a_{k,j\neq i}^{(2,1)} = -1/4$ and $a_{k,i}^{(1,2)} \, a_{k,j=i}^{(2,1)} = 1/4$ so that

$$\mathbf{L}_{k+1} = \rho^2 \, \mathbf{L}_0, \tag{272}$$

where $k \in \{0, 1\}$ and $\rho^2 \equiv \lambda_1 \, \lambda_2$ denotes the squared spectral radius. Hence it follows that for the isotropic harmonic oscillator, in addition to the algorithmic total energy H_{k+1}, the algorithmic total angular momentum L_{k+1} also depends only on the squared spectral radius.

15.1 Constant time finite elements

We begin with investigating the algorithmic total angular momentum of the dG(0) method ($k = 0$). Since we do not have to distinguish between exactly evaluated integrals and using interpolating quadrature rules, we consider only the scheme which we obtained by exact quadrature. To use the equation (272) of the algorithmic total angular momentum for $k = 0$, we need only the squared spectral radius of the constituent matrices (237) which according to equation (239) takes the form

$$\rho^2 = \frac{1}{1 + \Omega^2}.$$

The relation (272) in connection with the squared spectral radius (239) shows that only for a sampling frequency $\Omega = 0$ conservation of the algorithmic total angular momentum $\mathbf{L}_1$ occurs and that for $\Omega \neq 0$ the algorithmic total angular momentum $\mathbf{L}_1$ decays; see Figure 36. According to Betsch & Steinmann [7] the algorithmic total angular momentum of the cG(1) method is preserved for the equivalent one-body problem which is why in Figure 36 the dotted line of the cG(1) method is covered by the solid line of the exact total angular momentum.

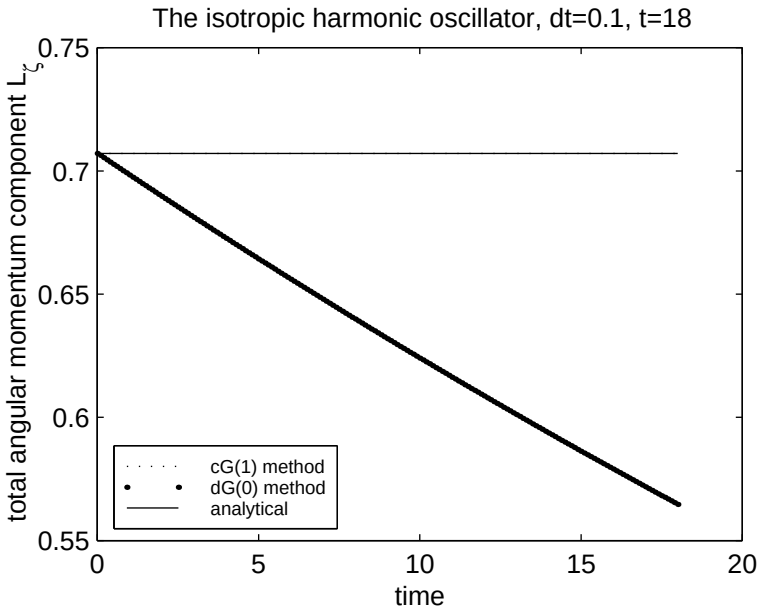

Figure 36: Total angular momentum component $L_\zeta = L_\zeta(t)$ of an isotropic harmonic oscillator with the reduced mass $\mu = 2$, total energy $E = 0.25$ and potential constant $c = -0.25$. Computed with the dG(0) method with $h_n = 0.1$.

15.2 Linear time finite elements

Here we elaborate on linear time finite elements ($k = 1$). The linear trial function implies in the dG(1) method a necessary distinction between exactly evaluated integrals and the use of quadrature rules.

15.2.1 Time-stepping scheme associated with exact quadrature

In this subsection we consider the time-stepping scheme which we gain by exact evaluation of the integrals. Owing to equation (272), the algorithmic total angular momentum $\mathbf{L}_2$ depends only on the squared spectral radius ρ. According to equation (245), the squared spectral radius in the case of exactly evaluated integrals is given by

$$\rho^2 = \frac{4\,\Omega^2 + 36}{\Omega^4 + 4\,\Omega^2 + 36}.$$

Thus it is obvious that the algorithmic total angular momentum $\mathbf{L}_2$ for $\Omega \neq 0$ decays (see Figure 37) and obeys the law of conservation of total angular momentum only for $\Omega = 0$.

15.2.2 Time-stepping schemes associated with specific quadrature rules

Now we consider the use of interpolating quadrature rules. Owing to relation (272), the squared spectral radius is exclusively of interest for the algorithmic total angular momentum $\mathbf{L}_1$, which is given by the equation (247) and reads

$$\rho_q^2 = \frac{1 + 4\,\beta_{12}^2\,\Omega^2}{1 + 4\,\beta_{12}^2\,\Omega^2 + (\beta_{22} - \beta_{11})^2\,\Omega^2 + 4\,(\beta_{12}^2 - \beta_{11}\,\beta_{22})^2\,\Omega^4}.$$

We refer to Table 4 for the coefficients β_{ij} of the considered quadrature rules. It is obvious that we get conservation of algorithmic total angular momentum only for $\beta_{11} = \beta_{12} = \beta_{22}$ because then $\rho_q^2 = 1$. Therefore, according to Table 4 only the midpoint rule preserves the algorithmic total angular momentum; see Figure 38. The other quadrature rules lead to a decay of the algorithmic total angular momentum because the numerator of the squared spectral radius (247) is for $\Omega \neq 0$ bigger than its denominator.

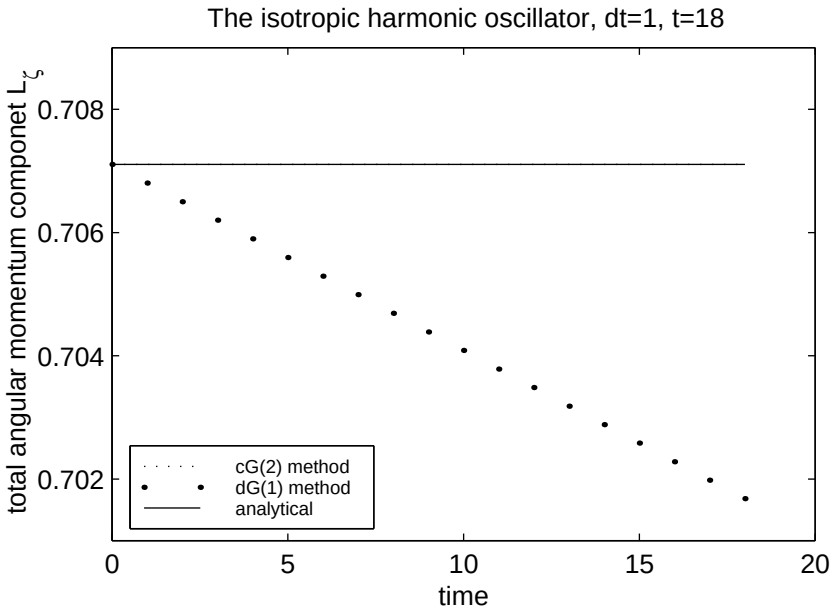

Figure 37: Total angular momentum component $L_\zeta = L_\zeta(t)$ of an isotropic harmonic oscillator with the reduced mass $\mu = 2$, total energy $E = 0.25$ and potential constant $c = -0.25$. Computed with the dG(1) method with $h_n = 1$.

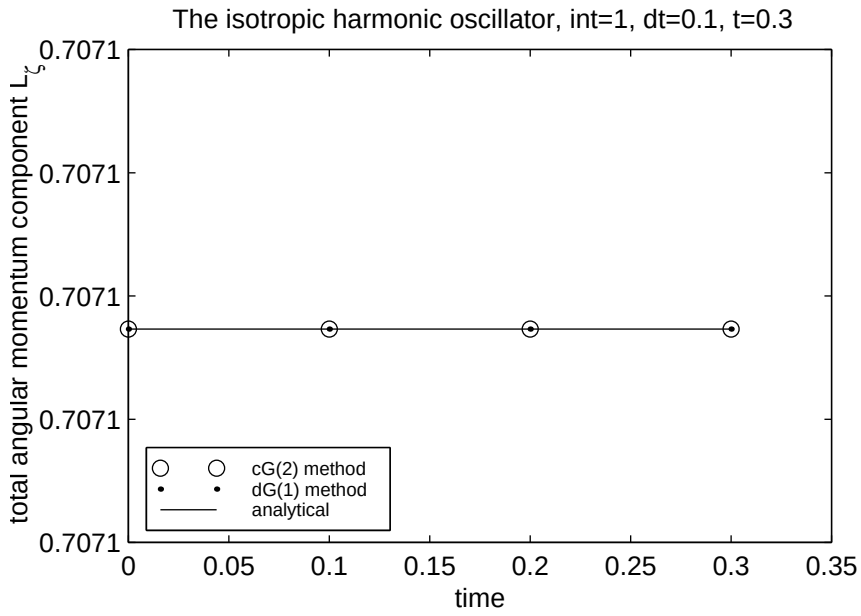

Figure 38: Total angular momentum component $L_\zeta = L_\zeta(t)$ of an isotropic harmonic oscillator with the reduced mass $\mu = 2$, total energy $E = 0.25$ and potential constant $c = -0.25$. Computed with the dG(1) method with midpoint rule ($N_q = 1$) and by a time step size $h_n = 0.1$.

16 A time finite element formulation for Kepler's problem

As an example for a nonlinear central force law, we consider the inverse square law of force which is the second of two central force laws that results in closed orbits for all bound particles; see GOLDSTEIN [14]. The inverse square law is the most important force law in celestial mechanics. Its potential V is called Kepler's potential and takes the shape

$$V = -\frac{c}{r}, \tag{273}$$

where $c > 0$ is the potential constant and $r \equiv \|\mathbf{r}\|$ designates the euclidean norm of the radius vector $\mathbf{r}$. Expressed by the generalized coordinate vector $\mathbf{q}$ the euclidean norm takes the form $r = \sqrt{\mathbf{q}^T\mathbf{q}}$. We refer to equation (225) for the hamiltonian

$$H(\mathbf{q}, \mathbf{p}) = \frac{1}{2\,\mu}\,\mathbf{p}^T\mathbf{I}\,\mathbf{p} + V(r). \tag{274}$$

We now determine the Jacobian matrix $DH(\mathbf{z})$ to present the time-stepping scheme in symplectic notation:

$$DH \equiv \begin{bmatrix} \partial_{\mathbf{q}} H \\ \partial_{\mathbf{p}} H \end{bmatrix} = \begin{bmatrix} \partial_{\mathbf{q}} V \\ 1/\mu\,\mathbf{I}\,\mathbf{p} \end{bmatrix} = \begin{bmatrix} -f(r)\,\partial_{\mathbf{q}} r \\ 1/\mu\,\mathbf{I}\,\mathbf{p} \end{bmatrix}, \tag{275}$$

where $f(r) \equiv -dV(r)/dr$ denotes the conservative central force according to equation (214). The derivative of the magnitude $r = \sqrt{\mathbf{q}^T\mathbf{I}\,\mathbf{q}}$ with respect to the generalized coordinate vector $\mathbf{q}$ results in

$$\partial_{\mathbf{q}} r = \frac{1}{r}\,\mathbf{I}\,\mathbf{q}, \tag{276}$$

where according to ZURMÜHL & FALK [35] the differentiation rule of quadratic forms was used. Hence it follows that the Jacobian matrix $DH(\mathbf{z})$ takes the form

$$DH = \begin{bmatrix} -f(r)/r\,\mathbf{I}\,\mathbf{q} \\ 1/\mu\,\mathbf{I}\,\mathbf{p} \end{bmatrix}. \tag{277}$$

Therefore, we are able to write the Jacobian matrix $DH(\mathbf{z})$ in symplectic notation as follows:

$$DH(\mathbf{z}) = \mathbf{H}(\mathbf{z})\,\mathbf{z}, \tag{278}$$

with

$$\mathbf{H}(\mathbf{z}) = \begin{bmatrix} -f(r)/r\,\mathbf{I} & \mathbf{O} \\ \mathbf{O} & 1/\mu\,\mathbf{I} \end{bmatrix}. \tag{279}$$

16.1 Constant time finite elements

This subsection begins the finite element formulation with the treatment of constant time finite elements ($k = 0$), where the trial function $\mathbf{z}^h = \mathbf{z}_1$ is constant. On account of the constant trial function the nonlinear matrix (279) is also constant:

$$\mathbf{H}(\mathbf{z}_1) = \begin{bmatrix} -f(r_1)/r_1\,\mathbf{I} & \mathbf{O} \\ \mathbf{O} & 1/\mu\,\mathbf{I} \end{bmatrix}, \tag{280}$$

where $r_1 = \sqrt{\mathbf{q}_1^T \mathbf{q}_1}$ designates the magnitude of the radius vector at the unknown node $k+1 = 1$ of the master element I_α. Since interpolating quadrature rules lead to exactly evaluated integrals for constant integrands, we only consider the time-stepping scheme (46) generated by the dG(0) method which we obtained by exact evaluation of the remaining integral:

$$(\mathbf{1} - h_n\,\mathbf{J}\mathbf{H}(\mathbf{z}_1))\,\mathbf{z}_1 = \mathbf{z}_0.$$

Thus the used time-stepping scheme is a system of generally nonlinear algebraic equations owing to $\mathbf{H} = \mathbf{H}(\mathbf{z}_1)$. Accordingly, we solve this time-stepping scheme by the Newton-Raphson method according to Table 7. However, first we have to determine the tangent $\mathbf{K}_T \equiv \partial_{\mathbf{z}_1}\mathbf{R}(\mathbf{z}_1)$. In consideration of the equations (275) and (278) we obtain

$$\mathbf{K}_T = \mathbf{1} - h_n\,\mathbf{J}\mathcal{H}_H^h, \tag{281}$$

where $\mathcal{H}_H^h \equiv D^2H(\mathbf{z}^h)$, the $2n_{dof} \times 2n_{dof}$ Hessian matrix of the hamiltonian (274), takes the shape

$$\mathcal{H}_H^h = \begin{bmatrix} \partial_{\mathbf{q}}^2 V(\mathbf{q}^h) & \mathbf{O} \\ \mathbf{O} & 1/\mu\,\mathbf{I} \end{bmatrix}. \tag{282}$$

Taking into account equation (275), the Hessian matrix $\partial_{\mathbf{q}}^2 V$ reads

$$\partial_{\mathbf{q}}^2 V = -\partial_{\mathbf{q}}\left(f(r)\,\partial_{\mathbf{q}} r\right). \tag{283}$$

According to Steinmann [33] the derivative formula for a product of a scalar-valued vector function and a vector-valued vector function implies

$$\partial_{\mathbf{q}}^2 V = -\left(f(r)\,\partial_{\mathbf{q}}^2 r + \partial_{\mathbf{q}} r \otimes \partial_{\mathbf{q}} f(r)\right) = -\left(f(r)\,\partial_{\mathbf{q}}^2 r + \partial_{\mathbf{q}} r \otimes \frac{df(r)}{dr}\,\partial_{\mathbf{q}} r\right), \tag{284}$$

where the operator $\otimes$ designates the dyadic product. With regard to equation (276), the equation (284) leads to

$$\partial_{\mathbf{q}}^2 V = -\left(f(r)\,\partial_{\mathbf{q}}^2 r + \frac{1}{r^2}\,\frac{df(r)}{dr}\,\mathbf{q} \otimes \mathbf{q}\right). \tag{285}$$

We determine the Hessian matrix $\partial_{\mathbf{q}}^2 r$ with equation (276) in the same way:

$$\partial_{\mathbf{q}}^2 r \equiv \partial_{\mathbf{q}}\left(\frac{1}{r}\,\mathbf{I}\,\mathbf{q}\right) = \frac{1}{r}\,\mathbf{I} + \mathbf{q} \otimes \frac{d}{dr}\left(\frac{1}{r}\right)\,\partial_{\mathbf{q}} r = \frac{1}{r}\,\mathbf{I} - \frac{1}{r^3}\,\mathbf{q} \otimes \mathbf{q}. \tag{286}$$

Given: initial condition $\mathbf{z}_0$, time step size h_n and residual tolerance $\epsilon = 10^{-13}$ set iteration counter $l = 1$
Find: nodal unknown $\mathbf{z}_1$
(a) compute residual vector $\mathbf{R}^{(l)} = (\mathbf{1} - h_n \mathbf{JH}(\mathbf{z}_1))\, \mathbf{z}_1^{(l)} - \mathbf{z}_0$ if $\|\mathbf{R}^{(l)}\| > \epsilon$ goto (b) else goto (c) (b) compute tangent $\mathbf{K}_T^{(l)} \equiv \partial_{\mathbf{z}_1} \mathbf{R}(\mathbf{z}_1^{(l)})$ solve for increment $\Delta\, \mathbf{z}_1^{(l)}$ $\Delta\, \mathbf{z}_1^{(l)} = -\left(\mathbf{K}_T^{(l)}\right)^{-1} \mathbf{R}^{(l)}$ update the nodal unknown $\mathbf{z}_1^{(l+1)} = \mathbf{z}_1^{(l)} + \Delta\, \mathbf{z}_1^{(l)}$ goto (a) with $l = l + 1$ (c) end.

Table 7: Newton-Raphson method to solve the dG(0) time-stepping scheme for an arbitrary central force law.

Employing equation (286) in equation (285) yields

$$\partial_{\mathbf{q}}^2 V = -\frac{f(r)}{r}\, \mathbf{I} + \frac{1}{r^2} \left(\frac{f(r)}{r} - \frac{df(r)}{dr} \right) \mathbf{q} \otimes \mathbf{q}. \tag{287}$$

The dyadic product $\mathbf{q} \otimes \mathbf{q}$ of a column matrix $\mathbf{q}$ with itself result in the following quadratic matrix:

$$\mathbf{q} \otimes \mathbf{q} = \mathbf{q}\, \mathbf{q}^T. \tag{288}$$

Therefore, the Hessian matrix of the potential V with respect to the generalized coordinate vector $\mathbf{q}$ results in

$$\partial_{\mathbf{q}}^2 V = -\frac{f(r)}{r}\, \mathbf{I} + \frac{1}{r^2} \left(\frac{f(r)}{r} - \frac{df(r)}{dr} \right) \mathbf{q}\, \mathbf{q}^T. \tag{289}$$

Thus the Hessian matrix $\mathcal{H}_H^h$ is determinated and with it the tangent $\mathbf{K}_T$.

Numerical Example 16.1 *Let the reduced mass be $\mu = 2$. The total energy and the potential constant of the reduced mass is supposed to be $E = -0.25$ and $c = 0.25$ respectively. Note that the sign of the potential constant has to be positive for Kepler's potential in the form of equation (273) and that Kepler's potential only results in closed orbits for*

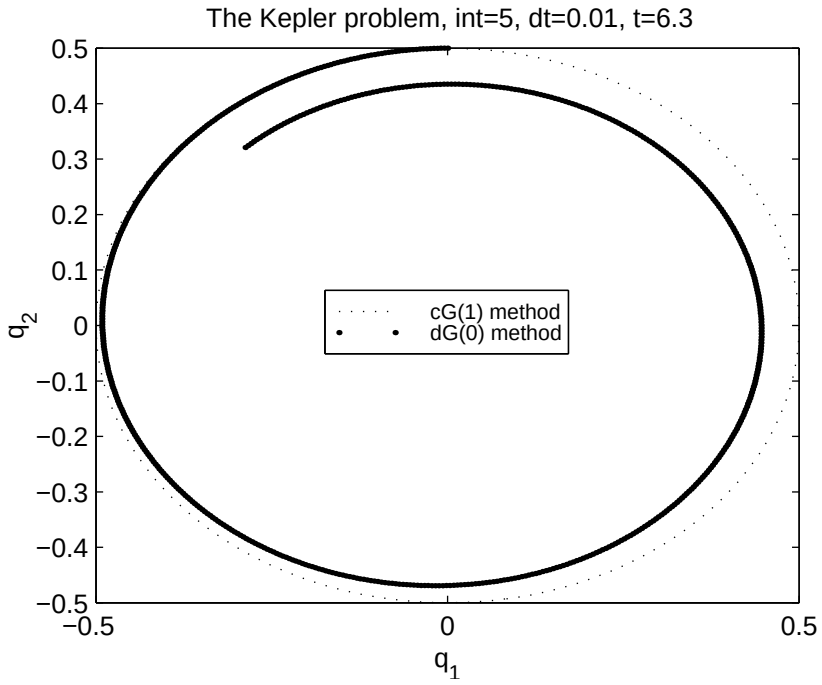

Figure 39: An orbit of the Kepler problem with the reduced mass $\mu = 2$, total energy $E = -0.25$ and potential constant $c = 0.25$. Computed with the dG(0) method with $h_n = 0.01$.

negative total energies; see eg Gross *[15]. We see in Figure 39 a full circle of the orbit of the reduced mass computed with the dG(0) method with exactly evaluted integral and by the energy conserving cG(1) method with five Gaussian quadrature points. The open orbit of the dG(0) method reveals the asymptotic annihilation of the components of the generalized coordinate vector* $\boldsymbol{q}$*. In contrast to the above numerical examples in the present thesis, the Newton-Raphson method needs a smaller time-step* $h_n = 0.01$*.*

16.2 Linear time finite elements

We continue the elaboration of a finite element formulation for Kepler's problem with linear time finite elements which means $k = 1$. Since we have formulated the dG(1) method for an arbitrary Jacobian matrix $DH(\mathbf{z})$ in Subsection 8.2, we are able to refer to equation (125) for the residual vector $\mathbf{R}(\mathbf{x})$ with $\mathbf{x} = [\mathbf{z}_1^T\ \mathbf{z}_2^T]^T$:

$$\mathbf{R}(\mathbf{x}) = \frac{1}{2}\begin{bmatrix} \mathbf{1} & \mathbf{1} \\ -\mathbf{1} & \mathbf{1} \end{bmatrix}\mathbf{x} - \begin{bmatrix} \mathbf{1} \\ \mathbf{0} \end{bmatrix}\mathbf{z}_0 - h_n \int_0^1 \begin{bmatrix} M_1(\alpha)\,\mathbf{1} \\ M_2(\alpha)\,\mathbf{1} \end{bmatrix} \mathbf{J}DH(\mathbf{z}^h(\alpha))d\alpha.$$

According to equation (278) $DH(\mathbf{z}^h)$ is given by

$$DH(\mathbf{z}^h) = \mathbf{H}(\mathbf{z}^h)\,\mathbf{z}^h, \tag{290}$$

with the matrix

$$\mathbf{H}(\mathbf{z}^h) = \begin{bmatrix} -f(r^h)/r^h\,\mathbf{I} & \mathbf{O} \\ \mathbf{O} & 1/\mu\,\mathbf{I} \end{bmatrix}. \tag{291}$$

The trial function reads $\mathbf{z}^h = \sum_{i=1}^2 M_i\,\mathbf{z}_i$ with the nodal shape functions $M_1 = 1-\alpha$ and $M_2 = \alpha$ according to Table 1. We introduce an interpolating quadrature rule to evaluate the integral in the residual vector (125) such that the approximated residual vector takes the form of equation (129):

$$\mathbf{R}(\mathbf{x}) \approx \frac{1}{2}\begin{bmatrix} \mathbf{1} & \mathbf{1} \\ -\mathbf{1} & \mathbf{1} \end{bmatrix}\mathbf{x} - \begin{bmatrix} \mathbf{1} \\ \mathbf{0} \end{bmatrix}\mathbf{z}_0 - h_n \sum_{l=1}^{N_q} \begin{bmatrix} M_1(\alpha_l)\,\mathbf{1} \\ M_2(\alpha_l)\,\mathbf{1} \end{bmatrix} \mathbf{J}DH(\mathbf{z}^h(\alpha_l))w_l.$$

To solve the residual vector in the way of Table 3, we need the approximated tangent $\mathbf{K}_T \approx \partial_{\mathbf{X}}\mathbf{R}(\mathbf{x})$ of the residual vector (125) according to equation (130):

$$\mathbf{K}_T \approx \frac{1}{2}\begin{bmatrix} \mathbf{1} & \mathbf{1} \\ -\mathbf{1} & \mathbf{1} \end{bmatrix} - h_n \sum_{l=1}^{N_q} \begin{bmatrix} M_{1,l}\,\mathbf{1} \\ M_{2,l}\,\mathbf{1} \end{bmatrix} \begin{bmatrix} M_{1,l}\,\mathbf{1} & M_{2,l}\,\mathbf{1} \end{bmatrix} \begin{bmatrix} \mathbf{J}\mathcal{H}_{H,l}^h & \mathbf{O}_2 \\ \mathbf{O}_2 & \mathbf{J}\mathcal{H}_{H,l}^h \end{bmatrix} w_l,$$

with the $2n_{dof} \times 2n_{dof}$ Hessian matrix $\mathcal{H}_H^h$ according to equation (282).
Since we have proved Theorem 8.1 by the general dG(1) method without a concrete Jacobian matrix $DH(\mathbf{z})$, we are able to also use Theorem 8.1 on the dG(1) method for the Kepler problem. Hence it follows that an orbit computed with the midpoint rule is continuous.

Numerical Example 16.2 *We consider the system of Example 16.1. Hence the reduced mass is $\mu = 2$. Further, the total energy and the potential constant of the reduced mass is $E = -0.25$ and $c = 0.25$ respectively. Figure 40 shows three time steps of the orbit which is computed with the midpoint rule. The continuous orbit corroborates the statement of Theorem 8.1. In contrast to it, five Gaussian quadrature points lead to jumps in the orbit; see Figure 41.*

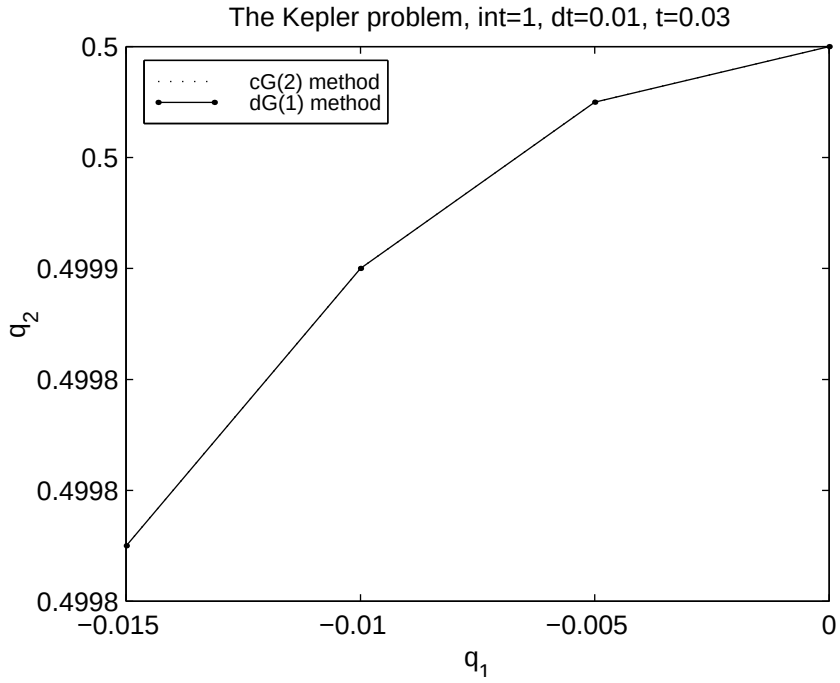

Figure 40: An orbit of the Kepler problem with the reduced mass $\mu = 2$, total energy $E = -0.25$ and potential constant $c = 0.25$. Computed with the dG(1) method with midpoint rule ($N_q = 1$) and by a time step size $h_n = 0.01$.

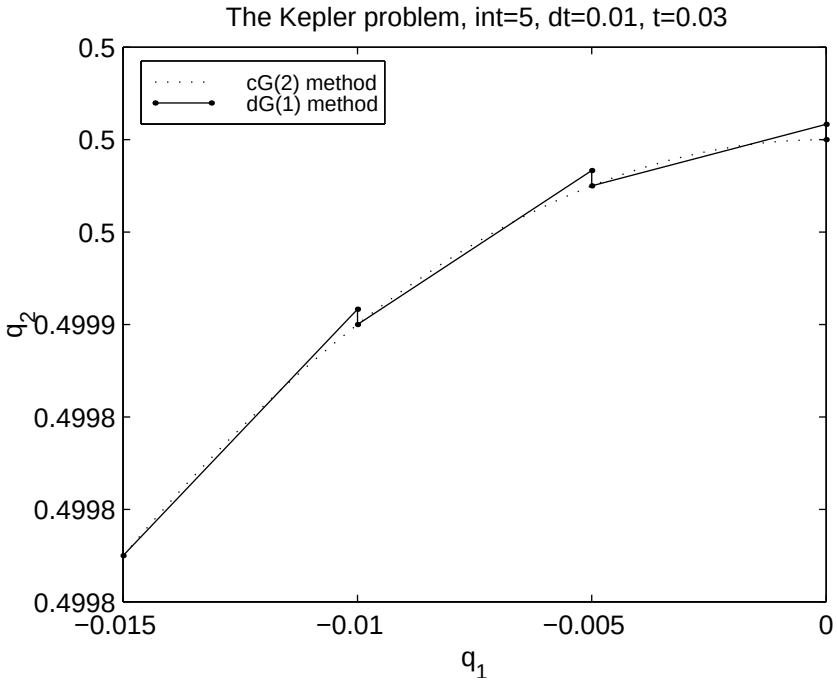

Figure 41: An orbit of the Kepler problem with the reduced mass $\mu = 2$, total energy $E = -0.25$ and potential constant $c = 0.25$. Computed with the dG(1) method with $h_n = 0.01$ and five Gaussian quadrature points.

17 The algorithmic total angular momentum of the equivalent one-body problem

We have investigated in Section 15 the algorithmic total angular momentum for Hooke's central force law. This section concerns the algorithmic total angular momentum for an arbitrary central force law. However, we refer to Section 15 for the introduction of the algorithmic total angular momentum $\mathbf{L}_{k+1}$ of the equivalent one-body problem which ends in equation (259):

$$\mathbf{L}_{k+1} = \mathbf{q}_{k+1} \bowtie \mathbf{p}_{k+1}.$$

17.1 Constant time finite elements

We begin with constant time finite elements ($k = 0$) which means a constant trial function $\mathbf{z}^h = \mathbf{z}_1 \equiv [\mathbf{q}_1^T \; \mathbf{p}_1^T]^T$. The starting point is the time-stepping scheme (46) which reads

$$(\mathbf{1} - h_n \, \mathbf{JH}) \; \mathbf{z}_1 = \mathbf{z}_0,$$

with respect to the matrix (280). To determine the algorithmic total angular momentum $\mathbf{L}_{k+1} \equiv \mathbf{L}_1$, we have to leave the symplectic notation and write the time-stepping scheme in an explicit representation:

$$\mathbf{q}_1 - \mathbf{q}_0 - \frac{h_n}{\mu}\mathbf{p}_1 = \mathbf{0}, \tag{292}$$

$$\mathbf{p}_1 - \mathbf{p}_0 - h_n \, \frac{f(r_1)}{r_1} \, \mathbf{q}_1 = \mathbf{0}, \tag{293}$$

where $r_1 = \sqrt{\mathbf{q}_1^T \mathbf{q}_1}$ denotes the magnitude of the radius vector at the node $k+1 = 1$ of the master element I_α. Further, $\mathbf{0}$ designates in the explicit representationa a $n_{dof} \times 1$ zero matrix.
As first step to obtain the algorithmic total angular momentum $\mathbf{L}_1$, we employ equation (292) instead of $\mathbf{q}_1$ in equation (259):

$$\mathbf{L}_1 = \left(\mathbf{q}_0 + \frac{h_n}{\mu}\mathbf{p}_1 \right) \bowtie \mathbf{p}_1. \tag{294}$$

Because of the properties (i) and (ii) of Theorem 15.1, we obtain

$$\mathbf{L}_1 = \mathbf{q}_0 \bowtie \mathbf{p}_1 + \frac{h_n}{\mu}\mathbf{p}_1 \bowtie \mathbf{p}_1. \tag{295}$$

Before we make use of property (iv) of Theorem 15.1, we apply the property (iii) of Theorem 15.1. Thus we gain in the end

$$\mathbf{L}_1 = \mathbf{q}_0 \bowtie \mathbf{p}_1. \tag{296}$$

Next we introduce equation (293) in equation (296) to eliminate the generalized momentum $\mathbf{p}_1$:

$$\mathbf{L}_1 = \mathbf{q}_0 \bowtie \left(\mathbf{p}_0 + h_n \frac{f(r_1)}{r_1} \mathbf{q}_1 \right). \tag{297}$$

Property (ii) of Theorem 15.1 yields

$$\mathbf{L}_1 = \mathbf{q}_0 \bowtie \mathbf{p}_0 + \mathbf{q}_0 \bowtie h_n \frac{f(r_1)}{r_1} \mathbf{q}_1. \tag{298}$$

$\mathbf{L}_0 = \mathbf{q}_0 \bowtie \mathbf{p}_0$ denotes the algorithmic total angular momentum at the initial node 0 of the master element I_α so that the algorithmic total angular momentum at the unknown node 1 takes the form

$$\mathbf{L}_1 = \mathbf{L}_0 + h_n \frac{f(r_1)}{r_1} \left(\mathbf{q}_0 \bowtie \mathbf{q}_1 \right), \tag{299}$$

where we place the scalar functions at the head with the properties (i) and (iii) of Theorem 15.1.
Because of the fact that $\mathbf{q}_0$ as well as $\mathbf{q}_1$ represents a vector which lies in the euclidean plane of motion $\mathcal{E}^2_m$, the product $\mathbf{q}_0 \bowtie \mathbf{q}_1$ yields for sufficiently brief time steps the matrix representation of a vector which direction always is identical with the direction of the initial total angular momentum $\mathbf{L}(t = 0)$; also see Figure 42. Since the radius is positive, the effect of the second term in equation (299) is determined by the central force law $f(r)$. Therefore, the sign of the central force law $f(r)$ determines whether the second term in equation (299) implies a decay (negative sign) or a growth (positive sign) of the algorithmic total angular momentum $\mathbf{L}_1$ with respect to the algorithmic total angular momentum $\mathbf{L}_0$ at the initial node.
Conservation of the algorithmic total angular momentum occurs for infinitesimal time steps ($h_n = 0$) and if the central force $\mathbf{F}$ vanishes which means the potential V is constant. The latter case is reasonable since a vanishing central force leads to (i) $f(r) = 0$ and (ii) according to Gross [15] to a line as orbit which implies $\mathbf{q}_1 = a\,\mathbf{q}_0$, $a \in \mathcal{R}$, so that because of the properties (i), (iii) and (iv) of Theorem 15.1 the product $\mathbf{q}_0 \bowtie \mathbf{q}_1$ vanishes.

Numerical Example 17.1 *For instance, we consider the algorithmic total angular momentum of the inverse square law of force in Example 16.1. According to equation (273) the Kepler potential takes the form $V = -c/r$, $c > 0$, so that the inverse square law of force $f(r) \equiv -dV/dr = -c/r^2$ is negative. Therefore, owing to equation (299) we expext a decay of the algorithmic total angular momentum which we also see in Figure 43. According to* Betsch & Steinmann *[7] the algorithmic total angular momentum of the cG(1) method is preserved for the equivalent one-body problem. Therfore, the dotted line of the cG(1) method in Figure 36 is covered by the solid line of the exact total angular momentum.*

Numerical Example 17.2 *We conclude the investigation of relation (299) with a second example. Here we consider a linear repulsive central force $f = c\,r$, $c > 0$, which results from Hooke's potential $V = -1/2\,c\,r^2$ with a positive potential constant. For*

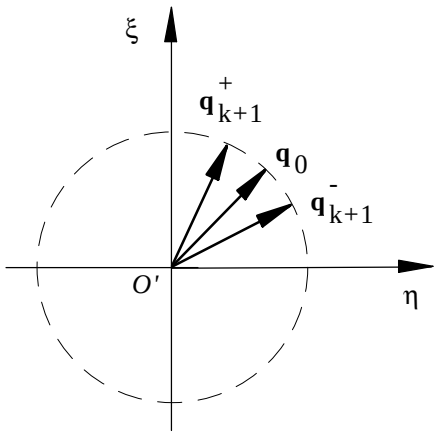

Figure 42: Generalized coordinate vectors at the initial node 0 and at the last node $k+1$ respectively of the master element I_α in the euclidean plane of motion $\mathcal{E}^2_m$ (eg here a closed orbit). The superscripts at the node $k+1$ designates the direction of the initial total angular momentum $\mathbf{L}(t=0)$: the plus means the direction of $\mathbf{u}_\zeta$ and the minus the opposite direction.

a concrete example we let $c = 0.25$ *and let the total energy of the reduced mass be* $E = 0.125$. *We expect by equation (299) an algorithmic total angular momentum growth which Figure 44 corroborates.*

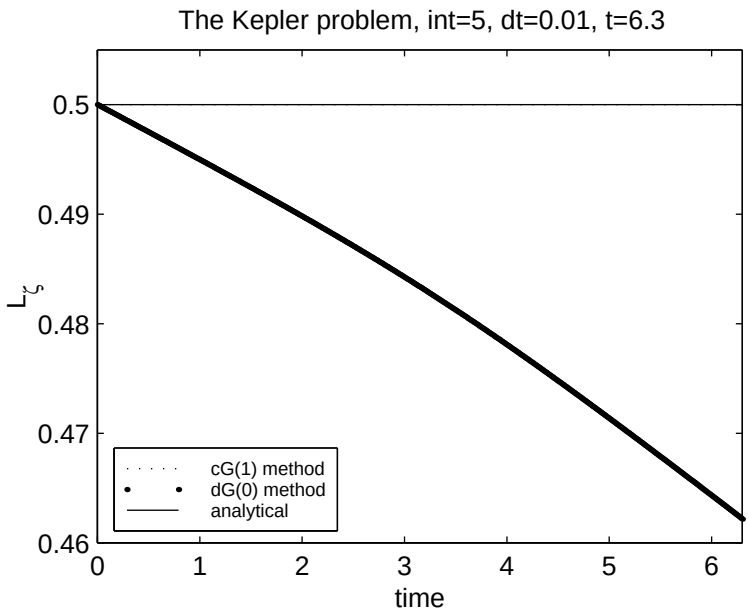

Figure 43: Total angular momentum component $L_\zeta = L_\zeta(t)$ of the Kepler problem with the reduced mass $\mu = 2$, total energy $E = -0.25$ and potential constant $c = 0.25$. Computed with the dG(0) method with $h_n = 0.01$.

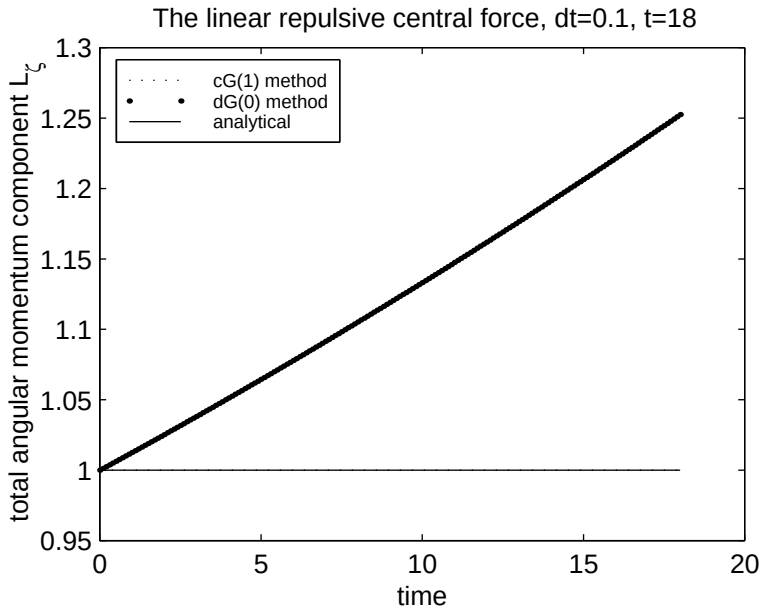

Figure 44: Total angular momentum component $L_\zeta = L_\zeta(t)$ of the reduced mass $\mu = 2$, total energy $E = 0.125$ and potential constant $c = 0.25$ within a linear repulsive central force field. Computed with the dG(0) method with $h_n = 0.01$.

17.2 Linear time finite elements

In this subsection we consider linear time finite elements to determine the algorithmic total angular momentum for an arbitrary central force law. Accordingly, we can evaluate the integrals of the Jacobian matrix of hamiltonian (274) with respect to the generalized coordinate vector $\mathbf{q}$ only by quadrature rules. Cf equation (275). On the other hand, we are able to integrate the Jacobian matrix of the hamiltonian (274) with respect to the generalized momentum vector $\mathbf{p}$ exactly; however, we want to preserve the possibility of considering interpolating quadrature rules in this subsection below. Therefore, we do not evaluate the integrals in the derivation of the algorithmic total angular momentum. The starting point is the general dG(1) method (57), (58):

$$\frac{1}{2}\,\mathbf{z}_2 + \frac{1}{2}\,\mathbf{z}_1 - \mathbf{z}_0 - h_n \int_0^1 M_1 \mathbf{J} DH(\mathbf{z}^h) d\alpha = \mathbf{0}, \tag{300}$$

$$\frac{1}{2}\,\mathbf{z}_2 - \frac{1}{2}\,\mathbf{z}_1 - h_n \int_0^1 M_2 \mathbf{J} DH(\mathbf{z}^h) d\alpha = \mathbf{0}. \tag{301}$$

However, the determination of the algorithmic total angular momentum demands the explicit representation of the general dG(1) method:

$$\frac{1}{2}\,\mathbf{q}_2 + \frac{1}{2}\,\mathbf{q}_1 - \mathbf{q}_0 - h_n \int_0^1 M_1\, \partial_{\mathbf{p}} H(\mathbf{q}^h, \mathbf{p}^h) d\alpha = \mathbf{0}, \tag{302}$$

$$\frac{1}{2}\,\mathbf{p}_2 + \frac{1}{2}\,\mathbf{p}_1 - \mathbf{p}_0 + h_n \int_0^1 M_1\, \partial_{\mathbf{q}} H(\mathbf{q}^h, \mathbf{p}^h) d\alpha = \mathbf{0}, \tag{303}$$

$$\frac{1}{2}\,\mathbf{q}_2 - \frac{1}{2}\,\mathbf{q}_1 - h_n \int_0^1 M_2\, \partial_{\mathbf{p}} H(\mathbf{q}^h, \mathbf{p}^h) d\alpha = \mathbf{0}, \tag{304}$$

$$\frac{1}{2}\,\mathbf{p}_2 - \frac{1}{2}\,\mathbf{p}_1 + h_n \int_0^1 M_2\, \partial_{\mathbf{q}} H(\mathbf{q}^h, \mathbf{p}^h) d\alpha = \mathbf{0}. \tag{305}$$

If we take the trial function $\mathbf{p}^h = \sum_{j=1}^2 M_j\, \mathbf{p}_j$ into consideration, owing to equation (275) we are in the position to write the integrals in the equations (302) and (304) as follows:

$$\int_0^1 M_i(\alpha)\, \partial_{\mathbf{p}} H(\mathbf{q}^h, \mathbf{p}^h) d\alpha = \frac{1}{\mu} \int_0^1 M_i(\alpha) \sum_{j=1}^2 M_j(\alpha)\, \mathbf{p}_j\, d\alpha \tag{306}$$

$$= \frac{1}{\mu} \sum_{j=1}^2 \int_0^1 M_i(\alpha)\, M_j(\alpha) d\alpha\, \mathbf{p}_j. \tag{307}$$

We introduce the following abbreviations for the integrals in equation (307):

$$\gamma_{ij} = \int_0^1 M_i(\alpha)\, M_j(\alpha) d\alpha. \tag{308}$$

Obviously, the coefficients γ_{ij} are symmetric, ie $\gamma_{ij} \equiv \gamma_{ji}$. In addition, the consideration of equation (275) lead to the following form of the equations (302)-(305):

$$\frac{1}{2}\,\mathbf{q}_2 + \frac{1}{2}\,\mathbf{q}_1 - \mathbf{q}_0 - \frac{h_n}{\mu}\,(\gamma_{11}\,\mathbf{p}_1 + \gamma_{12}\,\mathbf{p}_2) = \mathbf{0}, \tag{309}$$

$$\frac{1}{2}\,\mathbf{p}_2 + \frac{1}{2}\,\mathbf{p}_1 - \mathbf{p}_0 + h_n \int_0^1 M_1\,\partial_{\mathbf{q}} V(\mathbf{q}^h, \mathbf{p}^h) d\alpha \;=\; \mathbf{0}, \tag{310}$$

$$\frac{1}{2}\,\mathbf{q}_2 - \frac{1}{2}\,\mathbf{q}_1 - \frac{h_n}{\mu}\,(\gamma_{12}\,\mathbf{p}_1 + \gamma_{22}\mathbf{p}_2) \;=\; \mathbf{0}, \tag{311}$$

$$\frac{1}{2}\,\mathbf{p}_2 - \frac{1}{2}\,\mathbf{p}_1 + h_n \int_0^1 M_2\,\partial_{\mathbf{q}} V(\mathbf{q}^h, \mathbf{p}^h) d\alpha \;=\; \mathbf{0}, \tag{312}$$

where the symmetry of γ_{ij} has been taken into account. For the time being we do not approximate the integrals in the equations (310) and (312). For that resason we introduce the following abbreviation:

$$\mathbf{\Sigma}_i = \int_0^1 M_i\,\partial_{\mathbf{q}} V(\mathbf{q}^h, \mathbf{p}^h) d\alpha \equiv -\int_0^1 M_i\,\frac{f(r^h)}{r^h}\,\mathbf{q}^h d\alpha, \tag{313}$$

where $i \in \{1, 2\}$ and $r^h = \sqrt{(\mathbf{q}^h)^T \mathbf{q}^h}$ denotes the radius vector. Hence it follows that the general dG(1) method takes the following shape:

$$\frac{1}{2}\,\mathbf{q}_2 + \frac{1}{2}\,\mathbf{q}_1 - \mathbf{q}_0 - \frac{h_n}{\mu}\,(\gamma_{11}\,\mathbf{p}_1 + \gamma_{12}\,\mathbf{p}_2) \;=\; \mathbf{0}, \tag{314}$$

$$\frac{1}{2}\,\mathbf{p}_2 + \frac{1}{2}\,\mathbf{p}_1 - \mathbf{p}_0 + h_n\,\mathbf{\Sigma}_1 \;=\; \mathbf{0}, \tag{315}$$

$$\frac{1}{2}\,\mathbf{q}_2 - \frac{1}{2}\,\mathbf{q}_1 - \frac{h_n}{\mu}\,(\gamma_{12}\,\mathbf{p}_1 + \gamma_{22}\mathbf{p}_2) \;=\; \mathbf{0}, \tag{316}$$

$$\frac{1}{2}\,\mathbf{p}_2 - \frac{1}{2}\,\mathbf{p}_1 + h_n\,\mathbf{\Sigma}_2 \;=\; \mathbf{0}. \tag{317}$$

Henceforth we proceed close to the line of Betsch & Steinmann [7]. Since we aim at a relation which does not include the generalized coordinate vector $\mathbf{q}_1$ explicitly, we add equation (314) and equation (316). We obtain

$$\mathbf{q}_2 - \mathbf{q}_0 - \frac{h_n}{\mu}\,(\gamma_{11} + \gamma_{12})\,\mathbf{p}_1 - \frac{h_n}{\mu}\,(\gamma_{12} + \gamma_{22})\,\mathbf{p}_2 = \mathbf{0}. \tag{318}$$

Now we consider the algorithmic total angular momentum $\mathbf{L}_2$ by employing the relation (318) in equation (259):

$$\mathbf{L}_2 = \left(\mathbf{q}_0 + \frac{h_n}{\mu}\,(\gamma_{11} + \gamma_{12})\,\mathbf{p}_1 + \frac{h_n}{\mu}\,(\gamma_{12} + \gamma_{22})\,\mathbf{p}_2\right) \bowtie \mathbf{p}_2. \tag{319}$$

We dissolve the parenthesis with the properties (i) and (ii) of Theorem 15.1:

$$\mathbf{L}_2 = \mathbf{q}_0 \bowtie \mathbf{p}_2 + \frac{h_n}{\mu}\,(\gamma_{11} + \gamma_{12})\,\mathbf{p}_1 \bowtie \mathbf{p}_2 + \frac{h_n}{\mu}\,(\gamma_{12} + \gamma_{22})\,\mathbf{p}_2 \bowtie \mathbf{p}_2. \tag{320}$$

According to the properties (iii) and (iv) of Theorem 15.1 equation (320) can be also written in the form

$$\mathbf{L}_2 = \left(\mathbf{q}_0 + \frac{h_n}{\mu}\,(\gamma_{11} + \gamma_{12})\,\mathbf{p}_1\right) \bowtie \mathbf{p}_2. \tag{321}$$

Next we add the equations (315) and (317) to obtain a relation without generalized momentum vector $\mathbf{p}_1$ explicitly:

$$\mathbf{p}_2 - \mathbf{p}_0 + h_n (\mathbf{\Sigma}_1 + \mathbf{\Sigma}_2) = \mathbf{0}. \tag{322}$$

Therefore, we are able to substitute equation (322) for the generalized momentum vector $\mathbf{p}_2$ in equation (321):

$$\mathbf{L}_2 = \left(\mathbf{q}_0 + \frac{h_n}{\mu} (\gamma_{11} + \gamma_{12}) \mathbf{p}_1 \right) \bowtie (\mathbf{p}_0 - h_n (\mathbf{\Sigma}_1 + \mathbf{\Sigma}_2)) . \tag{323}$$

The partly expansion of the equation (323) enables taking into account the properties (i) and (ii) of Theorem 15.1. Moreover, the identity $\mathbf{L}_0 = \mathbf{q}_0 \bowtie \mathbf{p}_0$ yields

$$\mathbf{L}_2 = \mathbf{L}_0 + \frac{h_n}{\mu} (\gamma_{11} + \gamma_{12}) \mathbf{p}_1 \bowtie \mathbf{p}_0 + \left(\mathbf{q}_0 + \frac{h_n}{\mu} (\gamma_{11} + \gamma_{12}) \mathbf{p}_1 \right) \bowtie (-h_n (\mathbf{\Sigma}_1 + \mathbf{\Sigma}_2)) . \tag{324}$$

We place in equation (324) with the properties (i) and (iii) of Theorem 15.1 reals at the head and obtain

$$\mathbf{L}_2 = \mathbf{L}_0 + \frac{h_n}{\mu} (\gamma_{11} + \gamma_{12}) (\mathbf{p}_1 \bowtie \mathbf{p}_0) - h_n \left(\mathbf{q}_0 + \frac{h_n}{\mu} (\gamma_{11} + \gamma_{12}) \mathbf{p}_1 \right) \bowtie (\mathbf{\Sigma}_1 + \mathbf{\Sigma}_2) . \tag{325}$$

The elimination of the explicit generalized momentum vector $\mathbf{p}_0$ in equation (325) enables the result of the subtraction of equation (317) from equation (315). The subtraction yields

$$\mathbf{p}_1 - \mathbf{p}_0 + h_n (\mathbf{\Sigma}_1 - \mathbf{\Sigma}_2) = \mathbf{0}. \tag{326}$$

We take the $\bowtie$-product with $\mathbf{p}_1$ from the left on both sides of equation (326):

$$\mathbf{p}_1 \bowtie (\mathbf{p}_1 - \mathbf{p}_0 + h_n (\mathbf{\Sigma}_1 - \mathbf{\Sigma}_2)) = \mathbf{p}_1 \bowtie \mathbf{0}. \tag{327}$$

We dissolve the parenthesis in equation (327) with the properties (i) and (ii) of Theorem 15.1 and subsequently, we place reals at the head with property (iii) of Theorem 15.1:

$$\mathbf{p}_1 \bowtie \mathbf{p}_1 - \mathbf{p}_1 \bowtie \mathbf{p}_0 + h_n (\mathbf{p}_1 \bowtie (\mathbf{\Sigma}_1 - \mathbf{\Sigma}_2)) = \mathbf{p}_1 \bowtie \mathbf{0}. \tag{328}$$

Owing to the properties (i), (iv) and (v) of Theorem 15.1 the first term as well as the right side of equation (328) vanishes:

$$-\mathbf{p}_1 \bowtie \mathbf{p}_0 + h_n \mathbf{p}_1 \bowtie (\mathbf{\Sigma}_1 - \mathbf{\Sigma}_2) = \mathbf{0}, \tag{329}$$

where $\mathbf{0}$ denotes the 3×1 zero matrix. We employ equation (329) in the middle term of equation (325) and obtain

$$\mathbf{L}_2 = \mathbf{L}_0 + \frac{h_n^2}{\mu} (\gamma_{11} + \gamma_{12}) \mathbf{p}_1 \bowtie (\mathbf{\Sigma}_1 - \mathbf{\Sigma}_2) - h_n \left(\mathbf{q}_0 + \frac{h_n}{\mu} (\gamma_{11} + \gamma_{12}) \mathbf{p}_1 \right) \bowtie (\mathbf{\Sigma}_1 + \mathbf{\Sigma}_2) . \tag{330}$$

After we have sorted according to the abbreviations $\mathbf{\Sigma}_i$ with the properties (i), (ii) and (iii) of Theorem 15.1, the equation (330) takes the form

$$\mathbf{L}_2 = \mathbf{L}_0 - h_n\,\mathbf{q}_0 \bowtie \mathbf{\Sigma}_1 - h_n\,\mathbf{q}_0 \bowtie \mathbf{\Sigma}_2 - 2\,h_n\,(\gamma_{11}+\gamma_{12})\left(\frac{h_n}{\mu}\mathbf{p}_1 \bowtie \mathbf{\Sigma}_2\right). \tag{331}$$

On the other hand, we combine the equations (317) and (318) such that the result is the following relation which expressed the generalized momentum vector $\mathbf{p}_1$ only in generalized coordinate vectors as well as the integral $\mathbf{\Sigma}_2$:

$$\mathbf{q}_2 - \mathbf{q}_0 - \frac{h_n}{\mu}\,(\gamma_{11}+2\,\gamma_{12}+\gamma_{22})\,\mathbf{p}_1 + \frac{h_n^2}{\mu}\,(\gamma_{12}+\gamma_{22})\,\mathbf{\Sigma}_2 = \mathbf{0}. \tag{332}$$

We are able to simplify the contents of the parenthesis of the third term if we consider the meanings of the abbreviations γ_{ij}:

$$\begin{aligned}
\gamma_{11}+2\,\gamma_{12}+\gamma_{22} &= \int_0^1 \left(M_1^2(\alpha)+2\,M_1(\alpha)\,M_2(\alpha)+M_2^2(\alpha)\right)d\alpha && (333)\\
&= \int_0^1 \left(M_1(\alpha)+M_2(\alpha)\right)^2 d\alpha && (334)\\
&= \int_0^1 1\,d\alpha, && (335)
\end{aligned}$$

where the property $M_1+M_2=1$ was used. With regard to the application of interpolating quadrature rules, which according to Subsection 6.1.2 integrate a constant exactly, we can write

$$\gamma_{11}+2\,\gamma_{12}+\gamma_{22} = 1. \tag{336}$$

Consideration of identity (336) in equation (332) yields

$$\mathbf{q}_2 - \mathbf{q}_0 - \frac{h_n}{\mu}\mathbf{p}_1 + \frac{h_n^2}{\mu}\,(\gamma_{12}+\gamma_{22})\,\mathbf{\Sigma}_2 = \mathbf{0}. \tag{337}$$

Now we take the $\bowtie$-product with $\mathbf{\Sigma}_2$ from the right on both sides of equation (337) and obtain

$$\left(\mathbf{q}_2 - \mathbf{q}_0 - \frac{h_n}{\mu}\mathbf{p}_1 + \frac{h_n^2}{\mu}\,(\gamma_{12}+\gamma_{22})\,\mathbf{\Sigma}_2\right) \bowtie \mathbf{\Sigma}_2 = \mathbf{0} \bowtie \mathbf{\Sigma}_2. \tag{338}$$

We partly dissolve the outer parenthesis on the left with the properties (i) and (ii) of Theorem 15.1 and we apply the property (v) of Theorem 15.1 on the right side such that

$$(\mathbf{q}_2 - \mathbf{q}_0) \bowtie \mathbf{\Sigma}_2 - \frac{h_n}{\mu}\mathbf{p}_1 \bowtie \mathbf{\Sigma}_2 + \frac{h_n^2}{\mu}\,(\gamma_{12}+\gamma_{22})\,\mathbf{\Sigma}_2 \bowtie \mathbf{\Sigma}_2 = \mathbf{0}, \tag{339}$$

where $\mathbf{0}$ denotes the 3×1 zero matrix. Applying the properties (iii) and (iv) to the last term of equation (339) yields

$$(\mathbf{q}_2 - \mathbf{q}_0) \bowtie \mathbf{\Sigma}_2 - \frac{h_n}{\mu}\mathbf{p}_1 \bowtie \mathbf{\Sigma}_2 = \mathbf{0}. \tag{340}$$

Now we employ equation (340) into the last term of equation (331) and use the properties (i),(ii) and (iii) of Theorem 15.1. The result is

$$\mathbf{L}_2 = \mathbf{L}_0 - h_n\, \mathbf{q}_0 \bowtie \mathbf{\Sigma}_1 - h_n\, (\mathbf{q}_0 + 2\,(\gamma_{11} + \gamma_{12})\,(\mathbf{q}_2 - \mathbf{q}_0)) \bowtie \mathbf{\Sigma}_2. \tag{341}$$

Now we dissolve the last inner parenthesis with the properties (i) and (ii) of Theorem 15.1 and unite $\mathbf{q}_0$ to get:

$$\mathbf{L}_2 = \mathbf{L}_0 - h_n\, \mathbf{q}_0 \bowtie \mathbf{\Sigma}_1 - h_n\, ((1 - 2\,\gamma_{11} - 2\,\gamma_{12})\,\mathbf{q}_0 + 2\,(\gamma_{11} + \gamma_{12})\,\mathbf{q}_2) \bowtie \mathbf{\Sigma}_2. \tag{342}$$

The identity (336) implies a simplification of the coefficient of $\mathbf{q}_0$ in the last term of equation (342) such that the algorithmic total angular momentum in the end is as follows:

$$\mathbf{L}_2 = \mathbf{L}_0 + h_n\, \mathbf{N}_2, \tag{343}$$

where $\mathbf{N}_2$ denotes the following vector:

$$\mathbf{N}_2 = -\mathbf{q}_0 \bowtie \mathbf{\Sigma}_1 - ((\gamma_{22} - \gamma_{11})\,\mathbf{q}_0 + 2\,(\gamma_{11} + \gamma_{12})\,\mathbf{q}_2) \bowtie \mathbf{\Sigma}_2. \tag{344}$$

In consequence of the rate of change (36) of the total angular momentum we generally refer to $\mathbf{N}_{k+1}$ as the algorithmic total torque of the master element I_α of the dG(k) method. Simple transformations lead to

$$\mathbf{\Delta}^{(1)} = \mathbf{N}_2, \tag{345}$$

with

$$\mathbf{\Delta}^{(1)} = \frac{1}{h_n}\,(\mathbf{L}_2 - \mathbf{L}_0)\,, \tag{346}$$

where according to HILDEBRAND [16] $\mathbf{\Delta}^{(1)}$ denotes the first divided forward difference of the total angular momentum $\mathbf{L}(\alpha)$ of the master element I_α. Thus we may interprete equation (345) as the algorithmic counterpart of the rate of change (36) of the total angular momentum.
According to equation (343) the behavior of the algorithmic total angular momentum $\mathbf{L}_2$ depends only on the algorithmic total torque $\mathbf{N}_2$ and the time step size h_n. Hence it follows that $\mathbf{N}_2 = \mathbf{0}$, with $\mathbf{0} = [0, 0, 0]^T$, is the condition for the conservation of the algorithmic total angular momentum $\mathbf{L}_2$ in the sense that $\mathbf{L}_2 = \mathbf{L}_0$. Since the potential V is supposed to be arbitrary, we have to evaluate the integrals $\mathbf{\Sigma}_i$, $i \in \{1, 2\}$, by quadrature rules. Thus we may interprete $\mathbf{N}_2 = \mathbf{0}$ as a restriction on the quadrature rules.
In the following, we examine which interpolating quadrature rules obey the law of conservation of total angular momentum for linear time finite elements. According to the equations (343) and (344) the conservation condition takes the form

$$\mathbf{N}_2 \equiv -\mathbf{q}_0 \bowtie \mathbf{\Sigma}_1 - ((\gamma_{22} - \gamma_{11})\,\mathbf{q}_0 + 2\,(\gamma_{11} + \gamma_{12})\,\mathbf{q}_2) \bowtie \mathbf{\Sigma}_2 = \mathbf{0}, \tag{347}$$

where $\mathbf{0}$ denotes the 3×1 zero matrix. At first we approximate the integrals $\mathbf{\Sigma}_i$ according to equation (313) with an interpolating quadrature rule according to equation (51):

$$\mathbf{\Sigma}_i \approx \sum_{l=1}^{N_q} M_{i,l}\, \partial_{\mathbf{q}} V_l\, w_l, \tag{348}$$

where the index l designates the evaluation at the abscissae α_l. Since the condition (347) has to hold exactly for the conservation of algorithmic total angular momentum, we demand the following condition for the quadrature rules:

$$\mathbf{N}_2 \equiv -\mathbf{q}_0 \bowtie \sum_{l=1}^{N_q} M_{1,l}\, \partial_{\mathbf{q}} V_l\, w_l - \left(\left(\gamma_{22} - \gamma_{11}\right) \mathbf{q}_0 + 2\left(\gamma_{11} + \gamma_{12}\right) \mathbf{q}_2\right) \bowtie \sum_{l=1}^{N_q} M_{2,l}\, \partial_{\mathbf{q}} V_l\, w_l = \mathbf{0}. \tag{349}$$

We gain with the properties (i), (ii) and (iii) of the Theorem 15.1 the following simplifications:

$$\mathbf{N}_2 \equiv \sum_{l=1}^{N_q} \left(M_{1,l}\, \mathbf{n}_{0,l} + M_{2,l}\left(\left(\gamma_{22} - \gamma_{11}\right) \mathbf{n}_{0,l} + 2\left(\gamma_{11} + \gamma_{12}\right) \mathbf{n}_{2,l}\right)\right) w_l = \mathbf{0}, \tag{350}$$

where we used the fact that we are able to prove by induction the distributiv law (ii) of the Theorem 15.1 for arbitrary N_q and we introduced the following abbreviation to simplify the terms below:

$$\mathbf{n}_j = -\left(\mathbf{q}_j \bowtie \partial_{\mathbf{q}} V(\mathbf{q}^h, \mathbf{p}^h)\right) \equiv \mathbf{q}_j \bowtie \frac{f(r^h)}{r^h}\, \mathbf{q}^h, \tag{351}$$

where $j \in \{0, 1, 2\}$. Accordingly, we may write

$$\mathbf{N}_2 \equiv \sum_{l=1}^{N_q} \mathbf{\Gamma}(\alpha_l)\, w_l = \mathbf{0}, \tag{352}$$

with the vector-valued function

$$\mathbf{\Gamma}(\alpha) = \left(M_1(\alpha) + \left(\gamma_{22} - \gamma_{11}\right) M_2(\alpha)\right) \mathbf{n}_0(\alpha) + 2\left(\gamma_{11} + \gamma_{12}\right) M_2(\alpha)\, \mathbf{n}_2(\alpha). \tag{353}$$

On the other hand, we consider the residual vector of the general dG(1) method $\mathbf{R} \equiv \mathbf{R}(\mathbf{q}_1, \mathbf{q}_2) = \mathbf{0}$, where $\mathbf{0}$ denotes the $2n_{dof} \times 1$ zero matrix, which we obtain as a result of an elimination of the generalized momentum vectors $\mathbf{p}_1$ and $\mathbf{p}_2$:

$$\mathbf{R} \equiv \begin{bmatrix} \left(\gamma_{22} - \gamma_{11}\right) \mathbf{q}_2 + \mathbf{q}_1 - 2\left(\gamma_{12} + \gamma_{22}\right) \mathbf{q}_0 + 4\, h_n^2/\mu\, \left(\gamma_{12}^2 - \gamma_{11}\, \gamma_{22}\right) \mathbf{\Sigma}_2 \\ \mu/h_n\, \left(\mathbf{q}_2 - \mathbf{q}_1\right) - 2\left(\gamma_{12} + \gamma_{22}\right) \left(\mathbf{p}_0 - h_n\, \mathbf{\Sigma}_1\right) - 2\left(\gamma_{12} - \gamma_{22}\right) h_n\, \mathbf{\Sigma}_2 \end{bmatrix}. \tag{354}$$

We take the $\bowtie$-product with $\mathbf{\Sigma}_2$ from the right on both sides of the first component of the residual vector (354):

$$\left(\left(\gamma_{22} - \gamma_{11}\right) \mathbf{q}_2 + \mathbf{q}_1 - 2\left(\gamma_{12} + \gamma_{22}\right) \mathbf{q}_0 + 4\, h_n^2/\mu\, \left(\gamma_{12}^2 - \gamma_{11}\, \gamma_{22}\right) \mathbf{\Sigma}_2\right) \bowtie \mathbf{\Sigma}_2 = \mathbf{0}, \tag{355}$$

where property (v) of Theorem 15.1 implies that $\mathbf{0}$ denotes the 3×1 zero matrix. Using properties (i) and (ii) of Theorem 15.1 leads to a partly expanded equation (355). Subsequently, we place reals at the head of the $\bowtie$-products with the properties (i) and (iii) of Theorem 15.1. Finally, the property (iv) of Theorem 15.1 leads to the vanishing of the last term on the right side of equation (355). Thus we obtain

$$\left(\left(\gamma_{22} - \gamma_{11}\right) \mathbf{q}_2 + \mathbf{q}_1 - 2\left(\gamma_{12} + \gamma_{22}\right) \mathbf{q}_0\right) \bowtie \mathbf{\Sigma}_2 = \mathbf{0}. \tag{356}$$

The relation (356) has to be also fulfilled by the quadrature rules. Therefore, it has to be valid

$$\left(\left(\gamma_{22}-\gamma_{11}\right)\mathbf{q}_2+\mathbf{q}_1-2\left(\gamma_{12}+\gamma_{22}\right)\mathbf{q}_0\right)\bowtie\sum_{l=1}^{N_q}M_{2,l}\,\partial_{\mathbf{q}}V_l\,w_l=\mathbf{0}. \tag{357}$$

The properties (i), (ii) and (iii) of Theorem 15.1 gains

$$\sum_{l=1}^{N_q}\mathbf{\Lambda}(\alpha_l)\,w_l=\mathbf{0}, \tag{358}$$

with the vector-valued function

$$\mathbf{\Lambda}(\alpha)=-M_2(\alpha)\left(\left(\gamma_{22}-\gamma_{11}\right)\mathbf{n}_2(\alpha)+\mathbf{n}_1(\alpha)-2\left(\gamma_{12}+\gamma_{22}\right)\mathbf{n}_0(\alpha)\right). \tag{359}$$

To express the vector $\mathbf{n}_1$ through the vector $\mathbf{n}_2$ we consider the trial function $\mathbf{q}^h(\alpha)=\sum_{i=1}^{2}M_i(\alpha)\,\mathbf{q}_i$:

$$\mathbf{q}_1=\frac{1}{M_1(\alpha)}\left(\mathbf{q}^h(\alpha)-M_2(\alpha)\,\mathbf{q}_2\right),\qquad M_1(\alpha)\neq 0. \tag{360}$$

Taking the $\bowtie$-product with $\partial_{\mathbf{q}}V$ from the right on both sides of equation (360) yields

$$\mathbf{n}_1(\alpha)=\left(\frac{M_2(\alpha)}{M_1(\alpha)}\,\mathbf{q}_2-\frac{1}{M_1(\alpha)}\,\mathbf{q}^h(\alpha)\right)\bowtie\partial_{\mathbf{q}}V(\alpha), \tag{361}$$

where we introduced the abbreviation (351). We observe the properties (i) and (ii) of the Theorem 15.1 and obtain

$$\mathbf{n}_1(\alpha)=-\frac{M_2(\alpha)}{M_1(\alpha)}\,\mathbf{n}_2(\alpha)-\frac{1}{M_1(\alpha)}\,\mathbf{q}^h(\alpha)\bowtie\partial_{\mathbf{q}}V(\alpha). \tag{362}$$

According to equation (275) the last $\bowtie$-product of equation (362) reads

$$\mathbf{q}^h(\alpha)\bowtie\partial_{\mathbf{q}}V(\alpha)=\mathbf{q}^h(\alpha)\bowtie\left(-\frac{f(r(\alpha))}{r(\alpha)}\,\mathbf{q}^h(\alpha)\right). \tag{363}$$

The properties (i), (iii) and (iv) of the Theorem 15.1 lead to

$$\mathbf{q}^h(\alpha)\bowtie\partial_{\mathbf{q}}V(\alpha)=-\frac{f(r(\alpha))}{r(\alpha)}\left(\mathbf{q}^h(\alpha)\bowtie\mathbf{q}^h(\alpha)\right)=\mathbf{0}. \tag{364}$$

In consequence of equation (364) takes the vector $\mathbf{n}_1$ the following form:

$$\mathbf{n}_1(\alpha)=-\frac{M_2(\alpha)}{M_1(\alpha)}\,\mathbf{n}_2(\alpha). \tag{365}$$

Now we employ equation (365) in the vector $\mathbf{\Lambda}(\alpha)$ and obtain

$$\mathbf{\Lambda}(\alpha)=\frac{M_2(\alpha)}{M_1(\alpha)}\left(2\,M_1(\alpha)\left(\gamma_{12}+\gamma_{22}\right)\mathbf{n}_0(\alpha)+\left(M_2(\alpha)-M_1(\alpha)\left(\gamma_{22}-\gamma_{11}\right)\right)\mathbf{n}_2(\alpha)\right). \tag{366}$$

Here we devote to the evaluation of the coefficients in the vectors $\mathbf{\Gamma}$ and $\mathbf{\Lambda}$, which are algebraic functions of the integrals γ_{ij}:

$$\gamma_{22} - \gamma_{11} = \int_0^1 \left(M_2^2(\alpha) - M_1^2(\alpha) \right) d\alpha \tag{367}$$

$$= \int_0^1 \left(M_2(\alpha) - M_1(\alpha) \right) \left(M_1(\alpha) + M_2(\alpha) \right) d\alpha \tag{368}$$

$$\gamma_{22} - \gamma_{11} = \int_0^1 \left(M_2(\alpha) - M_1(\alpha) \right) d\alpha, \tag{369}$$

where the property $M_1 + M_2 = 1$ was applied. Furthermore, we obtain in the same line of argument:

$$\gamma_{11} + \gamma_{12} = \int_0^1 M_1(\alpha)\, d\alpha, \tag{370}$$

$$\gamma_{12} + \gamma_{22} = \int_0^1 M_2(\alpha)\, d\alpha. \tag{371}$$

We have reduced the coefficients to integrals of linear functions. To evaluate this integrals above with quadrature rules exactly we need quadrature rules which are at least second order accurate. The specific interpolating quadrature rules considered in the present paper, ie the midpoint rule, the trapezoidal rule and the Gaussian quadrature rule, fulfill this condition. According to Eriksson et al. [12] the midpoint rule and the trapezoidal rule are second order accurate and according to Isaacson & Keller [21] the Gaussian quadrature rules are $2N_q$th order accurate. Therefore, within the scope of the present paper we can use exact quadrature to calculate the coefficients. Exact quadrature in the equations (369), (370) and (371) yield

$$\gamma_{22} - \gamma_{11} = 0, \tag{372}$$

$$\gamma_{11} + \gamma_{12} = \frac{1}{2}, \tag{373}$$

$$\gamma_{12} + \gamma_{22} = \frac{1}{2}. \tag{374}$$

Taking into account the coefficients (372), (373) and (374), the vectors $\mathbf{\Gamma}$ and $\mathbf{\Lambda}$ owing to equations (353) and (366) respectively takes the form:

$$\mathbf{\Gamma}(\alpha) = M_1(\alpha)\, \mathbf{n}_0 + M_2(\alpha)\, \mathbf{n}_2, \tag{375}$$

$$\mathbf{\Lambda}(\alpha) = \frac{M_2(\alpha)}{M_1(\alpha)} \left(M_1(\alpha)\, \mathbf{n}_0 + M_2(\alpha)\, \mathbf{n}_2 \right). \tag{376}$$

A comparison of equation (375) with equation (376) results in

$$\mathbf{\Lambda}(\alpha) = C(\alpha)\, \mathbf{\Gamma}(\alpha), \quad \text{with} \quad C(\alpha) \equiv \frac{M_2(\alpha)}{M_1(\alpha)} = \frac{\alpha}{1-\alpha}. \tag{377}$$

Next we introduce equation (377) in equation (358):

$$\sum_{l=1}^{N_q} \mathbf{\Lambda}(\alpha_l)\, w_l = \sum_{l=1}^{N_q} C(\alpha_l)\, \mathbf{\Gamma}(\alpha_l)\, w_l = \mathbf{0}. \tag{378}$$

Considering the summation over the quadrature points with the index l in equation (378), a constant function $C = \text{const.}$ leads straight away to a satiesfied conservation property (352):

$$\sum_{l=1}^{N_q} \mathbf{\Lambda}(\alpha_l)\, w_l = C \sum_{l=1}^{N_q} \mathbf{\Gamma}(\alpha_l)\, w_l = \mathbf{0} \quad \overset{C\neq 0}{\Longrightarrow} \quad \sum_{l=1}^{N_q} \mathbf{\Gamma}(\alpha_l)\, w_l = \mathbf{0}. \tag{379}$$

Hence it follows that the condition on the quadrature rules in the end takes the form:

$$C = \frac{\alpha_l}{1-\alpha_l} = \text{const.}, \qquad C \neq 0, \tag{380}$$

for $l = 1, \ldots, N_q$. Because of the side conditions of equations (360), (380) we additionally obtain the following restriction: $\alpha_l \in I_{\alpha_l}$ with the open interval $I_{\alpha_l} = (0, 1)$. Therefore, quadrature points on the boundaries of the master element I_α are not allowed in this calculation. Accordingly, we have to neglect the trapezoidal rule and hence the quadrature rules considered in the present paper are confined to the midpoint rule ($N_q = 1$) and Gaussian quadrature rules with $N_q = 2, \ldots, 5$.

Remark 17.1 *In view of the conservation of the algorithmic total angular momentum the exclusion of the trapezoidal rule from the consideration is not disadvantageous because it proves that the trapezoidal rule does not obey the law of conservation of total angular momentum* $\boldsymbol{L}$*; see Figure 45.*

On account of the linear numerator and denominator of C in equation (380), for distinct quadrature points α_l the constants $C = \alpha_l/(1-\alpha_l)$ are also distinct. Thus only one quadrature point ($N_q = 1$) fulfills the condition (380). Equation (352) implies for one quadrature point that for a non-vanishing weight w_1 the conservation condition $\mathbf{N}_2 = \mathbf{0}$ is fulfilled only with the function $\mathbf{\Gamma}(\alpha) \equiv \mathbf{0}$. Therefore, we have to investigate under which circumstances $\mathbf{\Gamma}(\alpha)$ vanishes identically.
First we substitute in $\mathbf{\Gamma}(\alpha)$ equation (351) for the abbreviations $\mathbf{n}_j$:

$$\mathbf{\Gamma} = M_1\, \mathbf{q}_0 \bowtie \frac{f(r^h)}{r^h}\mathbf{q}^h + M_2\, \mathbf{q}_2 \bowtie \frac{f(r^h)}{r^h}\mathbf{q}^h. \tag{381}$$

Furthermore, we introduce the linear trial function $\mathbf{q}^h = \sum_{i=1}^{2} M_i\, \mathbf{q}_i$ and obtain

$$\mathbf{\Gamma} = M_1\, \mathbf{q}_0 \bowtie \frac{f(r^h)}{r^h}\left(M_1\, \mathbf{q}_1 + M_2\, \mathbf{q}_2\right) + M_2\, \mathbf{q}_2 \bowtie \frac{f(r^h)}{r^h}\left(M_1\, \mathbf{q}_1 + M_2\, \mathbf{q}_2\right). \tag{382}$$

Using property (ii) of Theorem 15.1 to dissolve the parenthesis and the properties (i) and (iii) of Theorem 15.1 to place reals at the head, equation (382) takes the form:

$$\mathbf{\Gamma} = M_1 \frac{f(r^h)}{r^h}\left(M_1\left(\mathbf{q}_0 \bowtie \mathbf{q}_1\right) + M_2\left(\mathbf{q}_0 \bowtie \mathbf{q}_2\right) + M_2\left(\mathbf{q}_2 \bowtie \mathbf{q}_1\right)\right), \tag{383}$$

where the property (iv) of Theorem 15.1 is responsible that the term $\mathbf{q}_2 \bowtie \mathbf{q}_2$ vanishes. Now we apply property (i) on the last term and summarize the last two terms such that

$$\mathbf{\Gamma} = M_1 \frac{f(r^h)}{r^h}\left(M_1\left(\mathbf{q}_0 \bowtie \mathbf{q}_1\right) - M_2\left(\mathbf{q}_1 - \mathbf{q}_0\right) \bowtie \mathbf{q}_2\right). \tag{384}$$

If the jump $[\mathbf{q}]_0 = \mathbf{q}_1 - \mathbf{q}_0$ vanishes, the last term drops out of equation (384) owing to property (v) of Theorem 15.1 and the first term vanishes because of property (iv) of Theorem 15.1. Hence it follows that $\mathbf{\Gamma}(\alpha)$ vanishes identically and thus according to equation (352) the algorithmic total torque $\mathbf{N}_2$ also vanishes. Therefore, a continuous solution of the dG(1) method implies the conservation of the algorithmic total angular momentum $\mathbf{L}_2$ for linear time finite elements.
Since we know from Theorem 8.1 that the midpoint rule applied to all integrals of the general dG(1) method leads to a continuous solution, the midpoint rule is an interpolating quadrature rule which preserves the algorithmic total angular momentum $\mathbf{L}_2$ owing to the continuous solution for linear time finite elements.

Numerical Example 17.3 *We compute the total angular momentum of the Kepler problem in Example 16.2 with the midpoint rule. Note that the midpoint rule gains the constant $C = 1$ by which the conservation condition (347) is identical with the equation (356). The reduced mass is $\mu = 2$. Moreover, the total energy and the potential constant of the reduced mass is $E = -0.25$ and $c = 0.25$ respectively. The non-vanishing total angular momentum component L_ζ shows Figure 46. We see the conservation of the total angular momentum at each time step.*

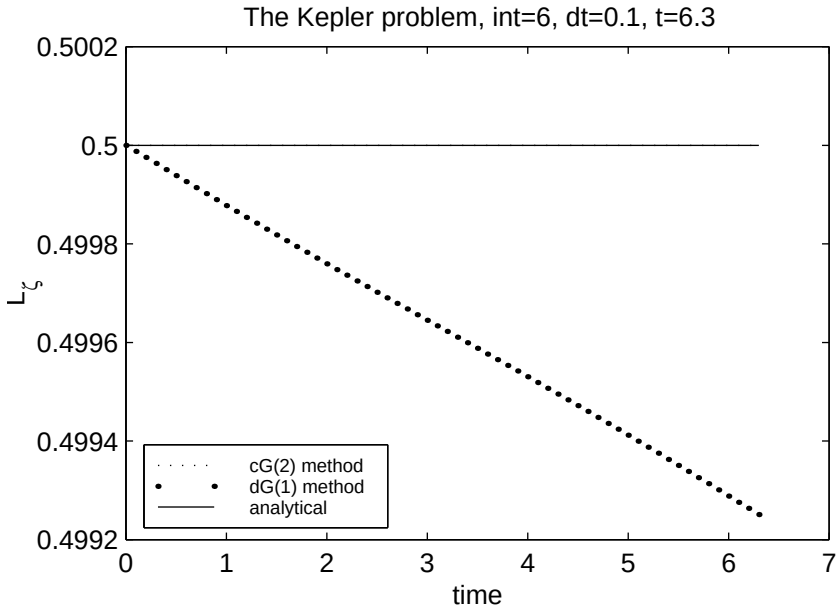

Figure 45: Total angular momentum component $L_\zeta = L_\zeta(t)$ of the Kepler problem with the reduced mass $\mu = 2$, total energy $E = -0.25$ and potential constant $c = 0.25$. Computed with the dG(1) method with trapezoidal rule ($N_q = 2$) and by a time step size $h_n = 0.1$.

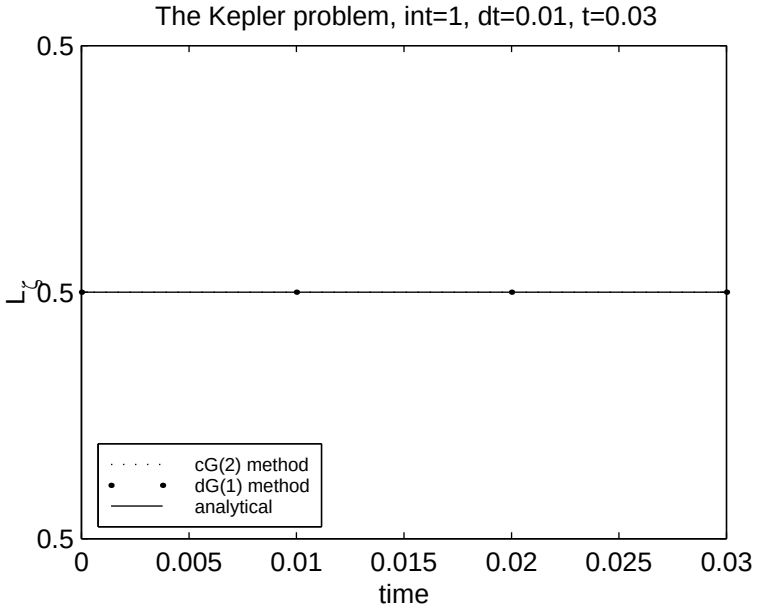

Figure 46: Total angular momentum component $L_\zeta = L_\zeta(t)$ of the Kepler problem with the reduced mass $\mu = 2$, total energy $E = -0.25$ and potential constant $c = 0.25$. Computed with the dG(1) method with midpoint rule ($N_q = 1$) and by a time step size $h_n = 0.01$.

18 The algorithmic total energy conservation of the equivalent one-body problem with linear time finite elements

In the present section we proceed along the lines of Section 10 and show the possibility in compliance with Betsch & Steinmann [7] to preserve the algorithmic total energy for an arbitrary central force law with linear time finite elements by the so-called modified midpoint rule.
According to Theorem 8.1, applying the standard midpoint rule to the general dG(1) method leads to the discrete cG(1) method emanating from the standard midpoint rule which not preserves the total energy in the nonlinear regime; cf Betsch & Steinmann [9]. However, according to Betsch & Steinmann [7] we gain algorithmic total energy conservation with the discrete cG(1) method emanating from the modified midpoint rule corresponding to equation (166). The starting point is also the discrete dG(1) method (137) which followed from the proof of Theorem 8.1:

$$\mathbf{z}_2 - \mathbf{z}_0 - h_n \, \mathbf{J} DH(\mathbf{z}^h(\frac{1}{2})) = \mathbf{0}.$$

Note that we have immediately employed equation (136). We leave the symplectic notation and take the explizit representation of the scheme (137). Simultaneously, we employ the Jacobian matrix (277) of the hamiltonian. Hence the explizit representation reads

$$\mathbf{q}_2 - \mathbf{q}_0 - \frac{h_n}{\mu} \, \mathbf{p}^h(\frac{1}{2}) = \mathbf{0}, \tag{385}$$

$$\mathbf{p}_2 - \mathbf{p}_0 - h_n \, \frac{f(r^h(1/2))}{r^h(1/2)} \, \mathbf{q}^h(\frac{1}{2}) = \mathbf{0}, \tag{386}$$

where $r = \sqrt{\mathbf{q}^T \mathbf{q}}$ and $f(r) = -dV(r)/dr$ denotes the magnitude of the radius vector $\mathbf{r}$ and the conservative central force law respectively. The matrix $\mathbf{0}$ designates the $n_{dof} \times 1$ zero matrix. Now we have to introduce a weight for each integral according to equation (166):

$$\mathbf{q}_2 - \mathbf{q}_0 - \frac{h_n}{\mu} \, \kappa_p \, \mathbf{p}^h(\frac{1}{2}) = \mathbf{0}, \tag{387}$$

$$\mathbf{p}_2 - \mathbf{p}_0 - h_n \, \kappa_q \, \frac{f(r^h(1/2))}{r^h(1/2)} \, \mathbf{q}^h(\frac{1}{2}) = \mathbf{0}. \tag{388}$$

Corresponding to Theorem 10.1 the solution is also continuous. According to Betsch & Steinmann [7], the condition for algorithmic energy conservation is the exact fulfillment of the Fundamental Theorem of Calculus for: (i) the kinetic energy $T = T(\mathbf{p}^h)$ which reads

$$T_2 - T_1 = \int_0^1 \partial_{\mathbf{p}} T(\mathbf{p}^h) \cdot \left(\mathbf{p}^h\right)' \, d\alpha \equiv \int_0^1 \partial_{\mathbf{p}} H(\mathbf{p}^h) \cdot \left(\mathbf{p}^h\right)' \, d\alpha, \tag{389}$$

and (ii) the potential $V = V(\mathbf{q}^h)$ in the form

$$V_2 - V_1 = \int_0^1 \partial_{\mathbf{q}} V(\mathbf{q}^h) \cdot \left(\mathbf{q}^h\right)' \, d\alpha \equiv \int_0^1 \partial_{\mathbf{q}} H(\mathbf{q}^h) \cdot \left(\mathbf{q}^h\right)' \, d\alpha. \tag{390}$$

The prime indicates differentiation with respect to α again. With regard to the equations (275) and (276), the equations (389) and (390) lead to:

$$T_2 - T_1 = \int_0^1 \frac{1}{\mu} \, \mathbf{p}^h \cdot \left(\mathbf{p}^h\right)' \, d\alpha, \tag{391}$$

$$V_2 - V_1 = -\int_0^1 \frac{f(r^h)}{r^h} \, \mathbf{q}^h \cdot \left(\mathbf{q}^h\right)' \, d\alpha. \tag{392}$$

Considering the linear trial functions, we first employ $\mathbf{p}^h = \sum_{i=1}^2 M_i \, \mathbf{p}_i$ in equation (391):

$$T_2 - T_1 = \int_0^1 \frac{1}{\mu} \left(\sum_{i=1}^2 M_i(\alpha) \, \mathbf{p}_i \right) \cdot (\mathbf{p}_2 - \mathbf{p}_1) \, d\alpha, \tag{393}$$

where $M_1 = 1 - \alpha$ and $M_2 = \alpha$ are the nodal shape functions. We aim at fulfilling the equation (393) with the modifiied midpoint rule corresponding to equation (166). Hence, we obtain

$$T_2 - T_1 = \frac{\kappa_p}{2\,\mu} \, (\mathbf{p}_1 + \mathbf{p}_2) \cdot (\mathbf{p}_2 - \mathbf{p}_1) \, . \tag{394}$$

Expanding equation (394) leads to

$$T_2 - T_1 = \kappa_p \left(\frac{1}{2\,\mu} \, \mathbf{p}_2^T \mathbf{p}_2 - \frac{1}{2\,\mu} \, \mathbf{p}_1^T \mathbf{p}_1 \right). \tag{395}$$

Taking into account the hamiltonian $H = T + V$ in equation (274), equation (395) can be written as

$$T_2 - T_1 = \kappa_p \, (T_2 - T_1) \, . \tag{396}$$

Therefore, the Fundamental Theorem of Calculus for the kinetic energy T is fulfilled for $\kappa_p = 1$, ie the standard midpoint rule.
Next we employ the trial function $\mathbf{q}^h = \sum_{i=1}^2 M_i \, \mathbf{q}_i$ in equation (392) and get

$$V_2 - V_1 = -\int_0^1 \frac{f(r^h(\alpha))}{r^h(\alpha)} \left(\sum_{i=1}^2 M_i(\alpha) \, \mathbf{q}_i \right) \cdot (\mathbf{q}_2 - \mathbf{q}_1) \, d\alpha. \tag{397}$$

We apply the modified midpoint rule corresponding to equation (166) to equation (397) and obtain

$$V_2 - V_1 = -\kappa_q \, \frac{f(r^h(1/2))}{2\, r^h(1/2)} \, (\mathbf{q}_1 + \mathbf{q}_2) \cdot (\mathbf{q}_2 - \mathbf{q}_1) \, . \tag{398}$$

We take into account $r^2 = \mathbf{q} \cdot \mathbf{q} \equiv \mathbf{q}^T \mathbf{q}$, hence the equation (398) takes the form

$$V_2 - V_1 = -\kappa_q \, \frac{f(r^h(1/2))}{2\, r^h(1/2)} \left(r_2^2 - r_1^2 \right). \tag{399}$$

Hence it follows that we get the following weight if we consider the continuous solution:

$$\kappa_q = -\tilde{C}_{20}\,\frac{2\,r^h(1/2)}{f(r^h(1/2))}, \tag{400}$$

where

$$\tilde{C}_{20} = \frac{V_2 - V_0}{r_2^2 - r_0^2}. \tag{401}$$

The determined weights κ_p and κ_q of the modified midpoint rule yields the following time-stepping scheme:

$$\mathbf{q}_2 - \mathbf{q}_0 - \frac{h_n}{2\,\mu}\,(\mathbf{p}_0 + \mathbf{p}_2) = \mathbf{0}, \tag{402}$$

$$\mathbf{p}_2 - \mathbf{p}_0 + h_n\,\tilde{C}_{20}\,(\mathbf{q}_0 + \mathbf{q}_2) = \mathbf{0}. \tag{403}$$

The time-stepping scheme (402), (403) makes possible to formulate the following

Theorem 18.1 *The modified midpoint rule conserves the algorithmic total energy of the equivalent one-body problem for linear time finite elements.*

Proof. We consider the time-stepping scheme (402), (403). Equation (403) scalar multiplied by $(\mathbf{q}_2 - \mathbf{q}_0)$ reads

$$(\mathbf{p}_2 - \mathbf{p}_0)\cdot(\mathbf{q}_2 - \mathbf{q}_0) + h_n\,\tilde{C}_{20}\,(\mathbf{q}_0 + \mathbf{q}_2)\cdot(\mathbf{q}_2 - \mathbf{q}_0) = 0. \tag{404}$$

Taking into account the identity $r^2 = \mathbf{q}\cdot\mathbf{q}$ as well the identity (401), we obtain

$$(\mathbf{p}_2 - \mathbf{p}_0)\cdot(\mathbf{q}_2 - \mathbf{q}_0) + h_n\,(V_2 - V_0) = 0. \tag{405}$$

Employing equation (402), equation (405) takes the form

$$\frac{h_n}{2\,\mu}\,(\mathbf{p}_2 - \mathbf{p}_0)\cdot(\mathbf{p}_0 + \mathbf{p}_2) + h_n\,(V_2 - V_0) = 0. \tag{406}$$

Expansion of equation (406) yields

$$h_n\left(\frac{1}{2\,\mu}\,\mathbf{p}_2^T\mathbf{p}_2 - \frac{1}{2\,\mu}\,\mathbf{p}_0^T\mathbf{p}_0\right) + h_n\,(V_2 - V_0) = 0. \tag{407}$$

With regard to the hamiltonian $H = T + V$ of the equivalent one-body problem in equation (274), for a non-vanishing time step size h_n the equation (407) leads to

$$H_2 - H_0 = 0. \tag{408}$$

□

To solve the time-stepping scheme (402), (403) by using the Newton-Raphson method in Table 8, we need the residual vector $\mathbf{R} = \mathbf{R}(\mathbf{q}_2)$:

$$\mathbf{R}(\mathbf{q}_2) = \left(1 + \frac{h_n^2}{2\,\mu}\,\tilde{C}_{20}\right)\,\mathbf{q}_2 - \left(1 - \frac{h_n^2}{2\,\mu}\,\tilde{C}_{20}\right)\,\mathbf{q}_0 - \frac{h_n}{\mu}\,\mathbf{p}_0. \tag{409}$$

The tangent $\mathbf{K}_T = \partial_{\mathbf{q}_2}\mathbf{R}(\mathbf{q}_2)$ results from the application of the derivative formula for a product of a scalar-valued vector function and a vector-valued vector function according to STEINMANN [33]:

$$\mathbf{K}_T = \left(1 + \frac{h_n^2}{2\,\mu}\,\tilde{C}_{20}\right)\,\mathbf{I} + \frac{h_n^2}{2\,\mu}\,(\mathbf{q}_0 + \mathbf{q}_2) \otimes \partial_{\mathbf{q}_2}\tilde{C}_{20}, \tag{410}$$

where $\otimes$ denotes the dyadic product. We calculate $\partial_{\mathbf{q}_2}\tilde{C}_{20}$ with the chain rule for differentiating composite functions:

$$\partial_{\mathbf{q}_2}\tilde{C}_{20} = \partial_{r_2}\tilde{C}_{20}\,\partial_{\mathbf{q}_2} r_2. \tag{411}$$

With regard to relation (276), the tangent reads

$$\mathbf{K}_T = \left(1 + \frac{h_n^2}{2\,\mu}\,\tilde{C}_{20}\right)\,\mathbf{I} + \frac{h_n^2}{2\,\mu}\,\tilde{C}'_{20}\,(\mathbf{q}_0 + \mathbf{q}_2)\,\mathbf{q}_2^T, \tag{412}$$

where

$$\tilde{C}'_{20} = -\frac{f_2/r_2 + 2\,\tilde{C}_{20}}{r_2^2 - r_0^2}. \tag{413}$$

Note that the tangent (412) is unsymmetric.

Numerical Example 18.1 *We compute the total energy of the Kepler problem in Example 16.2 with the modified midpoint rule. The reduced mass is $\mu = 2$, the total energy and the potential constant of the reduced mass is $E = -0.25$ and $c = 0.25$ respectively. Figure 47 shows the conservation of the total energy at each time step. Figure 48 compares the dG(1) and cG(2) method with standard midpoint rule and the dG(1) method with modified midpoint rule. According to Remark 6.3 the dG(1) and cG(2) method lead to identical schemes by applying the standard midpoint rule, which is why the total energies are identical. Referring to* BETSCH & STEINMANN *[9] it is well-known that the standard midpoint rule does not conserve the total energy in the nonlinear regime, what is corroborated in Figure 48.*

On the other hand, in Subsection 17.2 we have found that a one-point quadrature rule which generates a continuous solution leads to conservation of the total angular momentum for an arbitrary central force law. Since the modified midpoint rule consists of one quadrature point and yields a continuous solution according to Theorem 10.1, we expect conservation of the total angular momentum.

Remark 18.1 *The proof in Subsection 17.2 requires an exact integration of the coefficients (369), (370) and (371). The origin of this coefficients lies in the integrals of the equations (302) and (304) of the dG(1) method. On account of $\kappa_p = 1$ the integrals in the equations (302) and (304) are evaluated by the standard midpoint rule. According to Subsection 17.2, the standard midpoint rule evaluates the coefficients (369), (370) and (371) exactly. Therefore, the proof in Subsection 17.2 holds for the time-stepping scheme (402), (403) in the present section.*

Given: initial conditions $\mathbf{q}_0$ and $\mathbf{p}_0$, time step size h_n and residual tolerance $\epsilon = 10^{-13}$ set iteration counter $l = 1$
Find: nodal unknown $\mathbf{q}_2$ and $\mathbf{p}_2$
(a) initialization $\mathbf{q}_2^{(l)} = \mathbf{q}_0 + h_n/(2\,\mu)\,\left(\mathbf{p}_0 + \mathbf{p}_2^{(l)}\right)$ (b) compute residual vector $\mathbf{R}^{(l)} = \mathbf{R}(\mathbf{q}_2^{(l)})$ if $\|\mathbf{R}^{(l)}\| > \epsilon$ goto (c) else goto (d) (c) compute tangent $\mathbf{K}_T^{(l)} = \mathbf{K}_T(\mathbf{q}_2^{(l)})$ solve for increment $\Delta\,\mathbf{q}_2^{(l)}$ $\Delta\,\mathbf{q}_2^{(l)} = -\left(\mathbf{K}_T^{(l)}\right)^{-1}\mathbf{R}^{(l)}$ update the nodal unknowns $\mathbf{q}_2^{(l+1)} = \mathbf{q}_2^{(l)} + \Delta\,\mathbf{q}_2^{(l)}$ goto (b) with $l = l + 1$ (d) update generalized momentum vector $\mathbf{p}_2^{(l)} = (2\,\mu)/h_n\,\left(\mathbf{q}_2^{(l)} - \mathbf{q}_0\right) - \mathbf{p}_0$ (e) end.

Table 8: Newton-Raphson method to solve the time-stepping scheme generated by the dG(1) method with modified midpoint rule for the equivalent one-body problem.

Numerical Example 18.2 *We compute the total angular momentum of the Kepler problem in Example 16.2 with the modified midpoint rule. The reduced mass is* $\mu = 2$*, the total energy is* $E = -0.25$ *and the potential constant is* $c = 0.25$*. Figure 49 shows the algorithmic conservation of the total angular momentum of the dG(1) method integrated by the modified midpoint rule as well as the cG(2) and dG(1) method integrated by the standard midpoint rule.*

The upshot is that the modifed midpoint rule according to Betsch & Steinmann [7] preserves both the total energy and the total angular momentum at each time step for an arbitrary central force law.

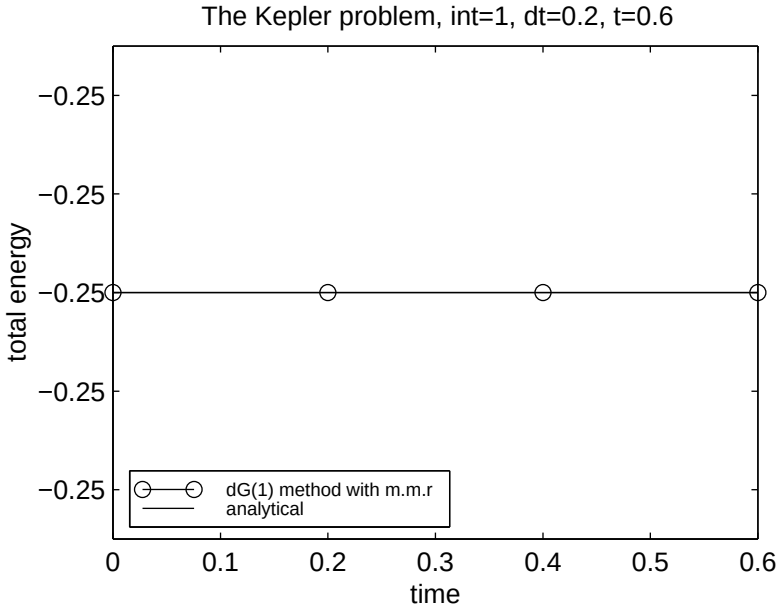

Figure 47: Total energy $E = E(t)$ of the Kepler problem with the reduced mass $\mu = 2$, total energy $E = -0.25$ and potential constant $c = 0.25$. Computed with the dG(1) method with the modified midpoint rule and by a time step size $h_n = 0.2$.

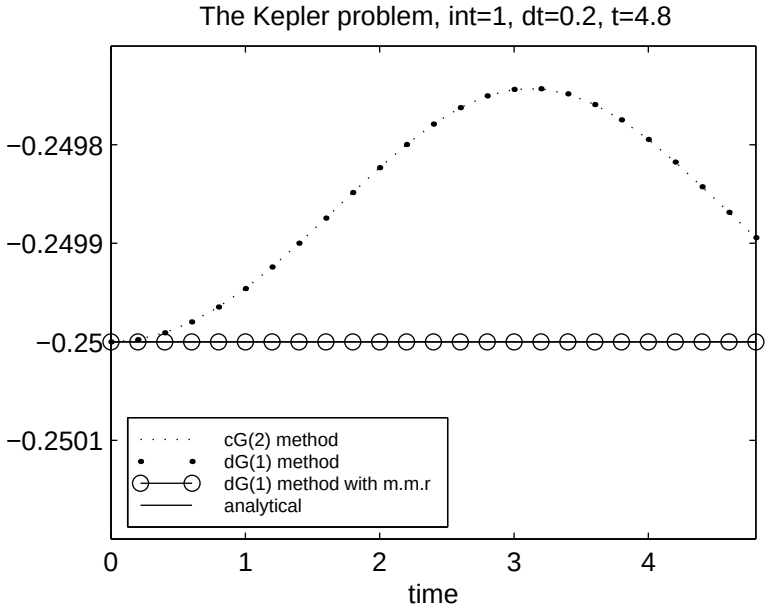

Figure 48: Total energy $E = E(t)$ of the Kepler problem with the reduced mass $\mu = 2$, total energy $E = -0.25$ and potential constant $c = 0.25$. Computed with the dG(1) method with the modified midpoint rule and by a time step size $h_n = 0.2$.

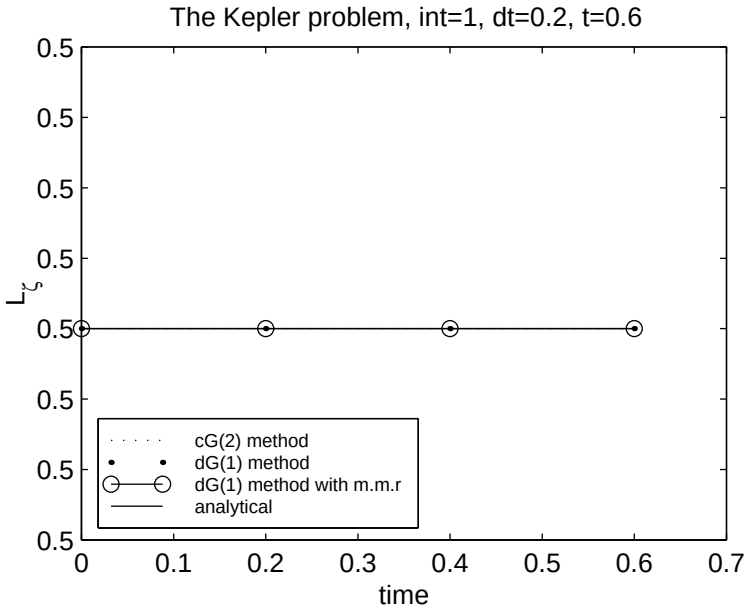

Figure 49: Total angular momentum component $L_\zeta = L_\zeta(t)$ of the Kepler problem with the reduced mass $\mu = 2$, total energy $E = -0.25$ and potential constant $c = 0.25$. Computed with the dG(1) method with modified midpoint rule and by a time step size $h_n = 0.2$.

19 Summary and conclusions

In Part I of the present thesis we gave a brief account of the Hamiltonian formulation of natural systems according to Arnold [3] and Goldstein [14]. Next we applied the discontinuous Galerkin (dG) finite element method according to Eriksson et al. [12] to Hamilton's canonical equations in symplectic notation. For the discontinuous Galerkin method based upon piecewise Lagrange polynomials of degree k (dG(k) method), we obtained a family of implicit multi-level one-step time-stepping schemes of which we got a specific member through a fixed polynomial degree k and a fixed quadrature rule used for the evaluation of the remaining integrals.
Further, we gave a proof for the decay of the algorithmic hamiltonian H_{k+1}; also see Bauchau & Joo [5]. We followed that the proof is valid as well for the dG(0) method without restrictions concerning test space and quadrature as for $k > 0$ under particular circumstances.

In Part II we were concerned with the application of the Galerkin finite element method to the planar circular pendulum for small oscillations (harmonic oscillator) and for arbitrary motions. We confined ourselves to constant ($k = 0$) and linear ($k = 1$) finite elements in time. To solve the equations of the implicit time-stepping schemes in the paper in hand, we applied the Newton-Raphson method.
First we introduced the law of conservation of total angular momentum of only one particle according to Goldstein [14] as Theorem 5.1.
It followed a time finite element formulation for the *harmonic oscillator*. We examined the time-stepping schemes emanating from as well exact quadrature as specific quadrature rules. We considered in the present thesis so-called interpolating quadrature rules according to Isaacson & Keller [21]. For constant time finite elements interpolating quadrature rules and exact quadrature led to identical time-stepping schemes. However, linear time finite elements generally implied an distinction between the use of quadrature rules and exactly evaluated integrals. We investigated in the present paper the midpoint rule, the trapezoidal rule and Gaussian quadrature rules with $N_q = 2, \ldots, 5$ quadrature points in particular. We found that for linear time finite elements the midpoint rule leads to a continuous solution. Furthermore, a comparison with Hughes [18] furnished that the trapezoidal rule would lead to the Crank-Nicholson algorithm (or average acceleration method in structural dynamics) if the jump $[\mathbf{z}^h]_0$ vanishes. The Gaussian quadrature with $N_q = 3, \ldots, 5$ quadrature points yielded the time-stepping schemes emanating from exact quadrature.
Next we examined the algorithmic total energy of the harmonic oscillator. We were able to relate the algorithmic total energy for constant and linear time finite elements to the spectral radius of the amplification matrix of the corresponding time-stepping schemes. This was possible through the Lagrange-Sylvester's interpolation polynomial according to Cadzow & Martens [10] or Gantmacher [13]. Therefore, we found that the spectral radius determined whether the algorithmic total energy decays, grows or is preserved. Accordingly, we showed that the algorithmic total energy of the dG(0) and dG(1) method decays if exact quadrature was carried out. Moreover, we took into

consideration the quadrature rules and found that only the midpoint rule conserves the algorithmic total energy for linear time finite elements. Thus it looks as if a continuous solution of the dG method is connected with algorithmic total energy conservation in the linear regime. The other considered quadrature rules led to algorithmic total energy decay and to jumps in the solution.
The next section was devoted to the planar circular pendulum for *arbitrary motions* and we also elaborated on constant and linear time finite elements. In contrast to the harmonic oscillator we had to use quadrature rules to evaluate the nonlinear integrals of the dG(1) method in symplectic notation. Further, we formulated Theorem 8.1 which states that the general dG(1) method can be converted into the discrete cG(1) method with a continuous solution by applying the midpoint rule. Moreover, we corroborated the fact according to Betsch & Steinmann [9] that in the nonlinear regime a continuous solution does not guarantee algorithmic total energy conservation.
In the subsequent section we determined the algorithmic total angular momentum of the circular pendulum for arbitrary motions with constant and linear time finite elements. We showed that the used polar coordinates immediately lead to conservation of algorithmic total angular momentum if the external total force $\mathbf{F} = m\,\mathbf{g}$ of the circular pendulum vanishes.
Concluding this part, we showed how algorithmic total energy conservation of the circular pendulum for arbitrary motions can be obtained with linear time finite elements by a nonstandard quadrature rule. We showed that a modification of the standard midpoint rule according to Betsch & Steinmann [7] gains total energy conservation at each time step. Further, we found that the general dG(1) method in connection with the modified midpoint rule leads to the discrete cG(1) method with a continuous solution (Theorem 10.1).

In Part III we dealed with the two-body central force problem. We first derived an equivalent one-body problem of which we developed the Hamiltonian formulation. Next we evolved a time finite element formulation of the so-called *isotropic harmonic oscillator* based upon the equivalent one-body problem. We considered constant and linear time finite elements. The time-stepping schemes for constant time finite elements emanated from exact quadrature whereas the schemes for linear time finite elements resulted from exact as well as numerical quadrature. We found that the time-stepping schemes of the isotropic harmonic oscillator only differs from the schemes of the harmonic oscillator in the matrix dimensions and so the results which we derived for the schemes of the harmonic oscillator we also found for the isotropic harmonic oscillator. Accordingly, we obtained a continuous solution by quadrature with midpoint rule.
We also examined the algorithmic total energy of the isotropic harmonic oscillator. Since the time-stepping schemes for the isotropic harmonic oscillator and the harmonic oscillator only differ in the matrix dimensions, we also used the Lagrange-Sylvester's interpolation polynomial to determine the algorithmic total energy. For constant and linear time finite elements the algorithmic total energy also depends only on the spectral radius of the amplification matrix. Moreover, the spectral radii were identical with the spectral radii of the harmonic oscillator so that we also got conservation of the algorithmic total

energy only by applying the midpoint rule and a decay of the algorithmic total energy in all the other cases.
Subsequent to the algorithmic total energy we determined the algorithmic total angular momentum of the isotropic harmonic oscillator as follows: We began with the introduction of the total angular momentum for the planar equivalent one-body problem. We gained a compact representation of the total angular momentum in matrix form through the definition of the new operator $\bowtie$. We got with the Theorem 15.1 the tool to calculate with the operator $\bowtie$. A further application of Lagrange-Sylvester's interpolation polynomial led to the algorithmic total angular momentum in dependence upon the spectral radius of the amplification matrix for constant and linear time finite elements. Thus we were able to show that the algorithmic total angular momentum of the isotropic harmonic oscillator with linear time finite elements is not preserved except by using the midpoint rule.
We next considered the *Kepler problem* as a concrete example of a nonlinear central force law. We developed a time finite element formulation whereby we computed orbits of the reduced mass with constant and linear time finite elements. Further, we corroborated Theorem 8.1 with a continuous orbit of the Kepler problem which we computed with the dG(1) method and midpoint rule.
Furthermore, we discussed whether constant and linear time finite elements obey the law of conservation of total angular momentum for arbitrary central forces. We obtained the result that constant time finite elements only lead to conservation of algorithmic total angular momentum, regardless of the kind of quadrature, in the uninteresting case of a constant central force potential V. However, we were able to show for sufficiently brief time steps that the sign of the central force law determines whether the algorithmic total angular momentum decays or grows. An approach of Betsch & Steinmann [7] made it possible to find that linear time finite elements obey the law of conservation of the algorithmic total angular momentum if the function $\mathbf{\Gamma}(\alpha)$ vanishes identically. We found that $\mathbf{\Gamma}(\alpha)$ vanishes identically only if the solution of the dG(1) method is continuous. Taking into consideration Theorem 8.1 implied that the midpoint rule is an interpolating quadrature rule which leads to algorithmic total angular momentum conservation with linear time finite elements owing to the fact that it leads to a continuous solution with the dG(1) method.
The last section showed how the algorithmic total energy for an arbitrary central force law can be conserved with linear finite elements in time by the modified midpoint rule according to Betsch & Steinmann [7]. Taking into account the results of the previous section, we were able to show that the modified midpoint rule also preserves the total angular momentum at each time step.

The upshot of it all is that constant time finite elements in connection with interpolating quadrature rules have not generally fulfilled the considered conservation laws for the circular pendulum and the two-body central force problem. On the other hand, linear time finite elements applied to the circular pendulum have led to algorithmic total energy conservation by using the modified midpoint rule. Furthermore, linear time finite elements applied to the two-body central force problem have led to algorithmic total

angular momentum conservation by using the midpoint rule; the modified midpoint rule according to Betsch & Steinmann [7] have led to algorithmic total energy and total angular momentum conservation. The conservation properties of the standard midpoint rule and the modified midpoint rule is attributed to the disappearance of the jumps (continuous solution). Further, a continuous solution emanated from the midpoint rule and also implied a conservation of algorithmic total energy in the linear regime of both natural systems.

We conclude by giving impulses for further investigations: Since we have not shown the behavior of the algorithmic total energy of the considered natural systems in the nonlinear case for $k > 0$, this issue can be the starting point for a follow-up paper. Furthermore, the application of the Lagrange-Sylvester's interpolation polynomial applied for quadratic potentials is not limited to the cases $k = 0$ and $k = 1$ for which we have shown the relation of the conservation properties to the spectral radius in the linear case. Therefore, an improvement upon the expositions about the algorithmic conservation properties in the linear case would be to determine the constituent matrices for arbitrary k. And finally, in Subsection 17.2 we have not determined the decay and growth of the algorithmic total angular momentum of the dG(1) method for an arbitrary central force law.

A The content of the enclosed CD-ROM

The time-stepping schemes presented in the present thesis are implemented in MATLAB 5.0. The MATLAB-Files are provided on the enclosed CD-ROM of which the directory tree is organized as follows:

(i) The first level separates the various time finite element formulations with respect to the polynomial degree k, ie $k = 0$ and $k = 1$ respectively.

(ii) The second level contains the specific problems which have been investigated, namely the circular pendulum and the two-body problem.

(iii) The third level is divided corresponding to the form of the conservative force; on the one hand the harmonic oscillator and the circular pendulum for arbitrary motions, on the other hand the isotropic harmonic oscillator and Kepler's problem.

Moreover, for $k = 1$ we had to distinguish between exact and numerical quadrature. In addition, the directory 'Spectral Radii' on the first level includes the MATLAB-File for computing the spectral radii of the dG(0) and dG(1) method.
The MATLAB-Files for a specific problem consist of several components. One component computes the first and second derivative of the potential. A further component calculates the potential V itself. The last components compute the residual and tangent for the Newton-Raphson method of the considered dG or cG method respectively. The names of the executable Files begin with 'cp' for circular pendulum or with 'tbp' for two-body problem.

References

[1] T.M. Apostol. *Calculus*, volume 2. John Wiley & Sons, New York, 2nd edition, 1967.

[2] T.M. Apostol. *Calculus*, volume 1. Xerox College Publishing, Lexington, Massachusetts, 2nd edition, 1967.

[3] V.I. Arnold. *Mathematical Methods of Classical Mechanics*. Springer, 2nd edition, 1989.

[4] V.I. Arnold. *Dynamical Systems*, volume 3. Springer, 2nd edition, 1991.

[5] O.A. Bauchau and T. Joo. Computational schemes for non-linear elasto-dynamics. *International Journal for Numerical Methods in Engineering.*, 45:693–719, 1999.

[6] O.A. Bauchau and N.J. Theron. Energy decaying scheme for non-linear beam models. *Comput. Methods Appl. Mech. Engrg.*, 134:37–56, 1996.

[7] P. Betsch and P. Steinmann. Conservation properties of a time fe method. Part I: Time-stepping schemes for n-body problems. To appear in Int. J. Numer. Methods Eng.

[8] P. Betsch and P. Steinmann. Conservation properties of a time fe method. Part II: Time-stepping schemes for nonlinear elastodynamics. Submitted to Int. J. Numer. Methods Eng.

[9] P. Betsch and P. Steinmann. Energy conserving time stepping schemes of arbitrary order for classical mechanics. To appear in Journal of Computational Physics.

[10] J.A. Cadzow and H.R. Martens. *Discrete-Time and Computer Control Systems*. Prentice-Hall, Inc., Englewood Cliffs, New Jersey, 1970.

[11] J. Chung and G.M. Hulbert. A time integration algorithm for structural dynamics with improved numerical dissipation: The generalized-α method. *Journal of Applied Mechanics*, 60:371–375, 1993.

[12] K. Eriksson, D. Estep, P. Hansbo, and C. Johnson. *Computational Differential Equations*. Cambridge University Press, 1996.

[13] F.R. Gantmacher. *Matrizenrechnung*, volume 1. VEB Deutscher Verlag der Wissenschaften, 3rd edition, 1970.

[14] H. Goldstein. *Classical Mechanics*. Addison-Wesley, Reading,Massachusetts, 2nd edition, 1980.

[15] M. Gross. *Numerische Untersuchungen diskreter dynamischer Systeme im Rahmen der Petrov-Galerkin-Methode*. Chair for Technical Mechanics, University of Kaiserslautern, Germany, 1999. Studienarbeit.

[16] F.B. Hildebrand. *Introduction to Numerical Analysis*. McGraw-Hill Book Company, New York, 2nd edition, 1974.

[17] C. Hoff and P.J. Pahl. Development of an implicit method with numerical dissipation from a generalized single-step algorithm for structural dynamics. *Computer Methods in Applied Mechanics and Engineering*, 67:367–385, 1988.

[18] T.J.R. Hughes. Stability, convergence and growth and decay of energy of the average acceleration method in nonlinear structural dynamics. *Computers & Structures*, 6:313–324, 1976.

[19] T.J.R. Hughes and W.K. Liu. Implicit-explicit finite elements in transient analysis: Stability theory. *Journal of Applied Mechanics*, 45:371–374, 1978.

[20] G.M. Hulbert. A unified set of single-step asymptotic annihilation algorithms for structural dynamics. *Comput. Methods Appl. Mech. Engrg.*, 113:1–9, 1994.

[21] E. Isaacson and H.B. Keller. *Analyse numerischer Verfahren*. Harri Deutsch, 1973.

[22] C. Johnson. Discontinous Galerkin finite element methods for second order hyperbolic problems. *Computer Methods in Applied Mechanics and Engineering*, 107:117–129, 1993.

[23] C. Johnson, U. Nävert, and J. Pitkäranta. Finite element methods for linear hyperbolic problems. *Computer Methods in Applied Mechanics and Engineering*, 45:285–312, 1984.

[24] H.J. Korsch and H.-J. Jodl. *Chaos*. Springer, 2nd edition, 1999.

[25] F. Kuypers. *Klassische Mechanik*. VCH-Verlag, 2nd edition, 1988.

[26] R.A. LaBudde and D. Greenspan. Energy and momentum conserving methods of arbitrary order for the numerical integration of equations of motion, I. Motion of a single particle. *Numer. Math.*, 25:323–346, 1976.

[27] P. Lasaint and P.A. Raviart. On a finite element method for solving the neutron transport equation. In Carl de Boor, editor, *Mathematical Aspects of Finite Elements in Partial Differential Equations*, pages 89–123. Academic Press, 1974.

[28] L.H. Loomis and S. Sternberg. *Advanced Calculus*. Addison-Wesley, Reading, Massachusetts, 1968.

[29] F. Lorenz. *Lineare Algebra*, volume 1. Wissenschaftsverlag, 3rd edition, 1991.

[30] J. Neumann and K. Schweizerhof. Analysis of shell structures under transient loading using adaptivity in time and space. In *European Conference on Computational Mechanics*, 1999.

[31] R.B. Richtmyer and K.W. Morton. *Difference Methods for Initial-Value Problems*. Interscience, New York, 2nd edition, 1967.

[32] P. Ruge. Hybrid time-finite-elements with time-step-adaption by discontinuity control. *Computational Mechanics*, 17:392–397, 1996.

[33] P. Steinmann. *Höhere Mechanik I*. Chair for Technical Mechanics, University of Kaiserslautern, Germany, 1997. Lecture notes.

[34] J.J. Sylvester. On the equation to the secular inequalities in the planetary theory. *Philosophical Magazine*, 16:267–269, 1883.

[35] R. Zurmühl and S. Falk. *Matrizen*, volume 1. Springer, 6th edition, 1992.

List of Figures

List of Tables

Notation

Latin symbols

a	real
$\mathbf{a}$	column matrix
$\mathbf{A}$	square matrices
$\mathbf{b}$	column matrix
$\mathbf{B}$	$2n_{dof} \times 2n_{dof}$ matrices
c	potential constant
$\mathbf{c}$	column matrix
$\mathbf{C}$	$2n_{dof} \times 2n_{dof}$ matrices
C	scalar coefficient
D	symplectic Jacobian matrix
D^2	symplectic Hessian matrix
E	total energy
f	conservative central force law
$\mathbf{F}$	external force
$\mathbf{F}_{ij}$	force of interaction
$\mathbf{g}$	gravitational acceleration vector
g	gravitational acceleration
h_n	time step size
H	hamiltonian
H_{k+1}	algorithmic hamiltonian
$\mathbf{H}$	matrix of symplectic hamiltonian
$\mathbf{I}$	identity matrix $(n_{dof} \times n_{dof})$
I	moment of inertia
I_t	time interval
I_n	nth subinterval of I
I_α	master element
I_{α_l}	an interval for abscissae
i	imaginary unit
$\mathbf{J}$	symplectic unit matrix
k	trial function degree
$\mathbf{K}_T$	tangent of the residual vector
$\mathbf{K}$	coefficient matrix
l	rod length
L	lagrangian
$\mathbf{L}$	angular momentum
$\mathbf{L}_{k+1}$	algorithmic angular momentum
M_I	Ith nodal shape function
m	mass of a particle
n	index, denotes time steps
n_{dof}	degrees of freedom
n_p	number of particles
$\mathbf{n}$	column matrix
N	index of end time
N_q	number of quadrature points
N_λ	number of eigenvalues
$\mathbf{N}$	total torque
$\mathbf{N}_{k+1}$	algorithmic total torque
$\mathbf{O}$	zero matrix $(n_{dof} \times n_{dof})$
$\mathbf{O}_2$	zero matrix $(2n_{dof} \times 2n_{dof})$
p	generalized momentum
$\mathbf{p}$	generalized momentum vector
$\mathbf{p}_I$	nodal value of $\mathbf{p}$
P_c	characteristic polynomial
P_m	minimal polynomial
$\mathbf{P}$	total linear momentum
q	generalized coordinate
$\mathbf{q}$	generalized coordinate vector
$\mathbf{q}_I$	nodal value of $\mathbf{q}$
$\dot{q}$	generalized velocity
$\dot{\mathbf{q}}$	generalized velocity vector
Q	generalized force
$\mathbf{Q}$	generalized force vector
r	magnitude of the radius vector
$\mathbf{r}$	radius vector
$\mathbf{R}$	residual vector, column matrix
$\mathbf{R}$	center of mass
t	time
t_n	nth time step
T	total kinetic energy
T	period of a harmonic solution
T_n	master element transformation
$\mathbf{u}$	unit vector
V	potential
w_l	quadrature weight
x	coordinate axis
$\mathbf{x}$	unknown column matrix
y,z	coordinate axis
$\mathbf{z}$	symplectic variable
$\mathbf{z}_I$	nodal value of $\mathbf{z}$

Greek and miscellaneous symbols

α	coordinate of I_α	η	coordinate axis
α_I	node in I_α	λ	eigenvalue
α_l	abscissae of quadrature	$\mathbf{\Lambda}$	matrix-valued function
β_{ij}	numerical quadrature coefficients	μ	reduced mass
γ_{ij}	exact quadrature coefficients	ν	positive integer
$\mathbf{\Gamma}$	matrix-valued function	ξ	coordinate axis
δ_{IJ}	Kronecker delta	ρ	spektral radius
δ	test function symbol	$\mathbf{\Sigma}_i$	matrix-valued integral terms
Δ	increment/difference symbol	ω	eigenfrequency
ϵ	residual tolerance	Ω	sampling frequency
ζ	coordinate axis		

$\mathcal{E}$	euclidean space	$\cdot$	scalar product
$\mathcal{H}$	Hessian matrix	$\times$	cross/cartesian product
$\mathcal{O}$	coordinate origin	$\otimes$	dyadic product
$\mathcal{P}^k$	space of polynomials of degree k	$\bowtie$	new matrix product
$\mathcal{R}$	the set of real numbers.	$()$	argument parentheses
$\mathcal{R}^{dim}$	dim-dimensional real space.	$^{(l)}$	denotes iterations
		$^{(l,m)}$	denotes block matrices
$\mathbf{0}$	column zero matrix	^{h}	denotes an employed trial function or an element of $\mathcal{P}^k$
$\mathbf{1}$	identity matrix $(2n_{dof} \times 2n_{dof})$		
		^{q}	denotes quadrature
∂	partial derivative	^{k}	designates the dG(k) method
∂^2	second partial derivative	$[\cdots]$	matrix representation
$\dot{(\bullet)}$	time derivative	$[\cdots]^T$	transposed matrix
$(\bullet)'$	derivative with respect to α	$[\bullet]_i$	designates a jump at node i
$d/d(\bullet)$	total derivative	$\{\}$	a set of scalars/matrices
$d^2/d(\bullet)^2$	second total derivative	$\square$	theorem is proved above
deg	degree of polynomials	$\| \bullet \|$	euclidean norm

Glossary

Miscellaneous general terms

Cross references are *italicized*.

Amplification matrix: Explained in the paper. See in the index.

Attractor: A geometrical object in *phase space* towards which *trajectories* converge in the long-time limit. Attractors can be of various dimensionality. The simplest case of an attractor is an *equilibrium point*, also called a *fixed point* in the context of maps. Cf Korsch & Jodl [24].

Configuration space: A n_{dof}-dimensional cartesian hyperspace where the generalized coordinates q_i, $i = 1, \ldots, n_{dof}$, form the n_{dof} coordinate axes. Cf Goldstein [14].

Damping: Asymptotic annihilation of a motion owing to forces of friction. Physical important is a frictional force which is proportional to the velocity of a moving particle (viscose damping). Algorithmic damping designates the effect of asymptotic annihilation of time evolutions determined by numerical algorithms. In general, damping leads to *dissipation*.

Damped harmonic oscillator: The *differential equation* $\ddot{x} + r\,\dot{x} + \omega_0^2\,x = 0$. The coefficient r is a measure for the *damping* and ω_0 denotes the eigenfrequency of the oscillator. This special kind of *damping*, the so-called viscose damping, leads to a resonance frequency ω_{res} which is smaller than the eigenfrequency and to an amplitude decay according to an exponential function. Cf Korsch & Jodl [24].

Degrees of freedom: The number of independent coordinates of a system.

Differential equation: Equation determining the dynamics of a sytem by relating variables of the system to their derivatives. Ordinary differential equations contain only derivatives with respect to time t, whereas partial differential equations additionally contain derivatives with respect to the variables. If a differential equation contains derivatives up to the kth order, it is called a differential equations of kth order.

Discontinuity: Let f be a given continuous function and let $W_h^{(q)}$ the space of discontinuous piecewise polynomials of degree q on (a,b). An interpolant $\pi_h f \in W_h^{(q)}$ is called discontinuous at node i if its right-hand limit $\pi_h f_i^+$ at node i and its left-hand limit $\pi_h f_i^-$ at node i exist but are unequal. In other words, the corresponding *jump* $[\pi_h f]_i$ is unequal to zero. Cf Eriksson et al. [12].

Dissipation: A *dynamical system*, for which the volume elements in *phase space* shrink under time evolution, is said to be dissipative. Dissipation is a prerequisite for the existence of *attractors* in the system. Cf KORSCH & JODL [24]. Numerical dissipation means that a numerical method has an *attractor* unequal to the exact solution by computing of algebraic equations. Prerequisite for numerical dissipation in numerical methods applied to linear problems is that the amount of the eigenvalues of the *amplification matrix* is less than one. Cf RICHTMYER & MORTON [31].

Dual space: The dual space V^* of the vector space V is the vector space $\mathrm{Hom}(V,\mathcal{R})$ of all linear mappings from V to $\mathcal{R}$. Its elements are called linear functionals. Cf LOOMIS & STERNBERG [28].

Dynamical system: A system described by time-dependent variables. The time evolution of the variables is given by a set of *differential equations* and *initial conditions*.

Equilibrium point: A point $\mathbf{x}_0$ of a system $\dot{\mathbf{x}} = \mathbf{f}(\mathbf{x})$, $\mathbf{x} \in \mathcal{R}^{dim}$, if $\mathbf{x}(t) \equiv \mathbf{x}_0$ is a solution of this system. In *dynamical systems* this usually means a *phase space* point with zero velocity. Equilibria can be either (Liapunov) stable or unstable. In the latter case, the slightest perturbation causes the system to move far away from the equilibrium state, whereas it stays forever in the vicinity of the equilibrium in the case of stability (in the sense of Liapunov). Cf ARNOLD [3] and KORSCH & JODL [24].

Finite element method: In basic form the *Galerkin method* with piecewise polynomial approximation. Cf ERIKSSON ET AL. [12].

Fixed point (of a mapping): A point which is mapped onto itself. Cf ERIKSSON ET AL. [12].

Galerkin method: Method for solving a general *differential equation*, which is based on searching for an (approximate) solution in a (finite-dimensional) space spanned by a set of basis functions which are easy to differentiate and integrate, together with an orthogonality condition determining the coefficients or coordinates in the given basis. With a finite number of basis functions, the Galerkin method leads to a system of algebraic equations with a finite number of unknowns which produces an approximate solution by numerical solving with a computer. Cf ERIKSSON ET AL. [12].

Hamiltonian system: *Dynamical system* with n_{dof} *degrees of freedom* in which the equations of motion can be derived from a scalar function $H(\mathbf{q},\mathbf{p},t)$, the hamiltonian, by partial differentiation: $\dot{\mathbf{p}} = -\partial_{\mathbf{q}} H$, $\dot{\mathbf{q}} = \partial_{\mathbf{p}} H$, where $\mathbf{q} = [q_1,\ldots,q_{n_{dof}}]^T$ and $\mathbf{p} = [p_1,\ldots,p_{n_{dof}}]^T$ denotes the generalized coordinates and momenta. This equations of motion, the canonical equations of Hamilton, generate *trajectories* in the $2n_{dof}$-dimensional *phase space*. In more global terms it is said that the hamiltonian produces

in the *phase space* a *phase flow* which preserves the phase space volume (Liouville's theorem). The name refers to the mathematician and astronomer W.R. Hamilton. Cf Arnold [3] and Korsch & Jodl [24].

Inertial system: A reference frame in which the Newton's law of motion is valid. Within classical mechanics the notion of an inertial system is something of an idealization. In practice, however, it is usually feasible to set up a coordinate system that comes as close to the desired properties as may be required. Cf Goldstein [14].

Initial condition: The values of the variables describing a *dynamical system* at a certain instant in time.

Isotropic: Along all directions of a space, eg *configuration space* or *phase space* but usually applied to an euclidean space (isotropic material), the physical properties are the same. This term comes from the Greek *isos* for 'same' and *tropos* for 'direction'.

Jump: Let f be a given continuous function and let $W_h^{(q)}$ the space of discontinuous piecewise polynomials of degree q on (a,b). A jump of an interpolant $\pi_h f \in W_h^{(q)}$ at the node i is denoted by $[\pi_h f]_i = \pi_h f_i^+ - \pi_h f_i^-$, where $\pi_h f_i^+$ and $\pi_h f_i^-$ denotes the right-hand and left-hand limit at node i respectively. Cf Eriksson et al. [12].

Legendre transformation: Let $y = f(x)$ be a convex function, $f''(x) > 0$. The Legendre transformation of the function f is a new function g of a new variable p, which is constructed in the following way: We draw the graph of f in the x, y plane. Let p a given number. Consider the straight line $y = p\,x$. We take the point $x = x(p)$ at which the curve is farthest from the straight line in the vertical direction: for each p the function $p\,x - f(x) = F(p,x)$ has a maximum with respect to x at the point $x(p)$. Now we define $g(p) = F(p, x(p))$. The point $x(p)$ is defined by the extremal condition $\partial_x F = 0$, ie $f'(x) = p$. Since f is convex, the point $x(p)$ is unique. Expressed in more global terms, the Legendre transformation transforms functions on a vector space to functions on the *dual space*. The name of the transformation refers to the French mathematician A.M. Legendre. Cf Arnold [3].

Linear: A *dynamical system*/function is linear if its response/value to the change in a variable is proportional to the value of the variable.

Nonlinear: *Dynamical systems*/functions in which the response/value to the change in a variable is not *linear*.

Phase flow: The one-parameter group of transformations of *phase space*

$$g^t : (\mathbf{q}(0), \mathbf{p}(0)) \mapsto (\mathbf{q}(t), \mathbf{p}(t)),$$

where $\mathbf{q}(t)$, $\mathbf{p}(t)$ are solutions of Hamilton's canonical equations. Cf Arnold [3].

Phase space: A $2n_{dof}$-dimensional space of generalized coordinates $\mathbf{q} = [q_1, \ldots, q_{n_{dof}}]^T$ and momenta $\mathbf{p} = [p_1, \ldots, p_{n_{dof}}]^T$. In the phase space the time evolution of a system can be described by first order *differential equations*. A point in the phase space uniquely determines the future of a system. Therefore, different *trajectories* in the phase space cannot intersect. Cf Arnold [3] and Korsch & Jodl [24].

Symplectic: This term comes from the Greek for 'intertwined.' The symplectic notation is particularly appropriate for Hamilton's equations where $\dot{\mathbf{q}}$ is connected with a partial derivative with respect to $\mathbf{p}$ and $\dot{\mathbf{p}}$ similarly with the negative of a $\mathbf{q}$ derivative. H. Weyl first introduced the term in 1939 in his book *The Classical Groups* (p. 165 in both the first edition, 1939, and second edition, 1946). Cf Goldstein [14].

Time-stepping scheme: A system of equations that relates the values of $m+1$ variables at one time to the values at a previous time (one-step). Typically, an implicit time-stepping scheme is given as $\mathbf{z}_m = \mathbf{f}(\mathbf{z}_0, \ldots, \mathbf{z}_m)$, where $\mathbf{f}$ is generally a *nonlinear* function. 'Implicit' reffers to the fact that $\mathbf{f}$ depends upon $\mathbf{z}_m$. A time-stepping scheme with $m+1$ variables is called a $(m+1)$-level scheme. Cf Richtmyer & Morton [31].

Trajectory: The image of the mapping $T : t \mapsto (\mathbf{q}(t), \mathbf{p}(t))$ is called a trajectory in *phase space*. Cf Arnold [3].

Index

German Supplements

S.1 Erklärung

Hiermit erkläre ich, dass ich die vorliegende Diplomarbeit selbstständig und ohne unerlaubte, fremde Hilfe angefertigt und die gesamte benutzte Literatur im Quellenverzeichnis angegeben habe.

Münchweiler
May 18, 2005 .....

S.2 Einleitung und Gliederung

Diese Arbeit beschäftigt sich mit der numerischen Integration der Hamiltonschen kanonischen Gleichungen. Zur temporalen Diskretisierung wird anstatt eines Differenzenverfahrens eine Finite-Elemente-Methode verwendet. Aus der Hamiltonschen Betrachtungsweise folgt die unabhängige Approximation der generalisierten Koordinaten und Impulse. Der Ausgangspunkt der vorliegenden temporalen Finite-Elemente-Methode ist die schwache Form der Hamiltonschen kanonischen Gleichungen in symplektischer Schreibweise. Das entsprechende System von gewöhnlichen Differentialgleichungen erster Ordnung wird mittels eines Zeitschrittverfahren gelöst, welches aus der sogenannten diskontinuierlichen Galerkin(dG)-Methode abgeleitet wird (siehe Eriksson u.a. [12]).

Diese oft Lasaint & Raviart [27] zugesprochene Galerkin-Finite-Elemente-Methode verwendet diskontinuierliche Lösungs- und Testfunktionen aus einem Funktionenraum. Im Vergleich dazu stützt sich die kontinuierliche Galerkin-Methode (cG-Methode) auf die Verwendung von Lösungs- und Testräume bei denen die Dimension des Testraumes gegenüber der Dimension des Lösungsraumes um eins niedriger ist. In Eriksson u.a. [12] stellte sich heraus, dass verglichen mit der cG-Methode die Verwendung lediglich eines Funktionenraumes einen Vorteil bei der Fehlerrechnung und eine Verbesserung der Stabilitätseigenschaften für parabolische Probleme erzielt. Dafür kann im allgemeinen, im Gegensatz zur cG-Methode, die Anfangsbedingung des Problems nicht mehr exakt erfüllt werden.

In dieser Arbeit werden für konstante und lineare temporale Finite-Elemente die Erhaltungseigenschaften untersucht, welche die folgenden zwei dynamischen Systeme mit skleronomen Zwangsbedingungen erfüllen:

- das ebene Kreispendel und
- das Zweikörperproblem.

Von besonderem Interesse ist die Energie und der Drehimpuls, da diese Konstanten der Bewegung in der Mechanik eine zentrale Rolle spielen und es sich deswegen auch als ein grosser Vorteil erweist wenn man in der Lage ist diese nach jedem Zeitschritt exakt

zu erhalten (algorithmische Erhaltung). Laut LaBudde & Greenspan [26] führt die Anwendung konventioneller numerischer Verfahren auf Systeme gewöhnlicher Differentialgleichungen der klassischen Mechanik lediglich zu einer Erhaltung der Energie und des Drehimpulses im Rahmen der Fehlerordnung des Verfahrens.
Ausserdem ist die Energieerhaltung vom numerischen Standpunkt aus wünschenswert um unbedingte Stabilität im nichtlinearen Fall zu gewährleisten (siehe dazu Betsch & Steinmann [9] und Hughes [18]).

Da zum Beispiel die wissenschaftlichen Arbeiten von Bauchau & Joo [5], Bauchau & Theron [6], Chung & Hulbert [11], Hoff & Pahl [17], Hulbert [20], Johnson [22], Johnson et al. [23], Neumann & Schweizerhof [30] und Ruge [32] für die dG-Approximation innerhalb von temporalen und temporal-räumlichen Finite-Elemente-Methoden numerische Dissipation nachweisen, kann eine Erfüllung der Erhaltungsgesetze nur aufgrund einer geeigneten numerischen Integration erfolgen. Im Rahmen der cG-Methode erzielten P. Betsch und P. Steinmann eine Drehimpulserhaltung durch spezielle Quadraturregeln (siehe Betsch & Steinmann [7, 8]). Generell werden in dieser Arbeit sogenannte interpolierende Quadraturregeln betrachtet (vgl. Isaacson & Keller [21]), im besonderen werden die Mittelpunktsregel, die Trapezregel und die Gaussschen Quadraturregeln untersucht.

Zusätzlich illustrieren numerische Beispielrechnungen die analytischen Resultate der Untersuchungen über die betrachteten dynamischen Systemen, wobei die energieerhaltenden cG-Methode als Referenz diente.

Der Rest der Arbeit ist wie folgt gegliedert: Das Ziel von Teil I ist die Ableitung des Zeitschrittverfahrens für beliebige temporale Finite-Elemente aus der Galerkin Finite-Element-Formulierung. Abschnitt 2 umfasst die Hamiltonsche Formulierung der Bewegungsgleichungen: Zuerst werden die kanonischen Hamiltonschen Gleichungen eingeführt und anschliessend wird die Hamiltonfunktion als Gesamtenergie und Erhaltungsgrösse von dynamischen Systemen mit skleronomen Zwangsbedingungen identifiziert. In Abschnitt 3 wird das implizite Zeitschrittverfahren aus der dG-Methode abgeleitet und Abschnitt 4 untersucht innerhalb der dG-Methode das algorithmische Verhalten der Hamiltonfunktion.
Teil II behandelt die Anwendung der Zeitschrittverfahren konstanter und linearer temporaler Finite-Elemente auf das ebene Kreispendel. Zu Anfang führt Abschnitt 5 das Gesetz der Erhaltung des Drehimpulses eines Massepunktes ein, welches sowohl beim Kreispendel als auch beim Zweikörperproblem Anwendung findet. In Abschnitt 6 wird eine temporale Finite-Elemente-Formulierung des Kreispendels für kleine Ausschläge bestimmt, wobei interpolierende Quadraturregeln berücksichtigt werden. Abschnitt 7 untersucht die algorithmische Gesamtenergie des Kreispendels ebenfalls für kleine Ausschläge unter Beachtung numerischer Integration. Abschnitt 8 behandelt die Erstellung einer temporalen Finite-Elemente-Formulierung des Kreispendels für beliebig grosse Ausschläge. Infolge des nichtlinearen Kraftgesetzes kann im Rahmen der symplektischen Notation bei linearen temporalen Finite-Elementen nur auf numerische Integration zurückgegriffen werden. Ausserhalb der symplektischen Notation zeigt Betsch &

Steinmann [9] eine Möglichkeit exakt zu integrieren. Abschnitt 9 widmet sich dem algorithmischen Gesamtdrehmpuls des Kreispendels für beliebig grosse Ausschläge. Da jedoch Polarkoordinaten als generalisierte Koordinaten verwendet werden, erweisst sich die Untersuchung als geradezu trivial. Abschnitt 10 zeigt wie die Gesamtenergie des Kreispendels durch eine nichtstandardisierte Quadraturregel algorithmisch erhalten werden kann.
Teil III befasst sich mit der Berechnung von Zentralkraftbewegungen zweier Massepunkte (Zweikörperproblem). Abschnitt 11 beginnt mit einer Reduzierung dieses Problems mit sechs Freiheitsgraden auf ein äquivalentes ebenes Einkörperproblem mit zwei Freiheitsgraden. Die Formulierung des äquivalenten Einkörperproblemes nach Hamilton wird in Abschnitt 12 ermittelt. Abschnitt 13 stellt eine temporale Finite-Elemente-Formulierung des äquivalentes Einkörperproblems für das Hookesche Zentralkraftgesetz vor. Abschnitt 14 beschäftigt sich mit der algorithmischen Gesamtenergie in Verbindung mit der Hookeschen Zentralkraft. Es wird gleichermassen exakte und numerische Integration behandelt. In Abschnitt 15 wird der algorithmische Gesamtdrehimpuls in Verbindung mit der Hookeschen Zentralkraft untersucht, wobei neben der exakten Integration auch eine Quadratur in Betracht gezogen wird. In Abschnitt 16 wird eine temporale Finite-Elemente-Formulierung beliebiger Zweikörperpotentiale aufgestellt und auf die nichtlineare Keplersche Zentralkraft angewendet (Keplerproblem). Abschnitt 17 untersucht die Erhaltungseigenschaften des algorithmischen Gesamtdrehimpulses für beliebige Zentralkräfte. Zur Integration werden nur interpolierende Quadraturregeln verwenden, da die Annahme eines beliebigen Kraftgesetzes eine exakte Integration ausschliesst. Abschnitt 18 zeigt eine Möglichkeit algorithmische Gesamtenergieerhaltung mit Hilfe einer nichtstandardisierten Quadraturregel zu erzielen. Abschnitt 19 umfasst eine Zusammenfassung und Diskussion der Arbeit.

S.3 Zusammenfassung und Schlussbemerkungen

In Teil I der vorliegenden Arbeit wurde nach einem kurzen Beitrag über die Hamiltonsche Formulierung von mechanischen Systemen mit holonomen, skleronomen Zwangsbedingungen gemäss Arnold [3] and Goldstein [14], die diskontinuierliche Galerkin-Finite-Elemente-Methode entsprechend Eriksson u.a. [12] auf die Hamiltonschen kanonischen Gleichungen in symplektischer Schreibweise angewendet. Da die entwickelte dG-Methode auf Lagrangesche Interpolationspolynome vom Grade k basiert (dG(k)-Methode), erhielt man eine Familie von impliziten Zeitschrittverfahren. Ein bestimmtes Mitglied dieser Familie erhielt man durch die Festlegung des Polynomgrades k und die Wahl einer Integrationsmethode für die verbleibenden Integrale.
Ferner wurde ein Beweis für die Abnahme der algorithmischen Hamiltonfunktion H_{k+1} geliefert (vgl. Bauchau & Joo [5]), woraus gefolgert wurde, dass der Beweis ohne Einschränkungen bezüglich Testraum und Integration auf die dG(0)-Methode anwendbar ist, jedoch für $k > 0$ bestimmten Einschränkungen unterliegt.

Teil II beschäftigte sich mit der Anwendung der Galerkin-Finite-Elemente-Methode auf das ebene Kreispendel für kleine Schwingungen und für beliebig grosse Auslenkungen. Es

wurden konstante und lineare temporale Finite-Elemente betrachtet. Die Gleichungen der impliziten Zeitschrittverfahren wurden in der gesamten Arbeit mittels der Newton-Raphson-Methode gelöst.
Zuerst wurde das Gesetz der Erhaltung des Gesamtdrehimpulses eines Massepunktes gemäss GOLDSTEIN [14] als Theorem 5.1 eingeführt.
Es folgte eine temporale Finite-Element-Formulierung des ebenen Kreispendels für kleine Schwingungen. Es wurden die Zeitschrittverfahren untersucht welche sowohl aus einer exakten Integration als auch aus einer numerische Integration herrührten. Der vorliegenden Arbeit wurden sogenannte interpolierende Quadraturregeln zu Grunde gelegt (siehe ISAACSON & KELLER [21]). Bei konstanten temporalen Finite-Elementen führten interpolierende Quadraturregeln und exakte Quadratur zu identischen Zeitschrittverfahren. Jedoch bei linearen temporalen Finite-Elementen ist im allgemeinen eine unbedingte Unterscheidung zwischen dem Gebrauch von Quadraturregeln und exakter Integration notwendig. Im besonderen wurde die Mittelpunktsregel, die Trapezregel und die Gausschen Quadraturregeln mit $N_q = 2, \ldots, 5$ Quadraturpunkten untersucht. Es stellte sich heraus, dass bei linearen temporalen Finite-Elementen die Mittelpunktsregel zu einer kontinuierlichen Lösung führte. Weiterhin erbrachte ein Vergleich mit HUGHES [18], dass eine numerischen Quadratur mit der Trapezregel den Crank-Nichelson-Algorithmus ergibt wenn die Sprünge $\mathbf{z}_0$ verschwinden würden. Eine Gausssche Quadratur mit $N_q = 3, \ldots, 5$ Quadraturpunkten ergab die Zeitschrittverfahren die auch durch eine exakte Quadratur erreicht wurden.
Als nächstes ist die algorithmische Gesamtenergie des Kreispendels für kleine Ausschläge untersucht worden. Es war möglich eine Verbindung zwischen der algorithmischen Gesamtenergie für konstante und lineare temporale Finite-Elemente und dem Spektralradius der zu den entsprechenden Zeitschrittverfahren gehörenden Übertragungsmatrix zu finden. Ermöglicht wurde dies durch die Anwendung des Lagrange-Sylvesterschen Interpolationspolynoms (siehe CADZOW & MARTENS [10] oder GANTMACHER [13]). Demzufolge bestimmt der Spektralradius ob die algorithmische Gesamtenergie abnimmt, zunimmt oder erhalten bleibt. Folglich konnte gezeigt werden, dass die algorithmische Gesamtenergie der dG(0)- und dG(1)-Methode bei exakter Integration abnimmt. Ausserdem zeigte sich bei linearen temporalen Finite-Elementen, dass lediglich eine der betrachteten Quadraturregeln die algorithmische Gesamtenergie erhält: die Mittelpunktsregel. Somit hat es den Anschein, als wäre im linearen Fall mit einer kontinuierlichen Lösung eine algorithmische Gesamtenergieerhaltung verbunden. Die anderen betrachteten Quadraturregeln führten zu einer algorithmischen Gesamtenergieabnahme und Sprüngen in der Lösung.
Anschliessend wurden beliebig grosse Auslenkungen des Kreispendels in Verbindung mit konstanten und linearen temporalen Finite-Elementen betrachtet. Im Gegensatz zu der Berechnung für kleine Ausschläge waren Quadraturregeln notwendig um die nichtlinearen Integrale der dG(1)-Methode auszuwerten. Ferner wurde das Theorem 8.1 formuliert welches besagt, dass die Anwendung der Mittelpunktsregel auf die dG(1)-Methode diese in die discrete cG(1)-Methode mit kontinuierlicher Lösung transformiert. Ausserdem wurde bestätigt, dass im nichtlinearen Fall eine kontinuierlichen Lösung keine algorith-

mische Gesamtenergieerhaltung garantiert (vgl. Betsch & Steinmann [9]).
Im nachfolgenten Abschnitt wurde der algorithmische Gesamtdrehimpuls beliebiger Bewegungen des Kreispendels unter Verwendung von konstanten und linearen temporalen Finite-Elementen bestimmt. Es wurde gezeigt, dass Polarkoordinaten sofort zu einer algorithmischen Erhaltung des Gesamtdrehimpulses führen, wenn die externe Gesamtkraft $\mathbf{F} = m\,\mathbf{g}$ des Kreispendels verschwindet.
Der letzte Abschnitt der dem Kreispendel gewidmet ist zeigte, wie eine algorithmische Erhaltung der Gesamtenergie des Kreispendel für beliebig grosse Auslenkungen mittels linearer temporaler Finite-Elemente durch eine nichtstandardisierte Quadraturregel erzielt werden kann. Es wurde gezeigt, dass eine Modifikation der gewöhnlichen Mittelpunktsregel nach Betsch & Steinmann [7] die Gesamtenergie nach jedem Zeitschritt erhält. Ferner konnte gezeigt werden, dass die dG(1)-Methode in Verbindung mit der modifizierten Mittelpunktsregel in eine discrete cG(1)-Methode übergeht und zu einer kontinuierlichen Lösung führt (Theorem 10.1).

Teil III befasste sich mit dem Zweikörperproblem. Begonnen wurde mit der Ableitung eines äquivalenten ebenen Einkörperproblems von welchem anschliessend die Hamiltonsche Formulierung verfasst wurde. Als nächstes wurde eine temporale Finite-Elemente-Formulierung der Hookeschen Zentralkraft bestimmt welche auf dem Einkörperproblem basiert. Es wurden konstante und lineare temporale Finite-Elemente betrachtet. Die Zeitschrittverfahren für konstante temporale Finite-Elemente ergaben sich aus einer exakten Integration wohingegen die Zeitschrittverfahren für lineare temporale Finite-Elemente sowohl aus einer exakten als auch aus einer numerischen Quadratur resultierten. Es stellte sich heraus, dass sich die Zeitschrittverfahren für die Hookesche Zentralkraft von den Zeitschrittverfahren für das Kreispendel mit kleinen Ausschlägen nur in den Dimensionen der Matrizen unterscheiden. Daraufhin waren die abgeleiteten Ergebnisse bezüglich der Zeitschrittverfahren identisch und man erhielt ebenfalls eine kontinuierliche Lösung durch eine Quadrature mit der Mittelpunktsregel.
Es wurde ebenfalls die algorithmische Gesamtenergie der Hookeschen Zentralkraft untersucht. Da sich die Zeitschrittverfahren des Kreispendels für kleine Ausschläge und die für die Hookesche Zentralkraft nur in den Matrizendimensionen unterschieden, war es möglich das Lagrange-Sylvestersche Interpolationspolynom zur Bestimmung der algorithmischen Gesamtenergie zu verwenden. Für konstante und lineare temporale Finite-Elemente hing die algorithmische Gesamtenergie ebenfalls nur vom Spektralradius der Übertragungsmatrix ab. Ausserdem waren die Spektralradii identisch mit denen des Kreispendels für kleine Ausschläge so dass die algorithmische Gesamtenergie nur nach einer Quadratur mit der Mittelpunktsregel erhalten blieb und in allen anderen Fällen abnahm.
Es folgte auf die algorithmische Gesamtenergie die Untersuchung des algorithmischen Gesamtdrehimpulses der Hookeschen Zentralkraft. Zuerst wurde der Drehimpuls des äquivalenten ebenen Einkörperproblemes eingeführt. Mit der Definition des Operators $\bowtie$ wurde eine kompakte Darstellung des Drehimpulses in Matrixform erzielt. Das Theorem 15.1 beinhaltete die notwendigen Rechenregeln für diesen neuen Operator. Eine weitere Anwendung des Lagrange-Sylvesterschen Interpolationspolynoms führte für kon-

stante und lineare temporale Finite-Elemente zu einem algorithmischen Gesamtdrehimpuls in Abhängigkeit von dem Spektralradius der Übertragungsmatrix. Damit konnte gezeigt werden, dass der algorithmische Gesamtdrehimpuls der dG(1)-Methode aussschliesslich durch eine Quadratur mit der Mittelpunktsregel erhalten wird.
Als nächstes wurde das Keplerproblem als konkretes Beispiel eines nichtlinearen Zentralkraftgesetzes betrachtet. Es wurde eine temporale Finite-Elemente-Formulierung entwickelt, womit Bahnkurven mit konstanten und linearen temporalen Finite-Elementen berechnet wurden. Ferner ist Theorem 8.1 durch eine Berechnung einer kontinuierlichen Bahnkurve nach einer Quadratur mit der Mittelpunktsregel bestätigten worden.
Weiterhin wurde für beliebige Zentralkraftgesetze diskutiert ob konstante und lineare temporale Finite-Elemente der Drehimpulserhaltung gehorchen. Konstante temporale Finite-Elemente führten zu dem Ergebnis, dass, ungeachtet der Art der Quadratur, eine Drehimpulserhaltung lediglich bei dem uninteressanten Fall eines konstanten Zentralkraftpotenitals zu erreichen ist. Jedoch für hinreichend kleine Zeitschritte konnte gezeigt werden, dass das Vorzeichen des Zentralkraftgesetzes bestimmt ob der algorithmische Gesamtdrehimpuls abnimmt oder zunimmt. Bei linearen temporalen Finite-Elementen führte ein Ansatz aus Betsch & Steinmann [7] zu folgendem Ergebnis: Interpoliernde Quadraturregeln mit einem Quadraturpunkt liefern eine Erhaltung des algorithmischen Gesamtdrehimpulses falls die Funktion $\mathbf{\Gamma}(\alpha)$ identisch verschwindet. Umformungen ergaben, dass $\mathbf{\Gamma}(\alpha)$ nur dann identisch verschwindet falls die Lösung der dG(1)-Methode kontinuierlich ist. Mit Hilfe von Theorem 8.1 liess sich dann folgern, dass nur die Mittelpunktsregel zur Erhaltung des algorithmischen Gesamtdrehimpulses bei linearen temporalen Finite-Elementen führt, aufgrund der Tatsache dass sich mit ihr eine kontinuierlichen Lösung ergibt.
Der letzte Abschnitt zeigte wie die algorithmische Gesamtenergie für ein beliebiges Zentralkraftgesetz mit linearen temporalen Finiten-Elementen mittels der modifizierten Mittelpunktsregel nach Betsch & Steinmann [7] erhalten werden kann. Zudem, unter Beachtung der Ergebnisse des vorherigen Abschnitts, war es möglich zu zeigen, dass die modifizierte Mittelpunktsregel ebenfalls den Gesamtdrehimpuls nach jedem Zeitschritt erhält.

Das Fazit ist somit: konstante temporale Finite-Elemente in Verbinding mit interpolierenden Quadraturregeln haben die betrachteten Erhaltungsgesetze für das Kreispendel und das Zweikörperproblem im allgemeinen nicht erfüllt. Dagegen haben lineare temporale Finite-Elemente beim Kreispendel mittels einer Quadratur mit der Mittelpunktsregel zur algorithmischen Erhaltung der Gesamtenergie geführt. Weiterhin haben lineare temporale Finite-Elemente im Rahmen des Zweikörperproblemes den Gesamtdrehimpuls durch die Anwendung der Mittelpunktsregel algorithmisch erhalten; die modifizierte Mittelpunktsregel nach Betsch & Steinmann [7] hat eine algorithmische Erhaltung der Gesamtenergie und des Gesamtdrehimpulses erzielt. Die Erhaltungseigenschaften der Mittelpunktsregel und der modifizierten Mittelpunktsregel beruhen auf dem Verschwinden der Sprünge in der Lösung. Ferner hat eine von der Mittelpunktsregel stammende kontinuierliche Lösung die algorithmische Erhaltung der Gesamtenergie im linearen Fall beider Systeme zur Folge.

Zum Abschluss werden noch Anregungen für weitere Untersuchungen gegeben: Da das algorithmische Verhalten der Gesamtenergie der betrachteten mechanischen Systeme im nichtlinearen Fall für $k > 0$ nicht ermittelt wurde, könnte dies ein Thema für eine nachfolgenden Arbeit sein. Die Anwendung des Lagrange-Sylvesterschen Interpolationspolynoms ist nicht auf die Fälle $k = 0$ und $k = 1$ beschränkt, für welche im linearen Fall die Verbindung der Erhaltungseigenschaften zu dem Spektralradius gezeigt wurde. Folglich ist die Bestimmung der Koeffizientenmatrizen des Lagrange-Sylvesterschen Interpolationspolynoms für beliebige k eine Verbesserung der Ausführungen über die Erhaltungseigenschaften im linearen Fall. Und abschliessend: In Abschnitt 17.2 wurde die Abnahme und das Ansteigen des algorithmischen Gesamtdrehimpulses der dG(1)-Methode für ein beliebiges Zentralkraftgesetz nicht bestimmt.